AD NUMBER

AD480402

NEW LIMITATION CHANGE

TO

Approved for public release, distribution unlimited

FROM

Distribution authorized to U.S. Gov't. agencies and their contractors; Critical Technology; 20 MAY 1964. Other requests shall be referred to Commanding Officer, Air Force Technical Applications Center, Patrick AFB, FL 32925.

AUTHORITY

USAF ltr, 25 Jan 1972

Atlas of Signals and Noise

Project VT/036

The Geotechnical Corporation
3401 Shiloh Rd. • Garland, Texas

TECHNICAL REPORT NO. 64-50

ATLAS OF SIGNALS AND NOISE

THE GEOTECHNICAL CORPORATION
3401 Shiloh Road
Garland, Texas

20 May 1964

CONTENTS

1. INTRODUCTION
   - 1.1 Authority
   - 1.2 Purpose
   - 1.3 Orientation of instrument arrays

2. EARTHQUAKE PHASES

3. P AND PKP PHASES FROM VARIOUS DISTANCES AND AZIMUTHS
   - 3.1 Distance = 0° to 16°
   - 3.2 Distance = 17° to 40°
   - 3.3 Distance = 41° to 60°
   - 3.4 Distance = 61° to 80°
   - 3.5 Distance = 81° to 100°
   - 3.6 Distance = 101° to 120°
   - 3.7 Distance = 121° to 140°
   - 3.8 Distance = 141° to 160°

4. NOISE SAMPLES

INDEX

ILLUSTRATIONS

Figure

1-1 Orientation of instrument arrays at WMSO

1-2 Normalized response characteristics of seismographs at WMSO

2-1 WMSO seismogram illustrating P and pP phase arrivals from the Kermadec Islands

2-2 WMSO seismogram illustrating P and pP phase arrivals from Central Peru

2-3 P-wave arrival recorded on all systems at WMSO. Epicenter: Kurile Islands

2-4 WMSO primary short-period seismogram illustrating a "Lonesome P." Epicenter: near the east coast of Kamchatka

2-5 WMSO seismogram illustrating S and sS phase arrivals (see figures 2-6 and 2-7 for the corresponding phase arrivals on the short-period system). Epicenter: Northern Chile

2-6 WMSO seismogram illustrating an S phase arrival on the short-period system. Epicenter: Northern Chile

2-7 WMSO seismogram illustrating an sS phase arrival on the short-period system. Epicenter: Northern Chile

2-8 WMSO seismogram illustrating an S phase arrival from Western Bolivia (see figure 2-9 for corresponding phase on the short-period system)

2-9 WMSO seismogram illustrating an S phase arrival from Western Bolivia

2-10 WMSO seismogram illustrating S and ScS phase arrivals from the Easter Islands region

2-11 WMSO seismogram illustrating S and SP phase arrivals from the Kurile Islands

ILLUSTRATIONS, Continued

Figure

2-12 WMSO seismogram illustrating a PP phase arrival from the New Hebrides Islands (see figure 2-13 for the corresponding phase on the short-period system)

2-13 WMSO primary short-period seismogram illustrating a PP phase from the New Hebrides Islands

2-14 WMSO seismogram illustrating a PP phase arrival from Western New Guinea (see figure 2-15 for the corresponding phase on the short-period system)

2-15 WMSO seismogram illustrating a PP phase arrival from Western New Guinea

2-16 WMSO seismogram illustrating PP and PPP phases from the Kurile Islands

2-17 WMSO seismogram illustrating SS and SSS phases from the Fiji Islands region

2-18 WMSO seismogram illustrating a PcP phase arrival. Epicenter: Northern Peru

2-19 WMSO seismogram illustrating an ScP phase arrival from the Peru-Bolivia border

2-20 WMSO seismogram illustrating ScP, S, and ScS phase arrivals from Northern Chile

2-21 ScS as recorded on the WMSO short-period seismogram. Epicenter: Northern Chile

2-22 WMSO seismogram illustrating PKP_1 and PKP_2 phase arrivals. Epicenter: near the west coast of Sumatra

2-23 WMSO seismogram illustrating an SKP phase arrival. Epicenter: near north coast of Java

ILLUSTRATIONS, Continued

Figure	
2-24	WMSO seismogram illustrating SKP_1 and SKP_2 phase arrivals. Epicenter: Western Macquarie Islands
2-25	WMSO primary short-period seismogram illustrating $PKKP_1$ and $PKKP_2$ phase arrivals from the Sandwich Islands
2-26	$PKKP_1$-$PKKP_2$-$PKKP_3$ as recorded on the WMSO short-period seismogram. Epicenter: Santa Cruz Island region
2-27	WMSO primary short-period seismogram illustrating an SKKP phase arrival. Epicenter: near north coast of Java
2-28	WMSO seismogram illustrating a PKPPKP (P'P') phase arrival. Epicenter: off the east coast of Kamchatka
2-29	WMSO seismogram illustrating a PKPPKPPKP (P'P'P') phase arrival. Epicenter: Kermadec Islands
2-30	WMSO seismogram illustrating a PKPPKPPKPPKP (P'P'P'P') phase arrival. Epicenter: Kermadec Islands
2-31	WMSO seismogram illustrating a PcPPKP phase arrival. Epicenter: Loyalty Islands region
2-32	WMSO seismogram illustrating SKS, S_c, and PS phase arrivals from the Fiji Islands region (see figure 2-33 for the corresponding short-period recording of SKS)
2-33	WMSO seismogram illustrating an SKS phase arrival from the Fiji Islands region
2-33a	WMSO seismogram illustrating an SKS phase arrival from the Fiji Islands region
2-34	WMSO seismogram illustrating SKS, PS, and PPS phase arrivals from the New Hebrides Islands
2-35	WMSO seismogram illustrating SKS, SP, and SPP phases from the Fiji Islands region

ILLUSTRATIONS, Continued

Figure

2-36 WMSO seismogram illustrating SKS and SKKS phase arrivals from Western New Guinea

2-37 WMSO seismogram illustrating PKKS and SKKS phase arrivals from the New Hebrides Islands

2-38 WMSO seismogram illustrating a PKP-PKS phase arrival from the Kermadec Islands

2-39 SKKKS as recorded on the WMSO short-period seismogram. Epicenter: Kermadec Islands

2-40 WMSO seismogram illustrating Love and Rayleigh phase arrivals from Sonoro, Mexico

2-41 WMSO seismogram illustrating the broad-band system response to surface waves. Epicenter: off the coast of Central Mexico

2-42 WMSO seismogram illustrating a $Rayleigh_1$ phase arrival (see figure 2-43 for $Rayleigh_2$ arrival from the same event). Epicenter: Kermadec Islands

2-43 WMSO seismogram illustrating a $Rayleigh_2$ phase arrival. Epicenter: Kermadec Islands

2-44 Rayleigh waves as recorded on the WMSO short-period seismogram. Epicenter: Santa Cruz Island region

3-1 WMSO seismogram illustrating a P phase arrival from the Gulf of California

3-2 WMSO short-period seismogram illustrating a P phase arrival from Central Idaho

3-3 WMSO seismogram illustrating a P phase arrival from Guerrero, Mexico

ILLUSTRATIONS, Continued

Figure

3-4 WMSO seismogram illustrating a P phase arrival from the Revilla Gigedo Island region

3-5 WMSO short-period seismogram illustrating a P phase arrival. Epicenter: Jalisco, Mexico

3-6 WMSO short-period seismogram illustrating a P phase arrival from the Ontario-Quebec border

3-7 WMSO seismogram illustrating a P phase arrival from off the coast of Oregon

3-8 WMSO seismogram illustrating a P phase arrival from off the coast of Oregon

3-9 WMSO short-period seismogram illustrating a P phase arrival. Epicenter: near the north coast of Venezuela

3-10 WMSO seismogram illustrating a P phase arrival from the Galapagos Islands

3-11 WMSO seismogram illustrating a P phase arrival Epicenter: near the coast of Southern Chile

3-12 WMSO short-period seismogram illustrating a P phase arrival from Ecuador

3-13 WMSO seismogram illustrating a P phase arrival from the North Atlantic Ocean

3-14 An event from Western Brazil as recorded at WMSO

3-15 WMSO seismogram illustrating a P phase arrival. Epicenter: south of Hawaii Island

3-16 WMSO seismogram illustrating a P phase arrival from the Andreanof Islands region

ILLUSTRATIONS, Continued

Figure

3-17 WMSO seismogram illustrating a P phase arrival from the Andreanof Islands region

3-18 WMSO primary short-period seismogram illustrating a P phase arrival from the Andreanof Islands region

3-19 WMSO seismogram illustrating a P phase arrival. Epicenter: near the coast of Northern Chile

3-20 WMSO seismogram illustrating a P phase arrival from the Bolivia-Brazil border

3-21 WMSO seismogram illustrating a P phase arrival from the Easter Island region

3-22 WMSO seismogram illustrating a P phase arrival from the Kurile Islands

3-23 WMSO seismogram illustrating a P phase arrival from the mid-Atlantic Ocean

3-24 WMSO seismogram illustrating a P phase arrival. Epicenter: near the east coast of Hokkaido

3-25 WMSO short-period seismogram illustrating a P phase arrival from the Ionian Sea

3-26 WMSO short-period seismogram illustrating a P phase arrival from the Aegean Sea

3-27 WMSO seismogram illustrating a P phase arrival from the Fiji Islands

3-28 WMSO seismogram illustrating a P phase arrival from the Fiji Islands

3-29 WMSO seismogram illustrating a P phase arrival from off the coast of Turkey

ILLUSTRATIONS, Continued

Figure

3-30 WMSO seismogram illustrating a PKP phase arrival from New Britain

3-31 WMSO seismogram illustrating a PKP phase arrival. Epicenter: near the coast of Southern Iran

3-32 WMSO short-period seismogram illustrating a PKP phase arrival. Epicenter: near the north coast of Luzon

3-33 WMSO short-period seismogram illustrating a PKP phase arrival from the Banda Sea

3-34 WMSO short-period seismogram illustrating a PKP phase arrival. Epicenter: off the southern coast of Java

3-35 WMSO seismogram illustrating a PKP phase arrival. Epicenter: off southern coast of Sumatra

3-36 WMSO seismogram illustrating a PKP phase arrival from the Sunda Strait

3-37 WMSO seismogram illustrating a PKP phase arrival from the Prince Edward Island region

3-38 WMSO seismogram illustrating a PKP phase arrival from the Chagos Archipelago region

3-39 WMSO seismogram illustrating a PKP phase arrival. Epicenter: south of Australia

3-40 WMSO short-period seismogram illustrating a PKP phase arrival from the Indian Ocean

4-1 WMSO short-period seismogram illustrating 1/2-second microseisms

4-2 WMSO seismogram illustrating the occurrence of 4- to 6-second microseisms at a low level on the short-period system

ILLUSTRATIONS, Continued

Figure

4-3 WMSO seismogram illustrating the occurrence of 4- to 6-second microseisms at a moderate level on the short-period system

4-4 WMSO seismogram illustrating the occurrence of 4- to 6-second microseisms at a high level on the short-period system

4-5 WMSO seismogram illustrating wind-generated noise on the short-period system. Wind speed is approximately 38 mph

4-6 WMSO seismogram illustrating the short-period system response to train noise

4-7 WMSO seismogram illustrating lightning spikes on the short-period system

4-8 WMSO seismogram illustrating overlining and a generally noisy condition caused by barometric pressure changes

4-9 WMSO seismogram illustrating artillery generated acoustic signals. No corresponding seismic signals were recorded

4-10 Seismic signal and corresponding acoustics from artillery fire as recorded on the WMSO short-period seismogram

4-11 WMSO seismogram illustrating the seismic signal and acoustics generated by the demolition of outdated ammunition and artillery duds on Fort Sill

4-12 WMSO seismogram illustrating a 2500-pound detonation of TNT on Fort Sill

4-13 WMSO seismogram illustrating an acoustical signal generated by a blast at Richard's Spur Quarry

4-14 WMSO seismogram illustrating the Lg (Sur) phase from a near regional (?) event. The P phase was not recorded

ATLAS OF SIGNALS AND NOISE

1. INTRODUCTION

1.1 AUTHORITY

The data included in this publication were collected under authority contained in Contract AF 33(657)-12007, Project VT/036 dated 1 March 1963. The Air Force Technical Applications Center (AFTAC) has technical supervision of the contract as a part of Project VELA UNIFORM, which is under the overall direction of the Advanced Research Projects Agency (ARPA).

1.2 PURPOSE

This atlas is designed as a guide for those interested in the signals recorded at the Wichita Mountains Seismological Observatory (WMSO). Examples of signals, phases, and noise are included. In many instances, the examples may be considered typical; however, due to the nature of several of the subjects, some of the examples given must be considered atypical. Reference to this atlas should provide assistance to those engaged in routine analysis of WMSO seismograms by illustrating the many different characteristics of signals and noise that appear on the seismograms.

The atlas is published in loose-leaf form so that new data may be readily added as they are encountered.

1.3 ORIENTATION OF INSTRUMENT ARRAYS AT WMSO

Figure 1-1 illustrates the orientation of the arrays and identifies the locations of the individual array elements at the observatory. The short-period horizontal seismometers are located in the walk-in vault with Z6; the three-component broad-band and intermediate-band systems are located in the tank farm; and the three-component long-period system is located in the walk-in vault between Z6 and Z10. All instrument traces are identified and their respective magnifications are shown on the seismograms included in this atlas.

The normalized response characteristics of the WMSO seismographs are shown in figure 1-2.

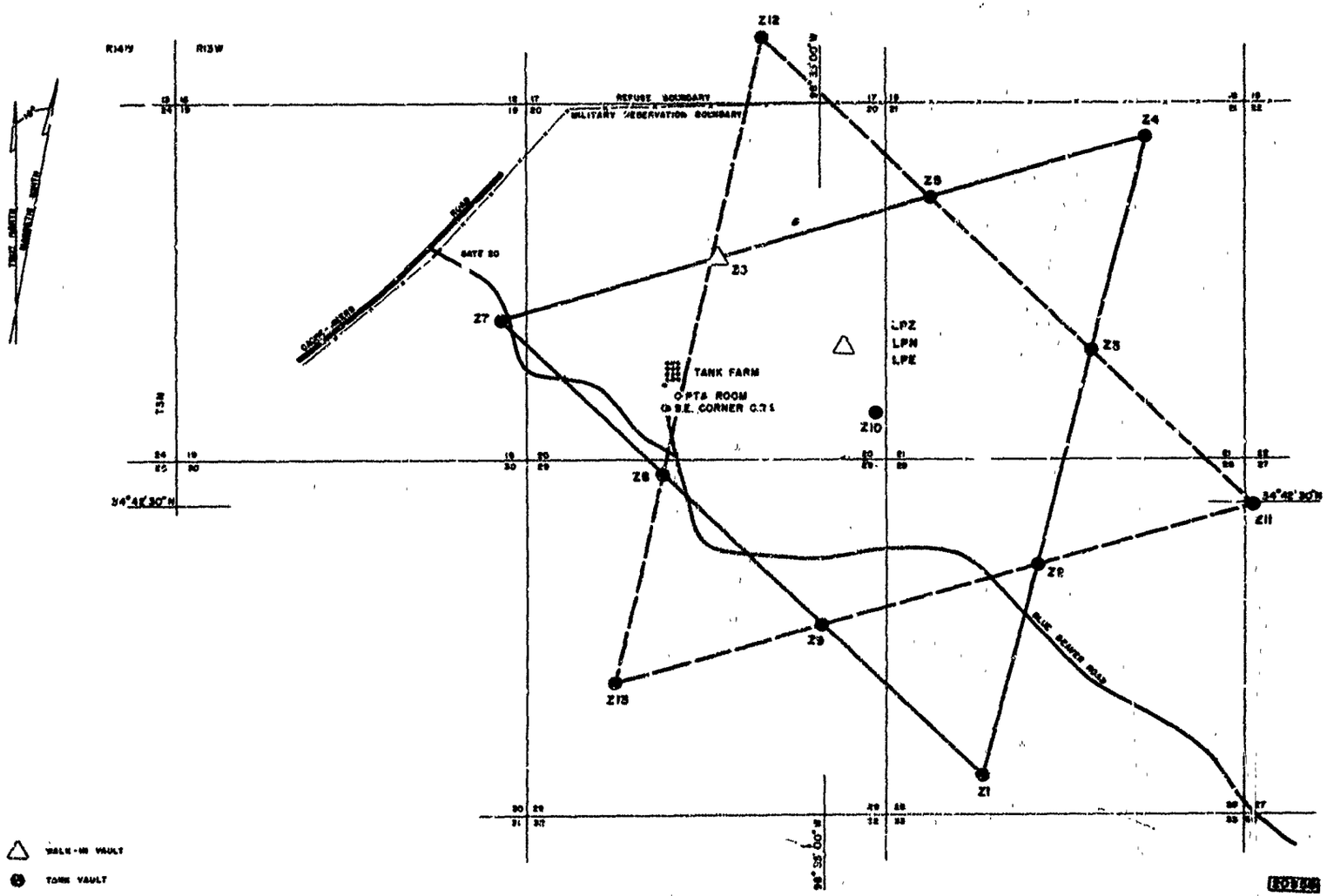

Figure 1-1. Orientation of instrument arrays at WMSO

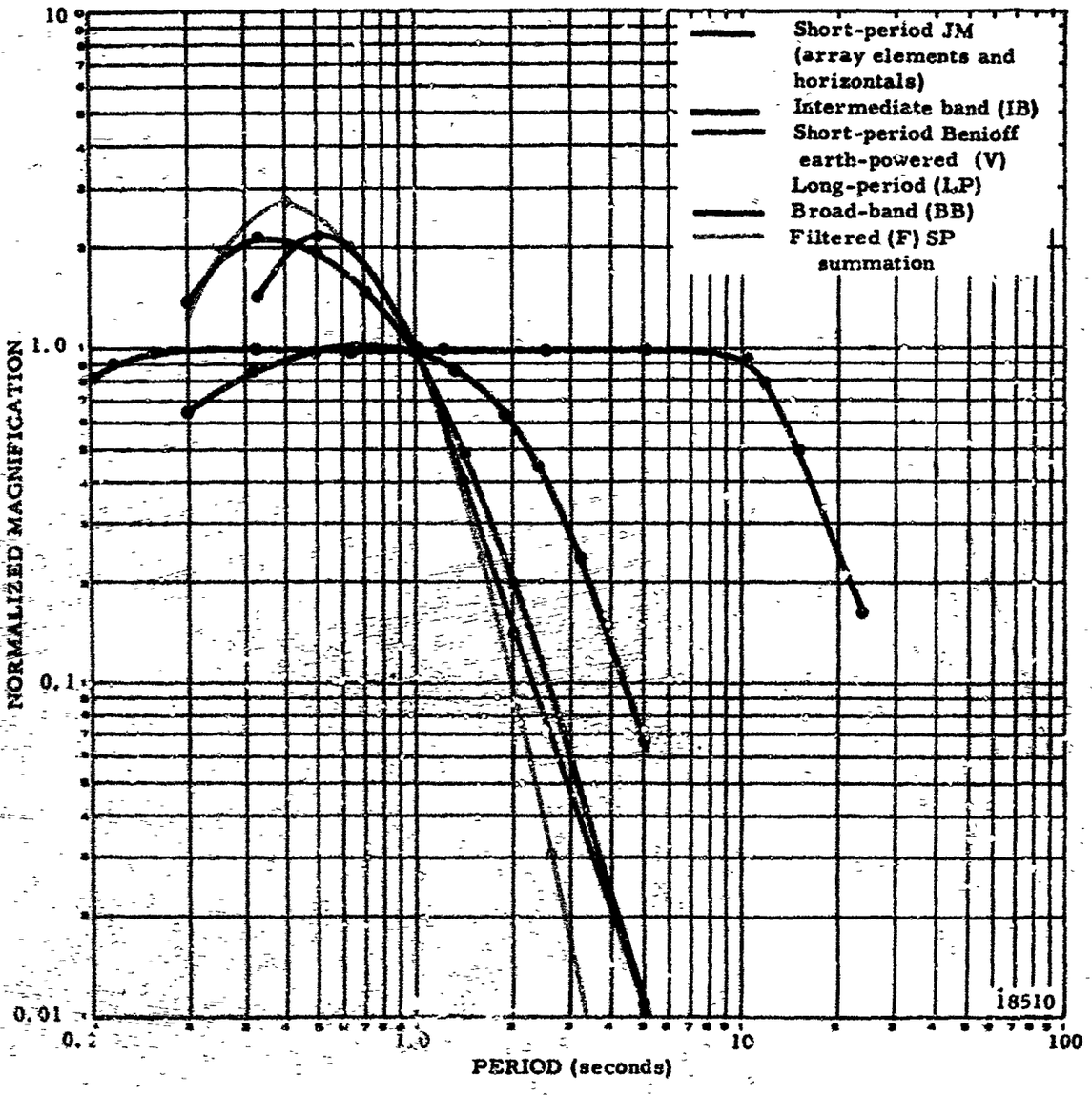

Figure 1-2. Normalized response characteristics of seismographs at WMSO

2. EARTHQUAKE PHASES

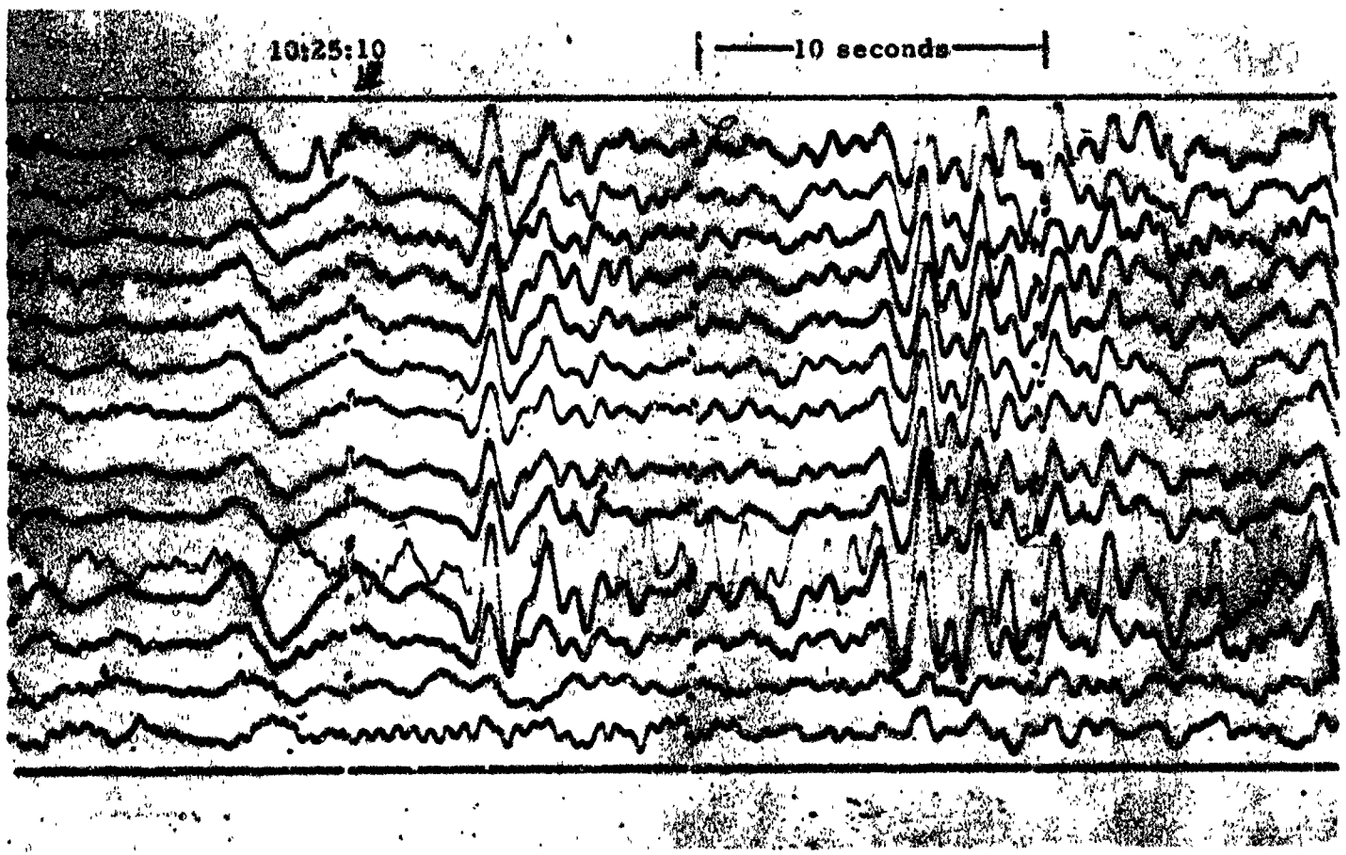

Figure 2-1. WMSO seismogram illustrating P and pP phase arrivals from the Kermadec Islands. Epicentral data: $\Delta \simeq 95^{\circ}$, h ≃ 31 km, azimuth ≃ 241°, magnitude ≃ 5.1 (X10 enlargement of 16-mm film)

WMSO
Run 005
5 Jan 1964
Data Group 311

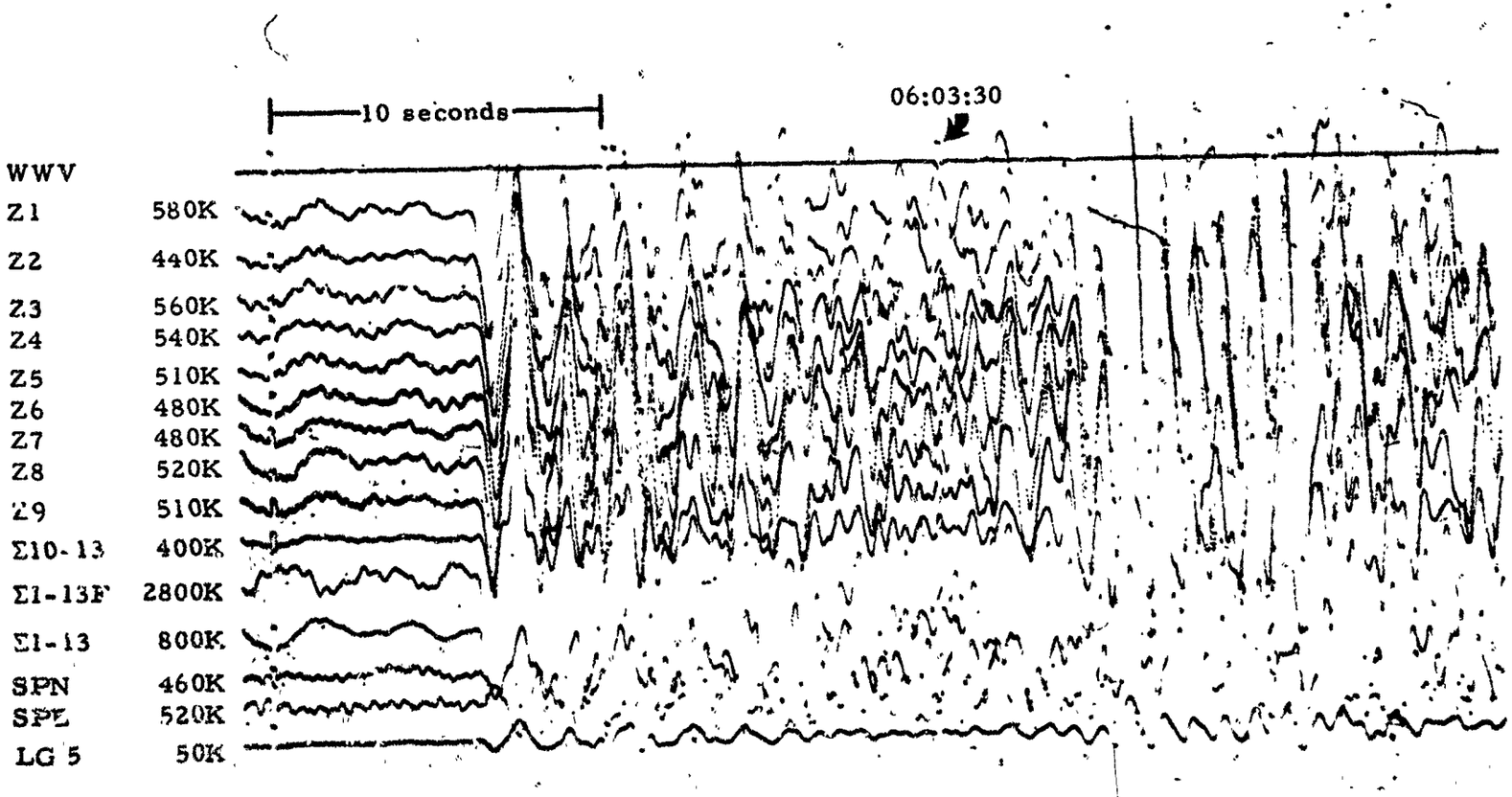

Figure 2-2. WMSO seismogram illustrating P and pP phase arrivals from Central Peru. Epicentral data: $\Delta \simeq 49^{\circ}$, h ≃ 61 km, azimuth ≃ 153°, magnitude ≃ 6.7 (X10 enlargement of 16-mm film)

WMSO
Rum 260
17 Sep 1963

Figure 2-3. P-wave arrival recorded on all systems at WMSO. Epicenter: Kurile Islands, $\Delta \simeq 80^{\circ}$, h $\simeq$ 40 km, azimuth $\simeq 318^{\circ}$, magnitude $\simeq$ 5.5 (X10 enlargement of 16-mm film)

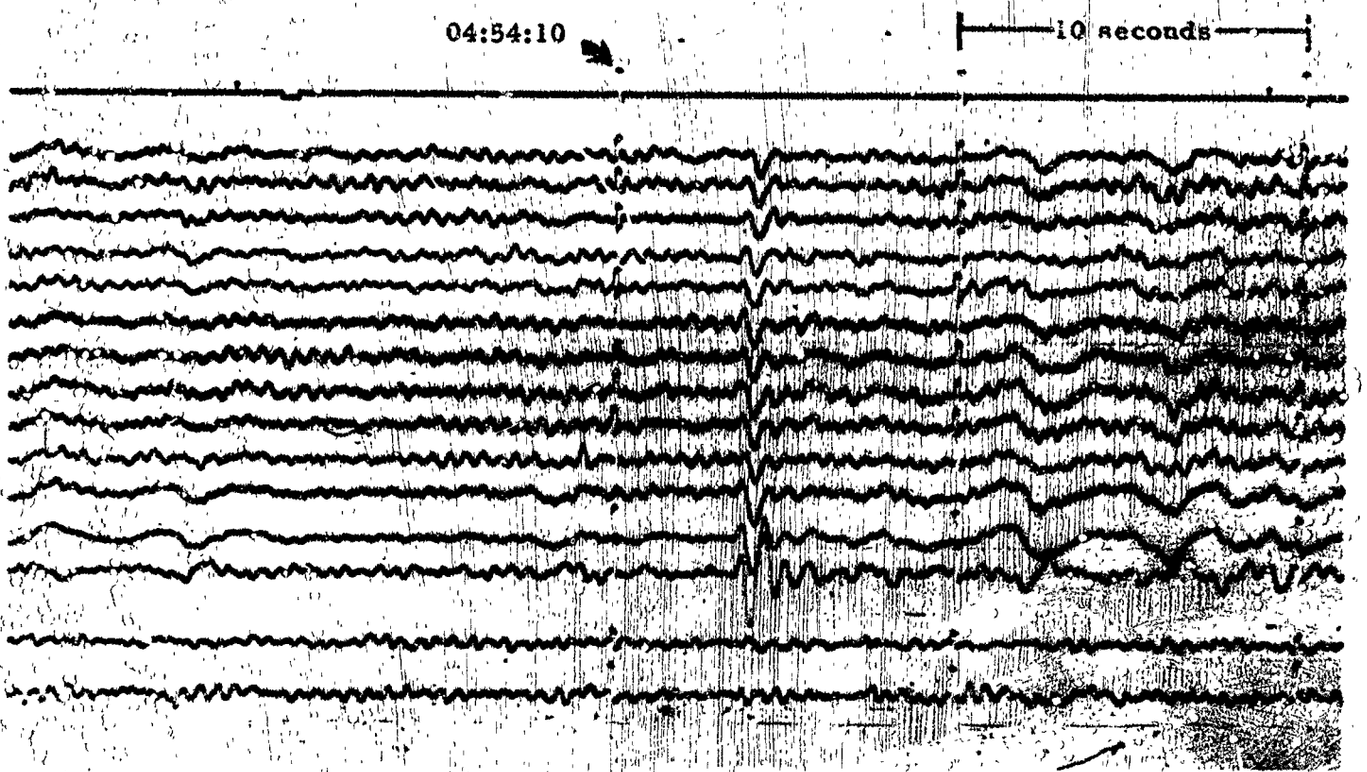

Figure 2-4. WMSO primary short-period seismogram illustrating a "Lonesome P." Epicenter: near the east coast of Kamchatka, $\Delta \simeq 69°$, $h \simeq 33$ km, azimuth $\simeq 321°$, magnitude $\simeq 4.6$ (X10 enlargement of 16-mm film)

WMSO
Run 146
26 May 1963

TX 64-50

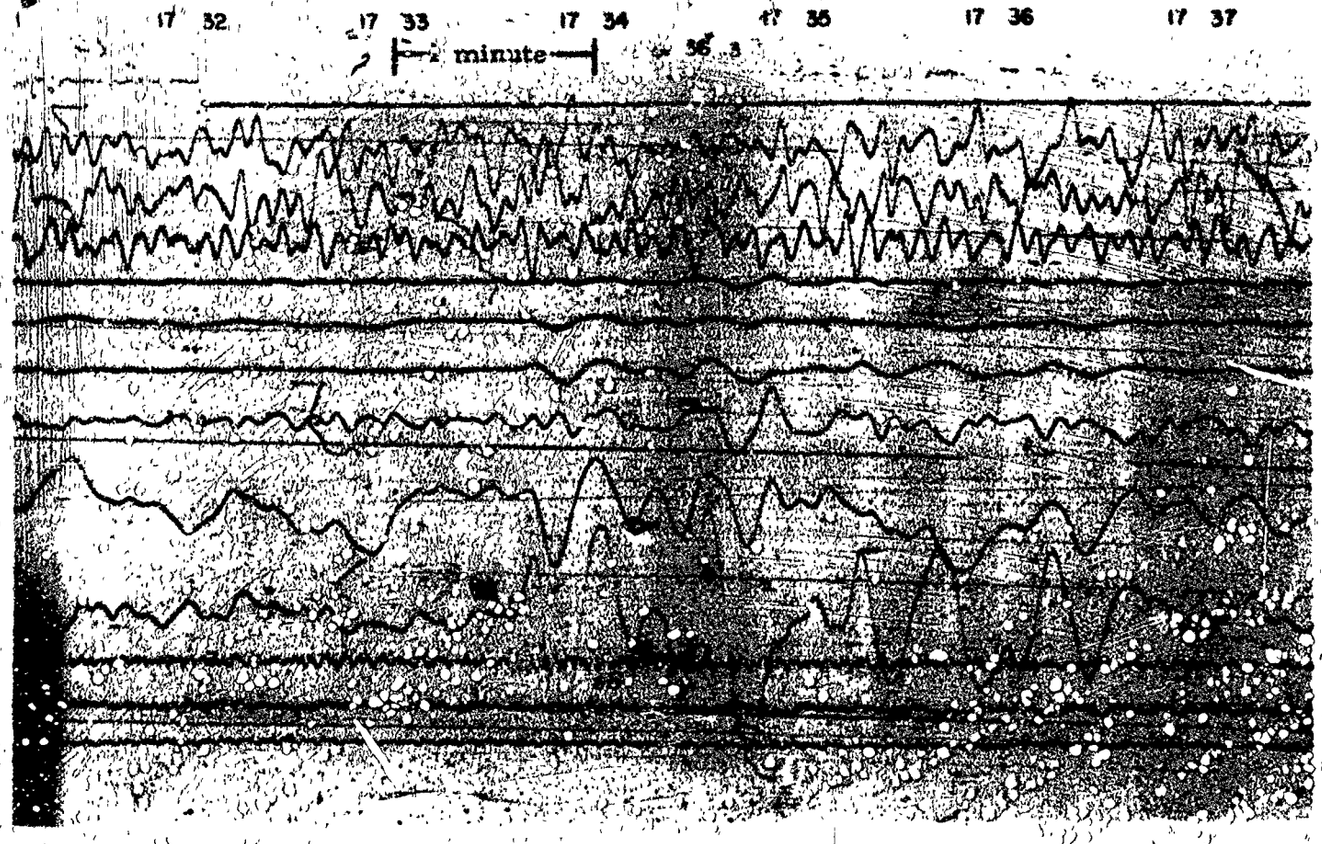

Figure 2-5. WMSO seismogram illustrating S and sP phase arrivals. See figures 2-6 and 2-7 for the corresponding phase arrivals on the short-period system. Epicenter: Northern Chile, $\Delta \simeq 60^{\circ}$, h ≃ 213 km, azimuth ≃ 248°, magnitude ≃ 5.5 (X10 enlargement of 16-mm film)

WMSO
Run 360
29 Dec 1963
Data Group 304

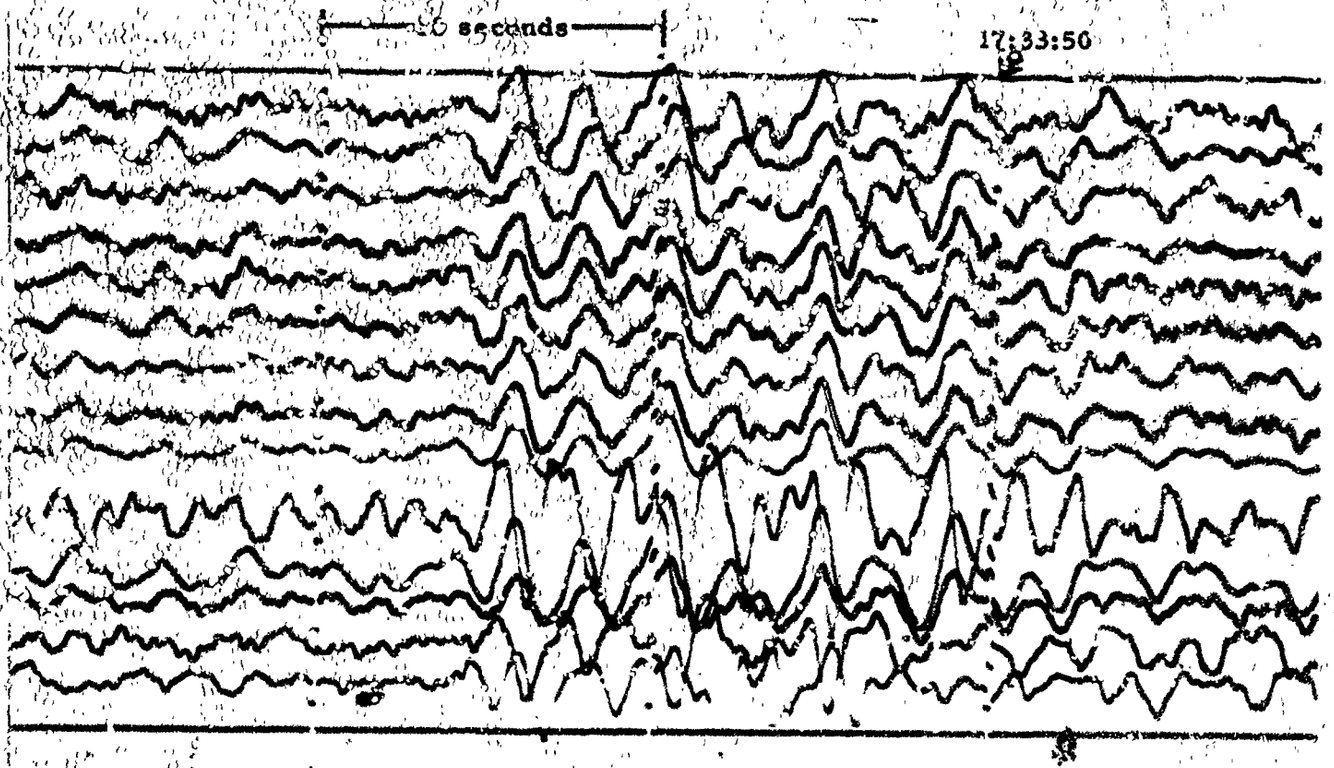

Figure 2-6. WMSO seismogram illustrating an S phase arrival on the short-period system. Epicenter: Northern Chile, $\Delta = 60^{\circ}$, $h = 113$ km, azimuth $= 148^{\circ}$, magnitude $= 5.5$ (X10 enlargement of 16-mm film)

WMSO
Run 333
29 Dec 1963
Data Group 311

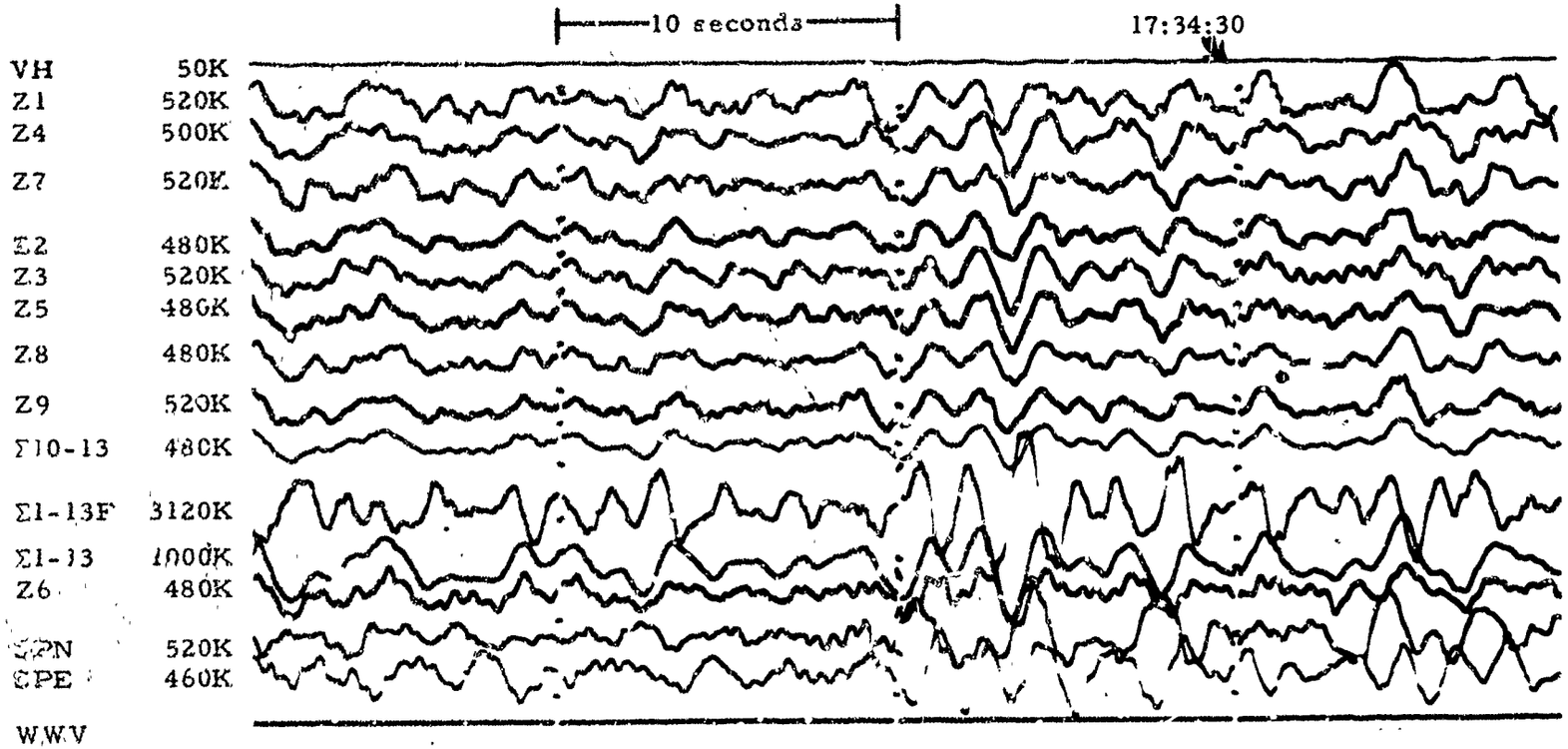

Figure 2-7. WMSO seismogram illustrating an sS phase arrival on the short-period system. Epicenter: Northern Chile, $\Delta \simeq 60^{\circ}$, $h \simeq 113$ km, azimuth $\simeq 148^{\circ}$, magnitude $\simeq 5.5$ (X10 enlargement of 16-mm film)

WMSO
Run 363
29 Dec 1963
Data Group 311

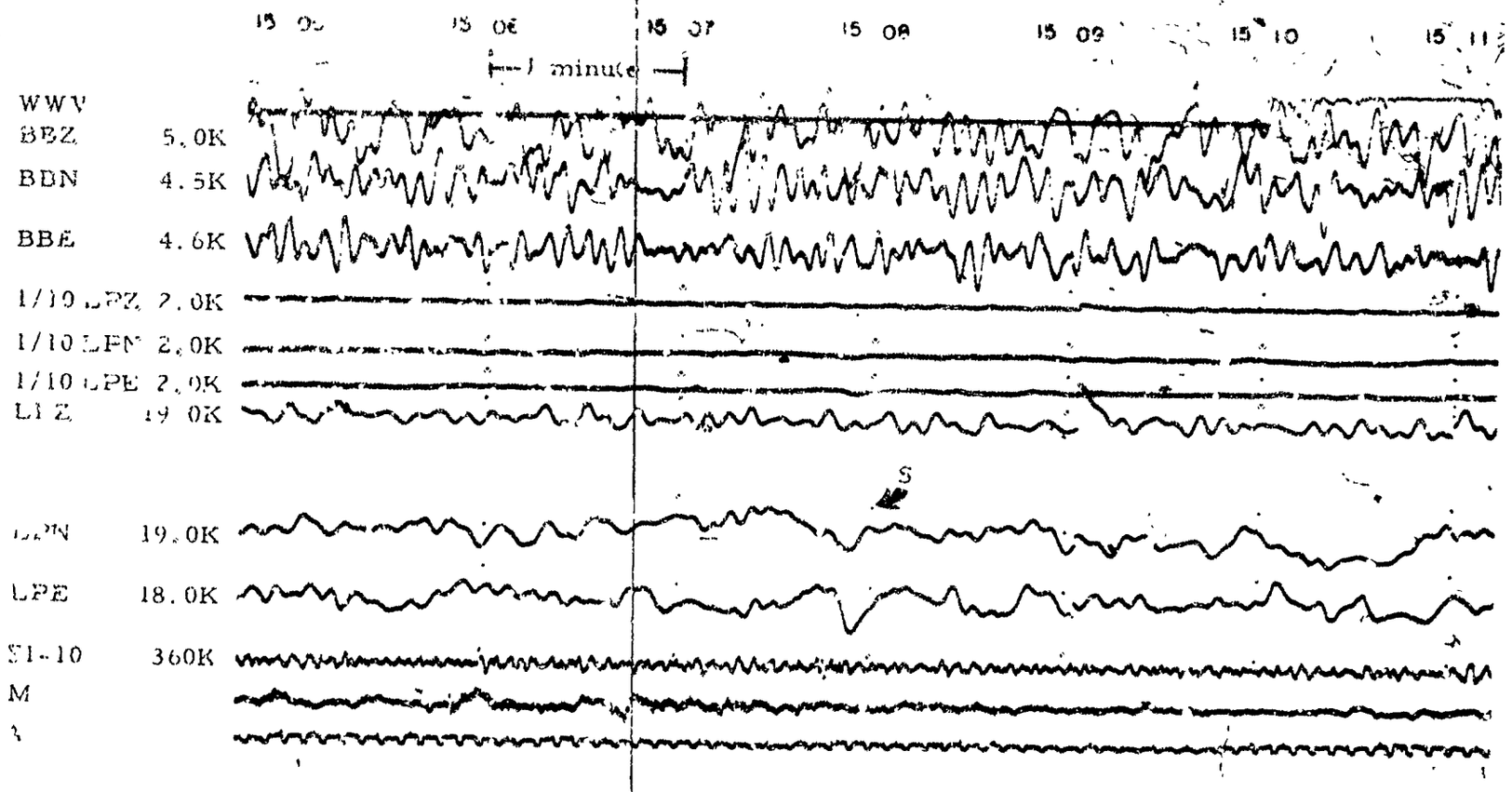

Figure 2-8. WMSO seismogram illustrating an S phase arrival from Western Bolivia. See figure 2-9 for corresponding phase on the short-period system. Epicentral data: $\Delta \simeq 60^{\circ}$, $h \simeq 79$ km, azimuth $\simeq 147^{\circ}$, magnitude $\simeq 5.3$ (X10 enlargement of 16-mm film)

WMSO
Run 344
10 Dec 1963
Data Group 304

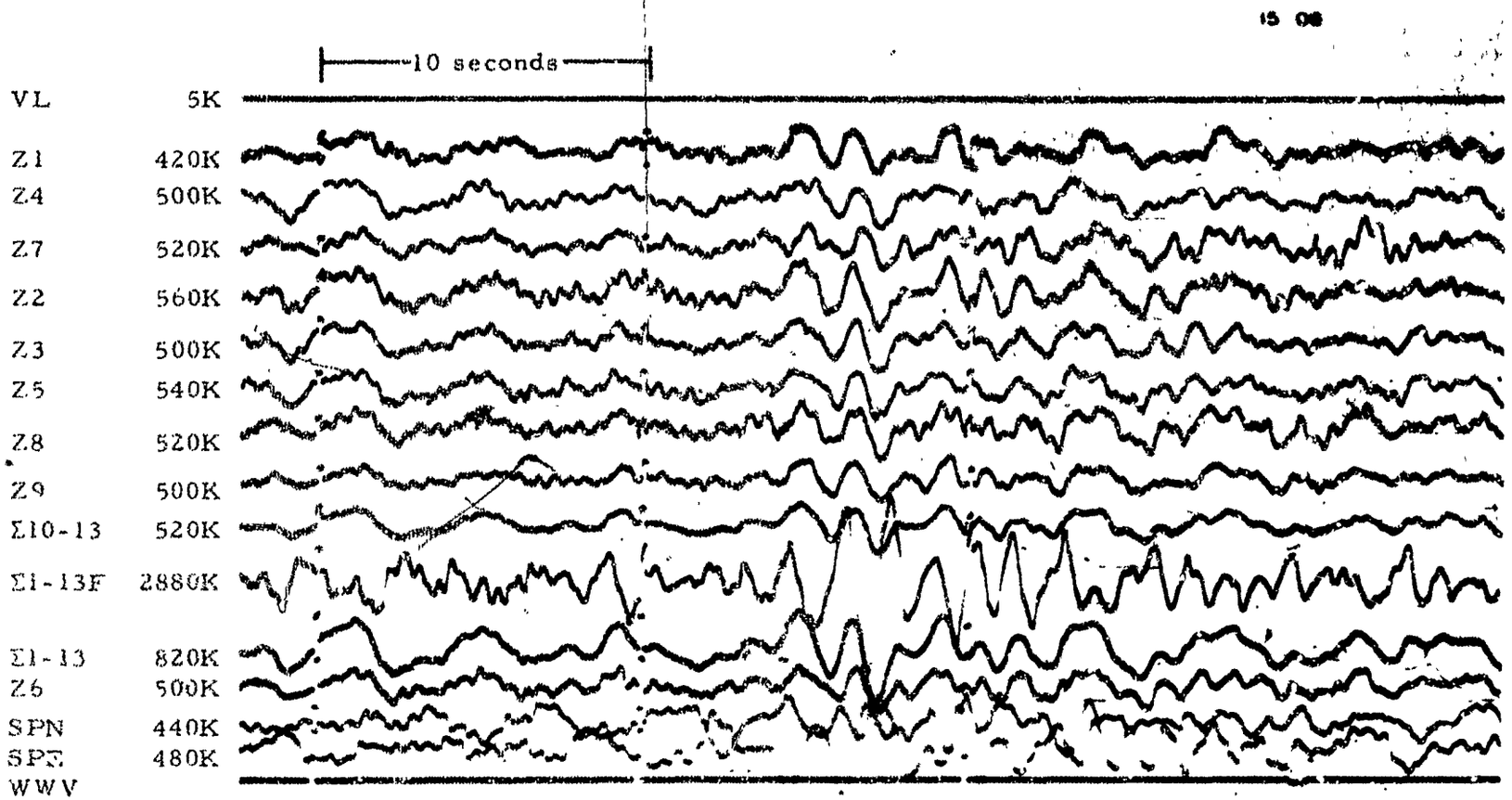

Figure 2-9. WMSO seismogram illustrating an S phase arrival from Western Bolivia.
Epicentral data: $\Delta \simeq 60^{\circ}$, h ≃ 79 km, azimuth ≃ 147°, magnitude ≃ 5.3
(X10 enlargement of 16-mm film)

WMSO
Run 344
10 Dec 1963
Data Group 311

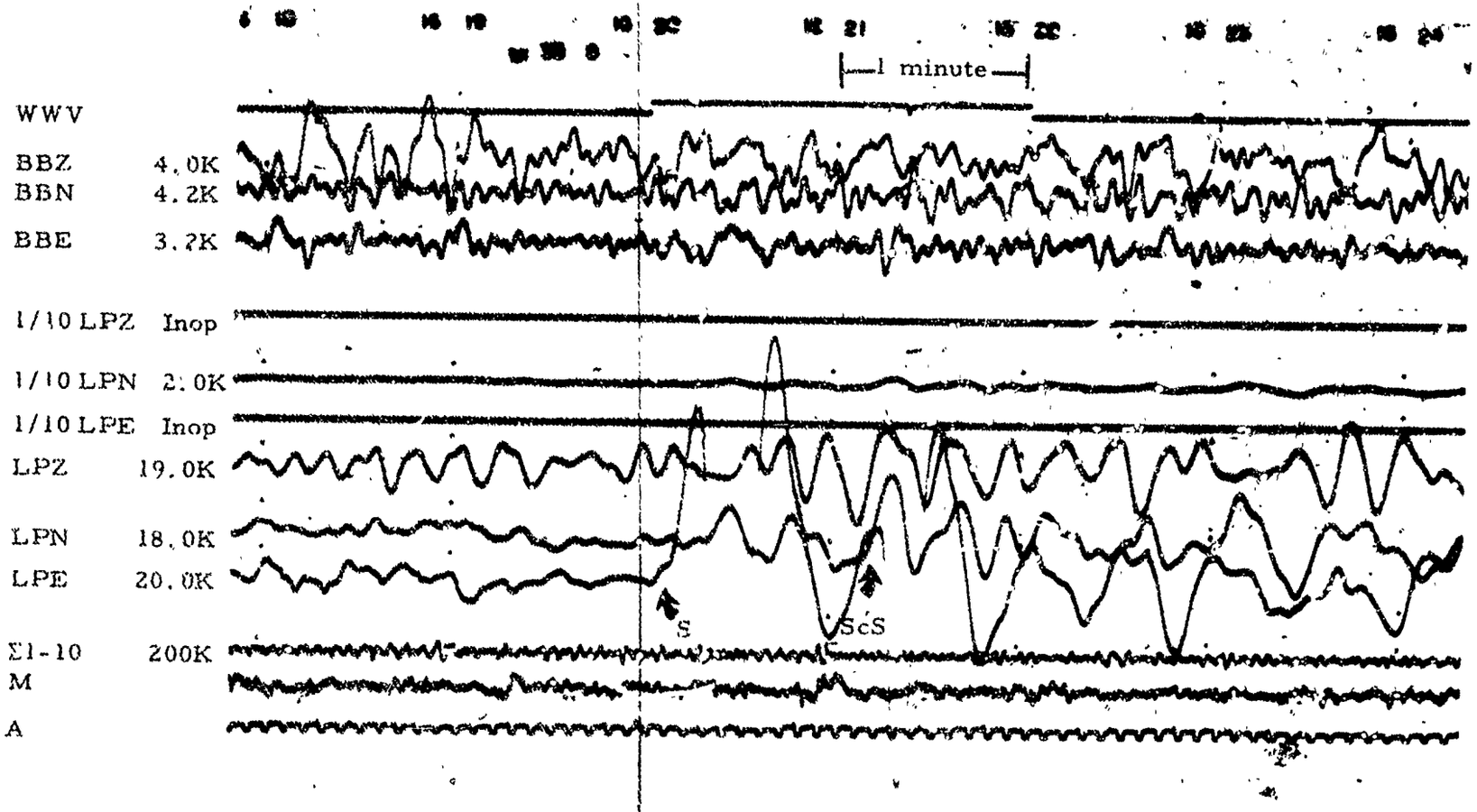

Figure 2-10. WMSO seismogram illustrating S and ScS phase arrivals from the Easter Islands region. Epicentral data: $\Delta \simeq 70^{\circ}$, h ≃ 33 km azimuth ≃ 18°, magnitude ≃ 4.6 (×10 enlargement of 16-mm film)

WMSO
Run 338
4 Dec 1963
Data Group 304

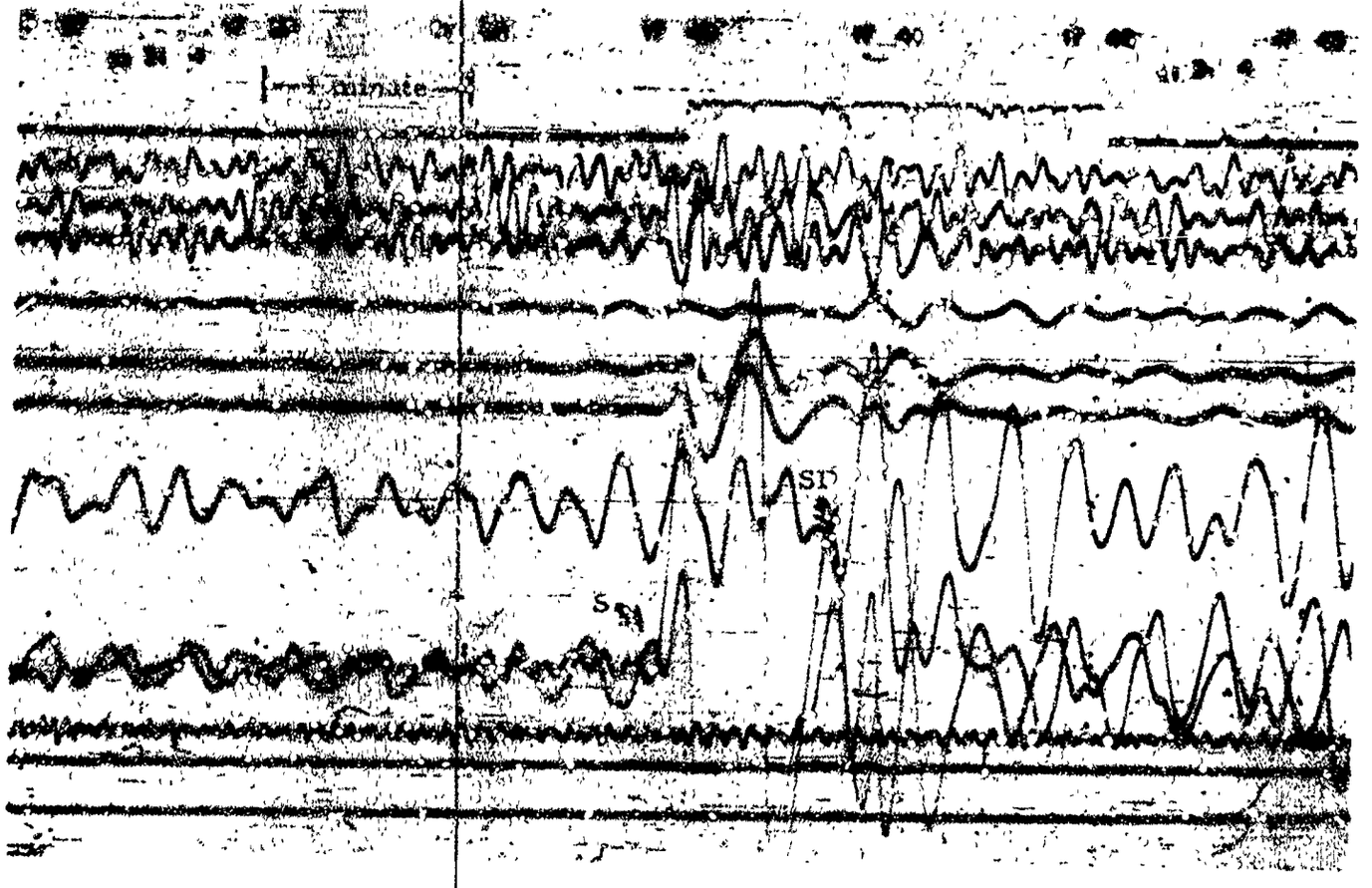

Figure 2-11. WMSO seismogram illustrating S and SP phase arrivals from the Kurile Islands. Epicentral data: $\Delta \simeq 80^{\circ}$, h ≃ 40 km, azimuth ≃ 318°, magnitude ≃ 5.5 (X10 enlargement of 16-mm film)

WMSO
Run 314
10 Nov 1963
Data Group 304

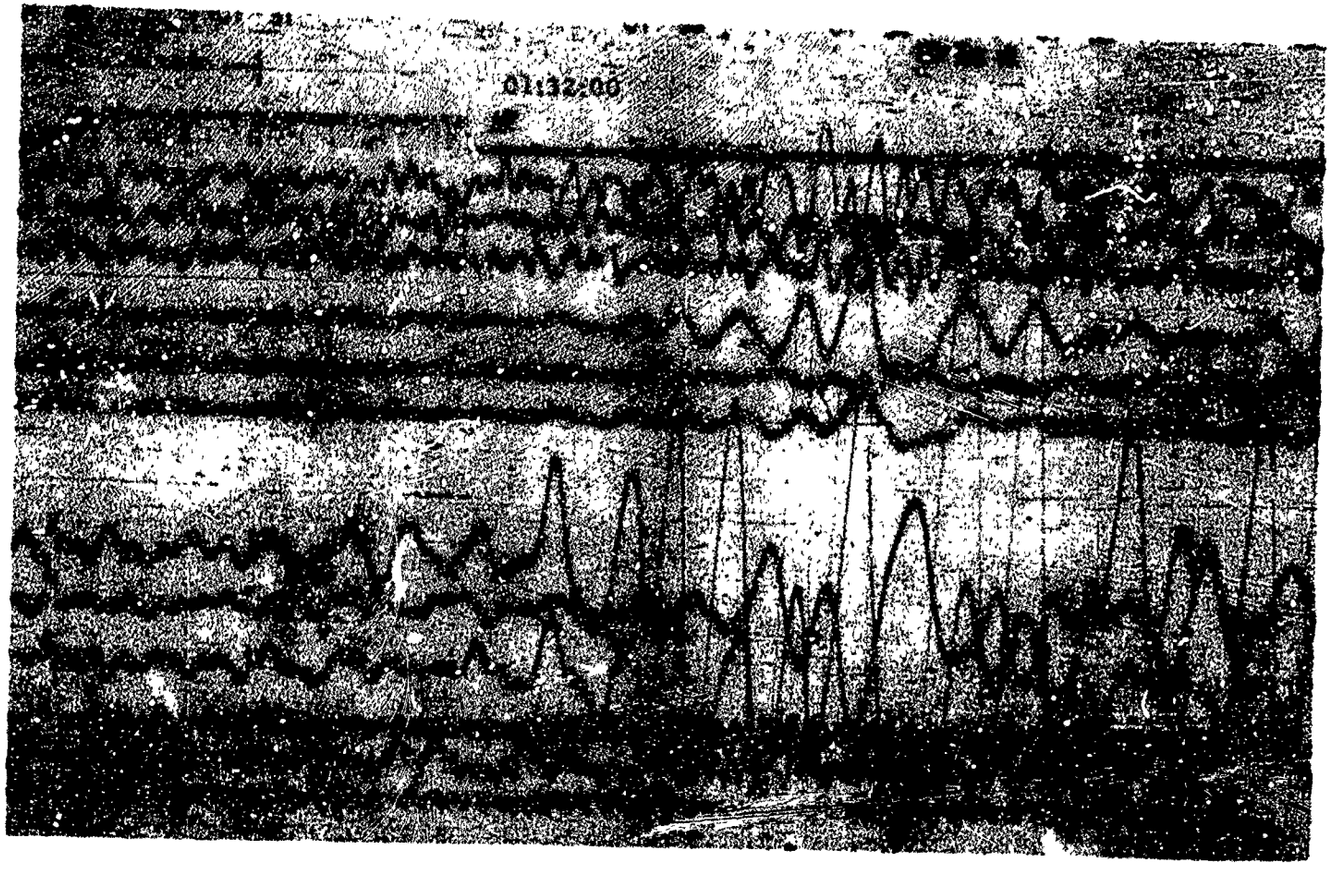

Figure 2-12. WMSO seismogram illustrating a PP phase arrival from the New Hebrides Islands. See figure 2-13 for the corresponding phase on the short-period system. Epicentral data: $\Delta \simeq 102^{\circ}$, h ≃ 154 km, azimuth ≃ 260°, magnitude ≃ 5.8 (X10 enlargement of 16-mm film)

WMSO
Run 308
4 Nov 1963
Data Group 304

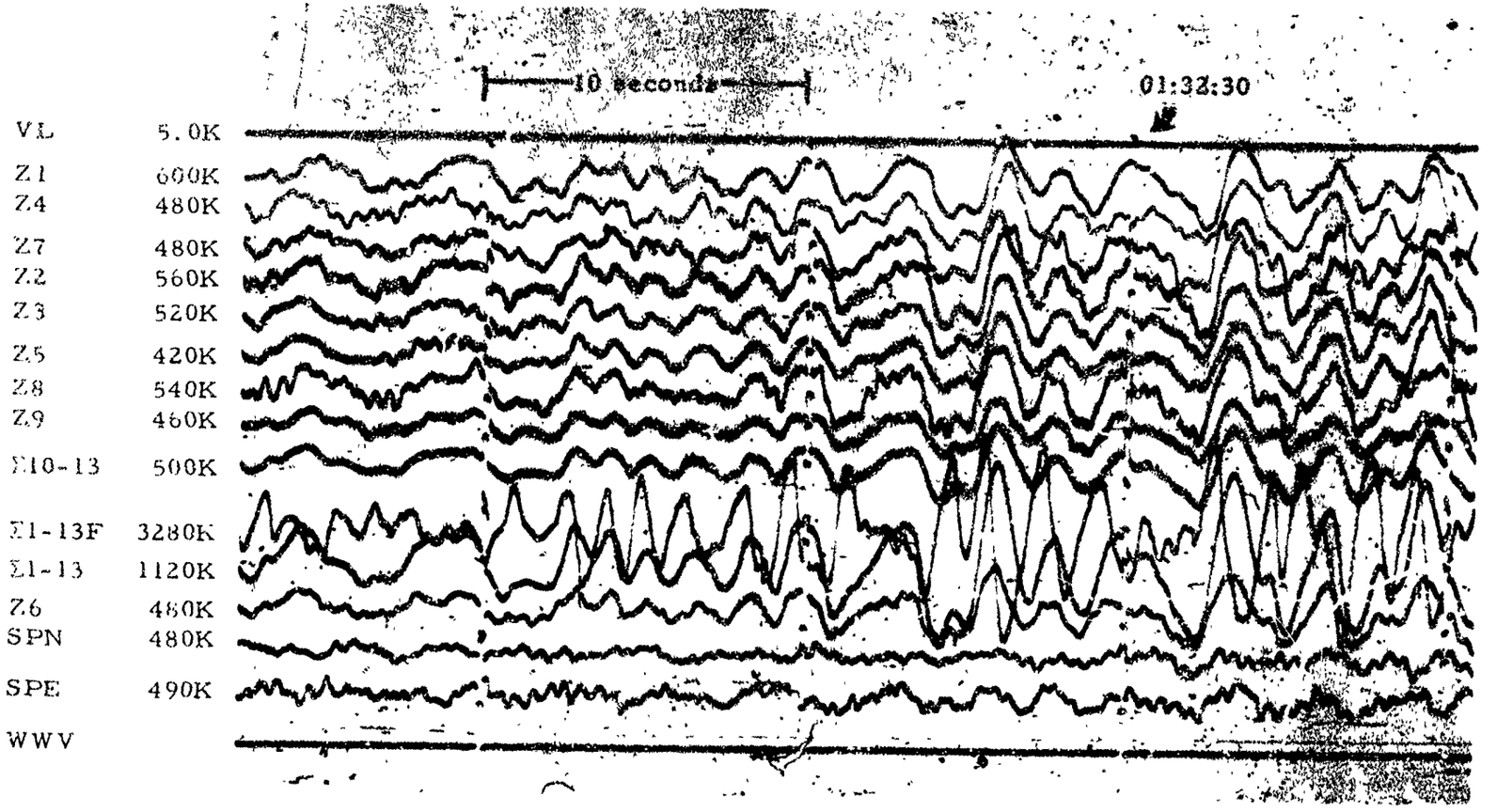

Figure 2-13. WMSO primary short-period seismogram illustrating a PP phase from the New Hebrides Islands. Epicentral data: $\Delta \simeq 102^{\circ}$, h ≃ 154 km, azimuth ≃ 260°, magnitude ≃ 5.8 (X10 enlargement of 16-mm film)

WMSO
Run 308
4 Nov 1963
Data Group 302

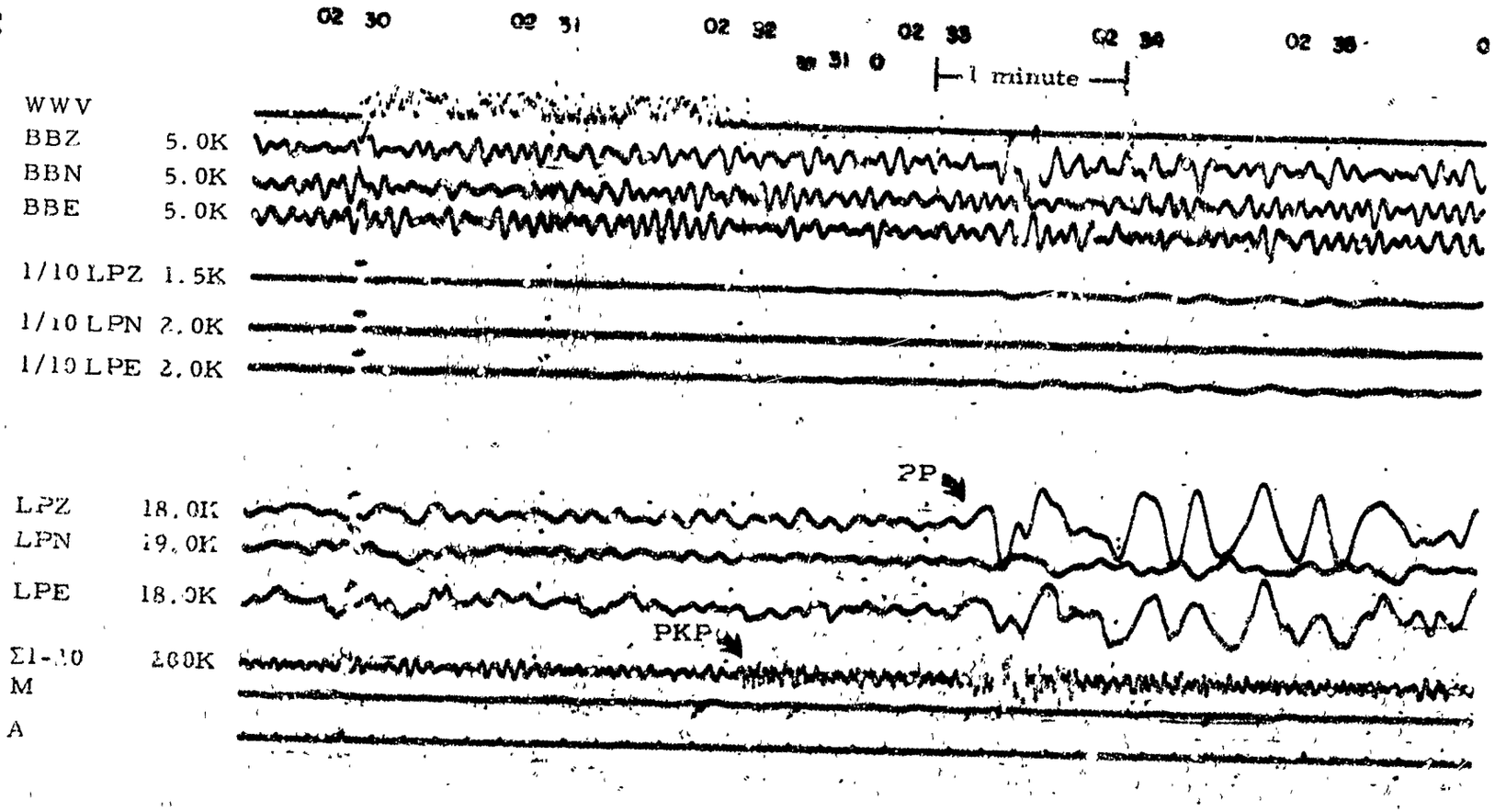

Figure 2-14. WMSO seismogram illustrating a PP phase arrival from Western New Guinea. See figure 2-15 for the corresponding phase on the short-period system. Epicentral data: $\Delta \approx 118^{\circ}$, $h \approx 33$ km, azimuth $\approx 288^{\circ}$, magnitude ≈ 5.7 (×10 enlargement of 16-mm film)

WMSO
Run 310
6 Nov 1963
Data Group 304

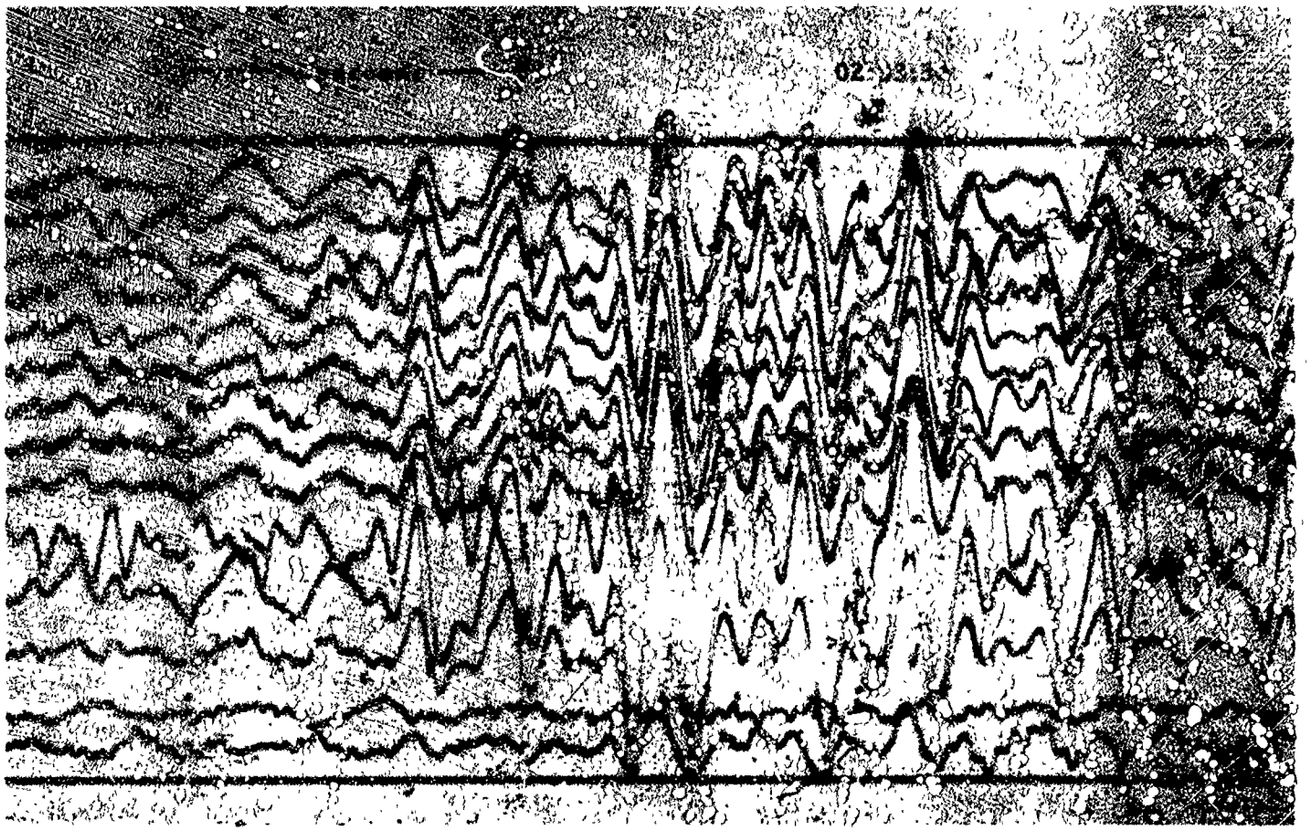

VL	5.0K
Z1	500K
Z4	490K
Z7	500K
Z2	520K
Z3	520K
Z5	480K
Z8	480K
Z9	580K
Σ10-13	500K
Σ1-13F	2720K
Σ1-13	1080K
Z6	490K
SPN	440K
SPE	440K
WWV	

Figure 2-15. WMSO seismogram illustrating a PP phase arrival from Western New Guinea. Epicentral data: $\Delta \simeq 118^{\circ}$, h ≃ 33 km, azimuth ≃ 288°, magnitude ≃ 5.7 (X10 enlargement of 10-mm film)

WMSO
Run 310
6 Nov 1963
Data Group 302

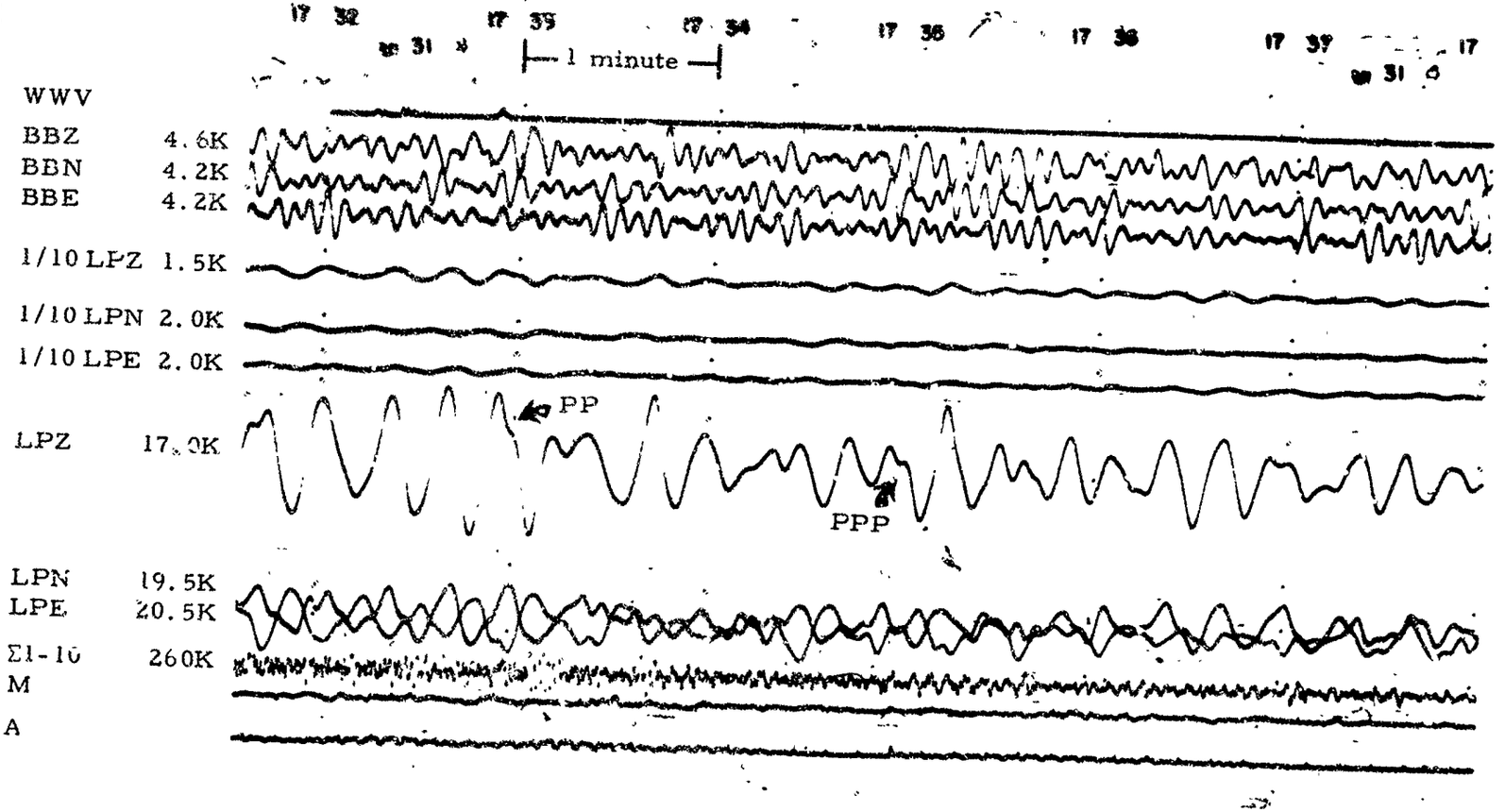

Figure 2-16. WMSO seismogram illustrating PP and PPP phases from the Kurile Islands. Epicentral data: $\Delta \simeq 80^{\circ}$, $h \simeq 40$ km, azimuth $\simeq 318^{\circ}$, magnitude $\simeq 5.5$ (×10 enlargement of 16-mm film)

WMSO
Run 314
10 Nov 1963
Data Group 304

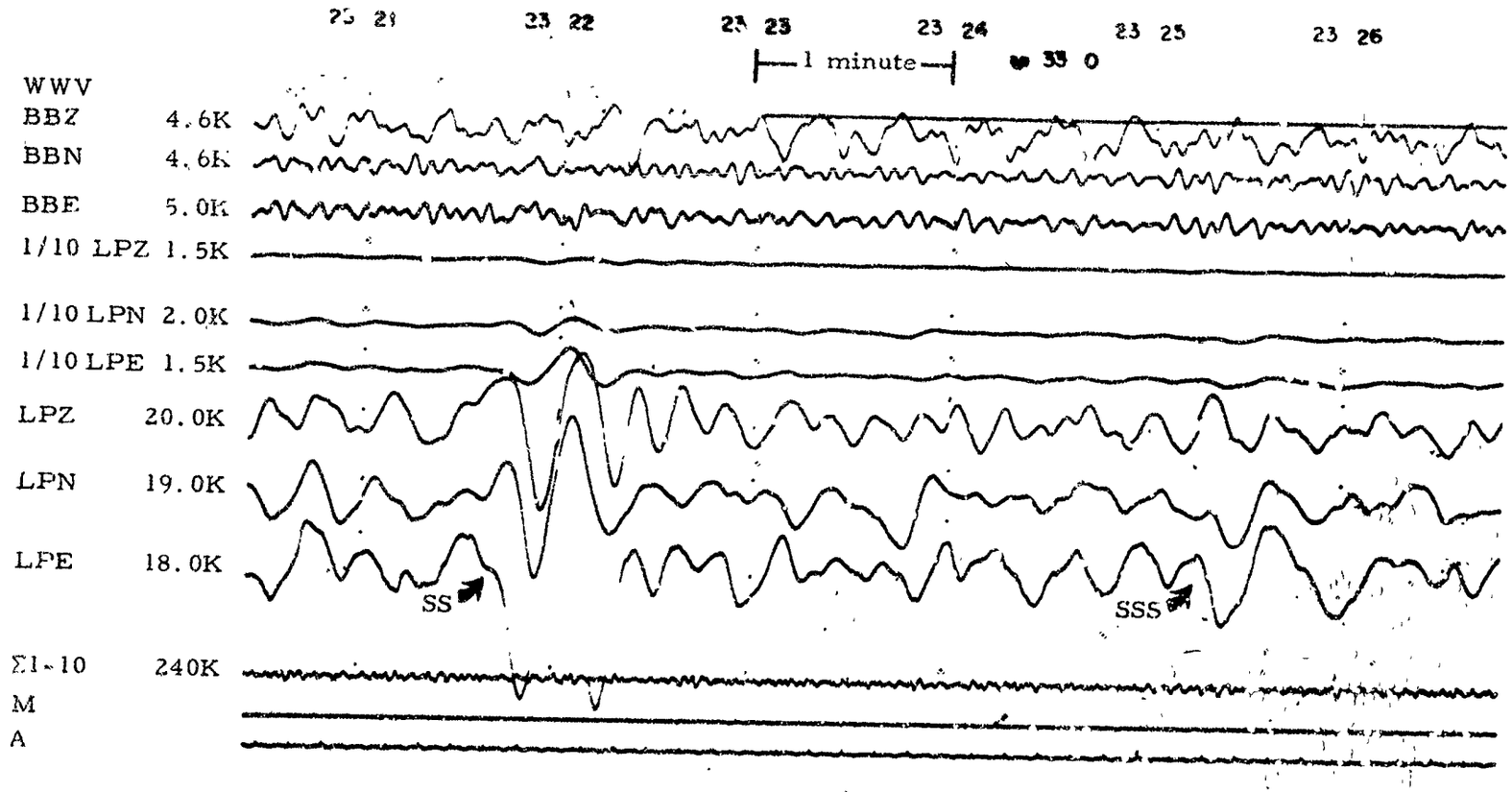

Figure 2-17. WMSO seismogram illustrating SS and SSS phases from the Fiji Islands region. Epicentral data: $\Delta \simeq 96^{\circ}$, h ≃ 33 km, azimuth ≃ 254°, magnitude ≃ 5.3 (X10 enlargement of 16-mm film)

WMSO
Run 330
26 Nov 1963
Data Group 304

WWV
Z1 540K
Z2 470K
Z3 480K
Z4 500K
Z5 530K
Z6 520K
Z7 510K
Z8 530K
Z9 570K
Z10-13 540K
Z1-10F 3200K
Z1-13 1760K
SPA 550K
SPE 530K
LG 5 50K

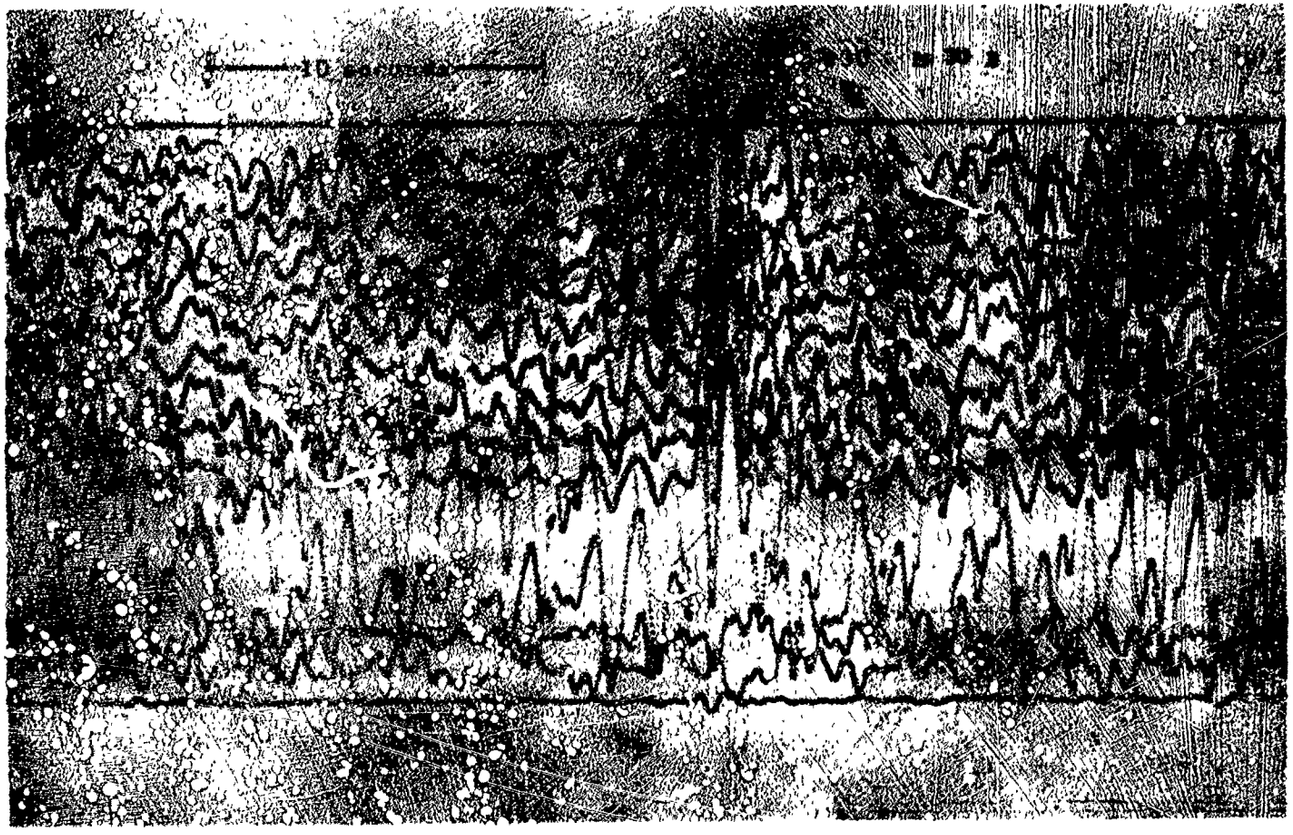

WMSO
Run 393
30 Oct 1963

Figure 2-18. WMSO seismogram illustrating a PcP phase arrival. Epicenter: Northern Peru, $\Delta = 44^{\circ}$, h = 20 km, azimuth = 149°, magnitude = 5.3 (X10 enlargement of 16-mm film)

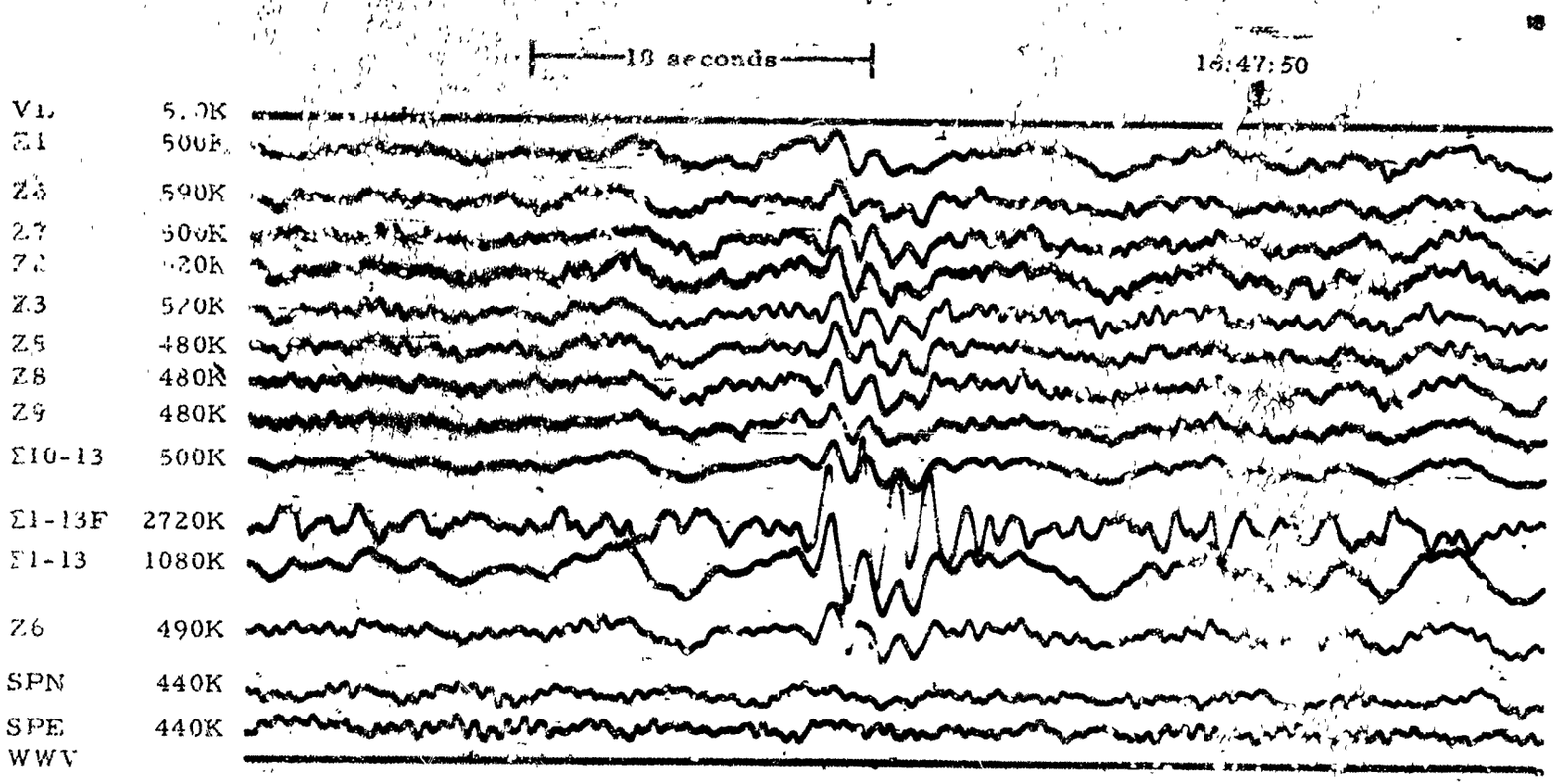

Figure 2-19. WMSO seismogram illustrating an ScP phase arrival from the Peru-Bolivia border. Epicentral data: $\Delta \simeq 58^{\circ}$, h ≃ 174 km, azimuth ≃ 147°, magnitude ≃ 4.7 (X10 enlargement of 16-mm film)

WMSO
Run 310
6 Nov 1963
Data Group 302

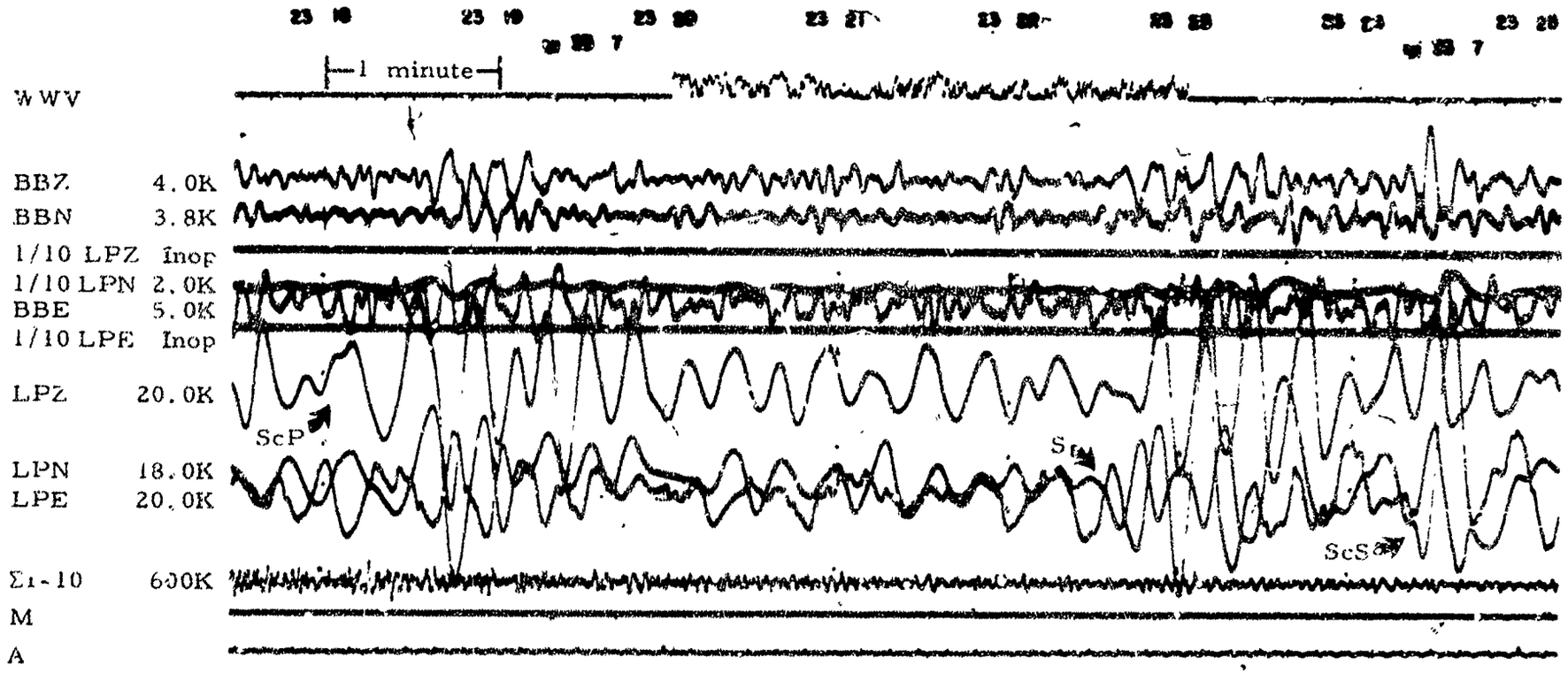

Figure 2-20. WMSO seismogram illustrating ScP, S, and ScS phase arrivals from Northern Chile. Epicentral data: $\Delta \approx 63^{\circ}$, h ≈ 18 km, azimuth ≈ 150°, magnitude ≈ 6.1 (X10 enlargement of 16-mm film)

WMSO
Run 337
3 Dec 1963
Data Group 304

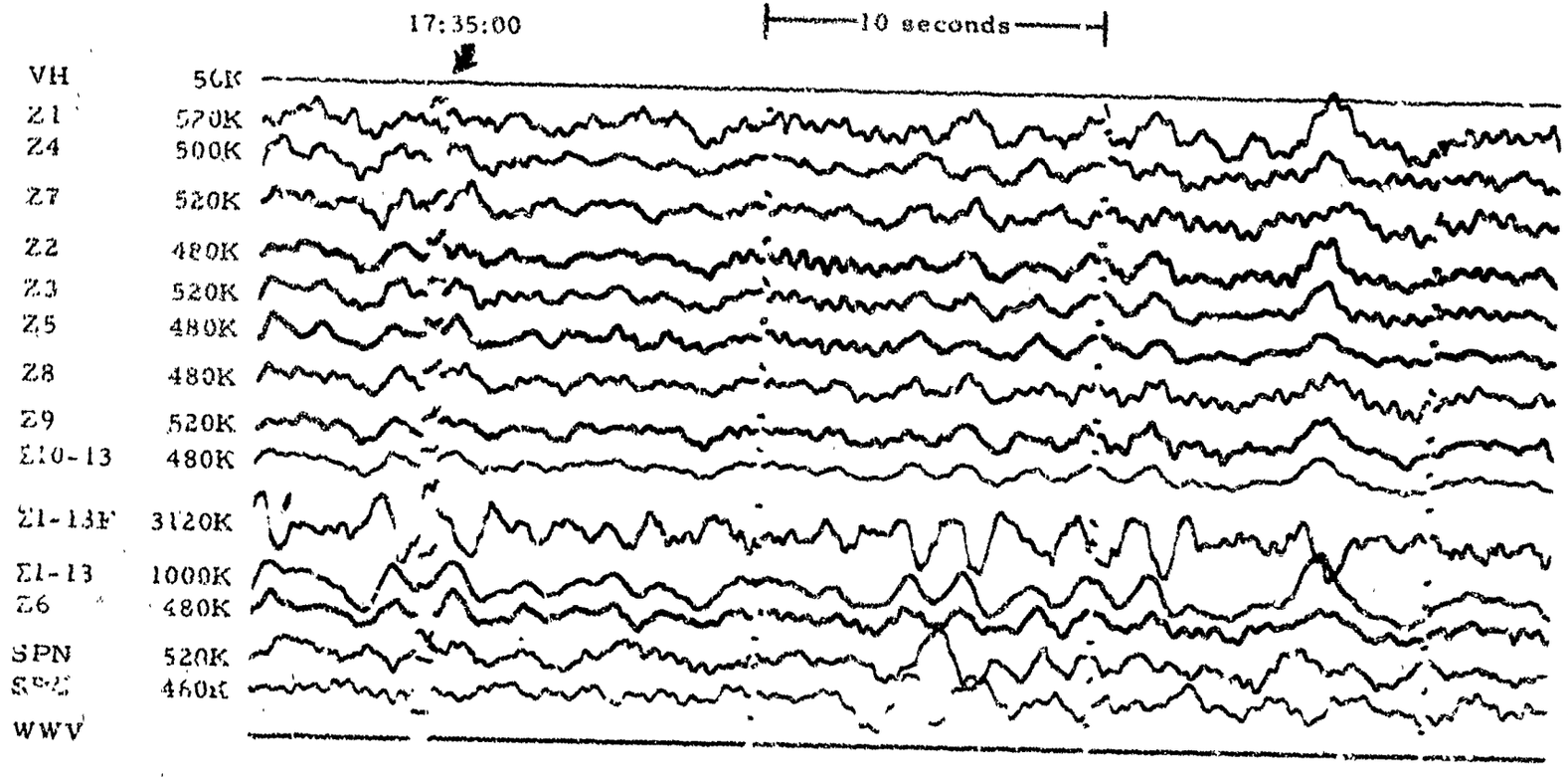

Figure 2-21. ScS as recorded on the WMSO short-period seismogram. Epicenter: Northern Chile, $\Delta \simeq 60^{\circ}$, h ≃ 113 km, azimuth ≃ 148°, magnitude ≃ 5.5
(X10 enlargement of 16-mm film)

WMSO
Rec. 363
29 Dec 1963
Data Group 311

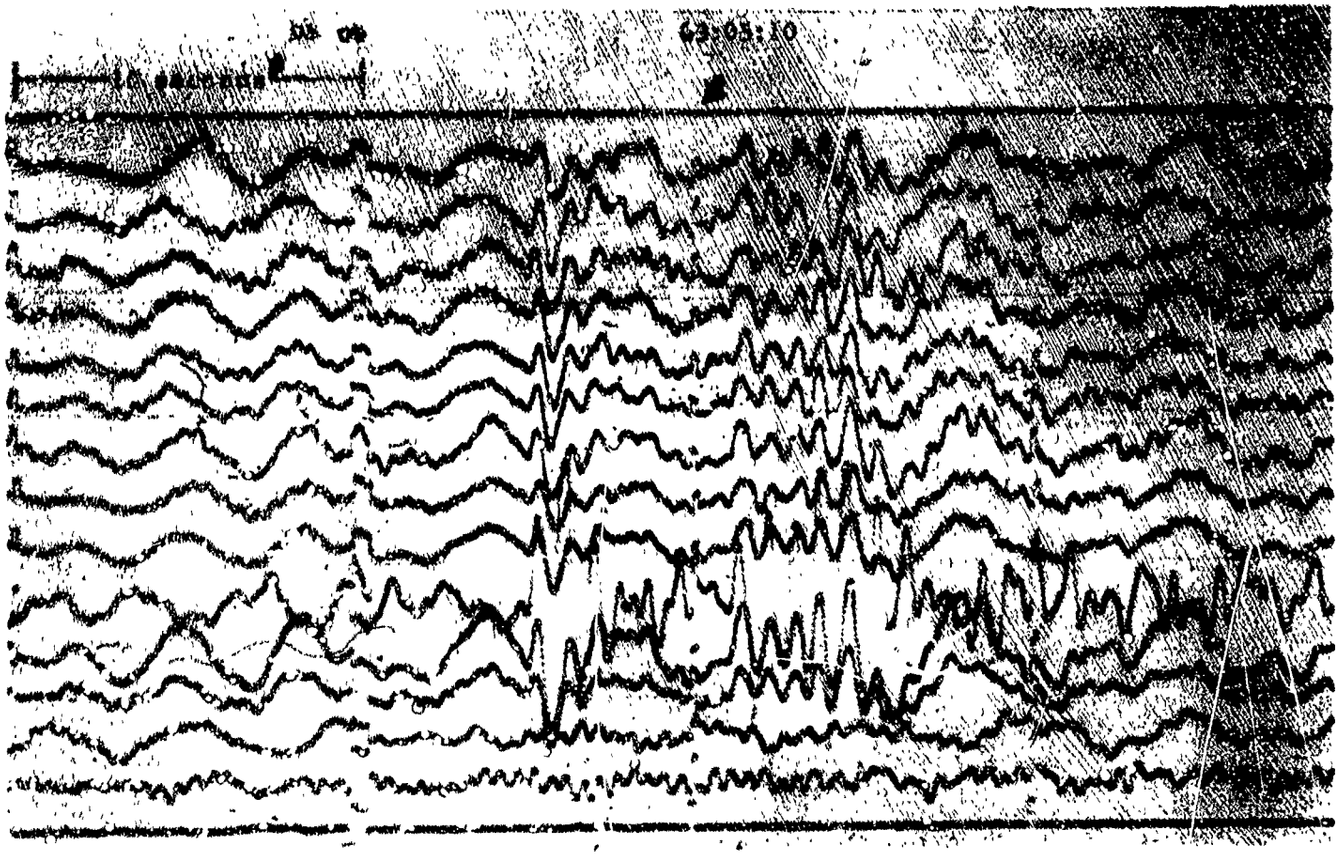

Figure 2-22. WMSO seismogram illustrating PKP_1 and PKP_2 phase arrivals. Epicenter: near the west coast of Sumatra, $\Delta \simeq 144^{\circ}$, h ≃ 55 km, azimuth ≃ 317°, magnitude ≃ 5.0 (X10 enlargement of 10-min film)

WMSO
Run 350
16 Dec 1953
Data Group 311

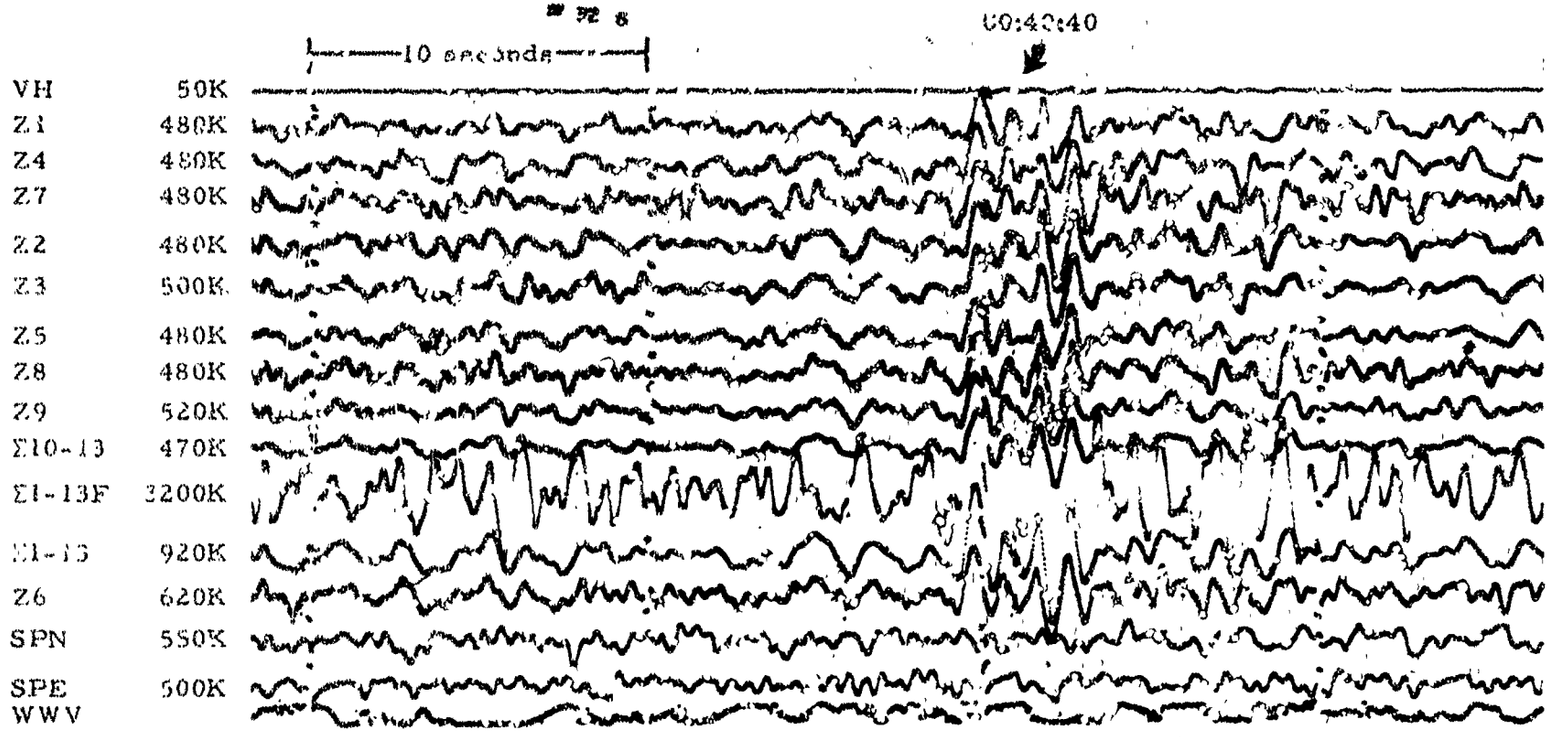

Figure 2-23. WMSO seismogram illustrating an SKP phase arrival. Epicenter: near north coast of Java, Δ ≈ 142°, h ≈ 333 km, azimuth ≈ 314°, magnitude ≈ 5.1 (X10 enlargement of 16-mm film)

WMSO
Run 326
22 Nov 1963
Data Group 311

WWV	
Z1	510K
Z2	470K
Z3	520K
Z4	450K
Z5	500K
Z6	540K
Z7	500K
Z8	480K
Z9	480K
Z10	500K
Σ1, 3, 5, 6	520K
Σ1-10	1080K
Σ1-10F	2000K
SFN	500K
SPE	500K

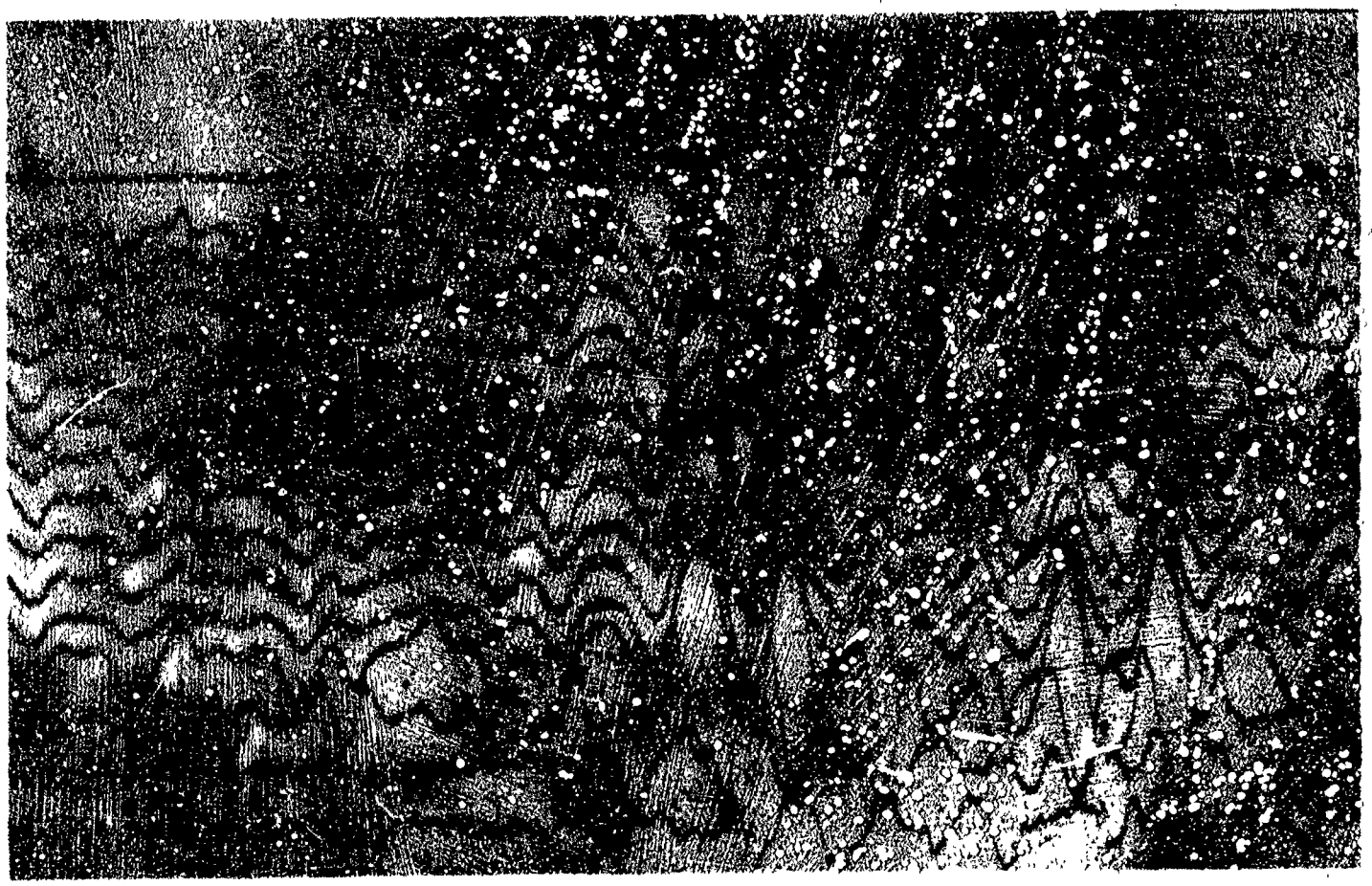

WMSO
Run 161
10 June 1963

Figure 2-24. WMSO seismogram illustrating SKP_1 and SKP_2 phase arrivals. Epicenter: Western Macquarie Islands, $\Delta \approx 132^{\circ}$, $h \approx 33$ km, azimuth $\approx 224^{\circ}$, magnitude ≈ 6.1 (X10 enlargement of 16-mm film)

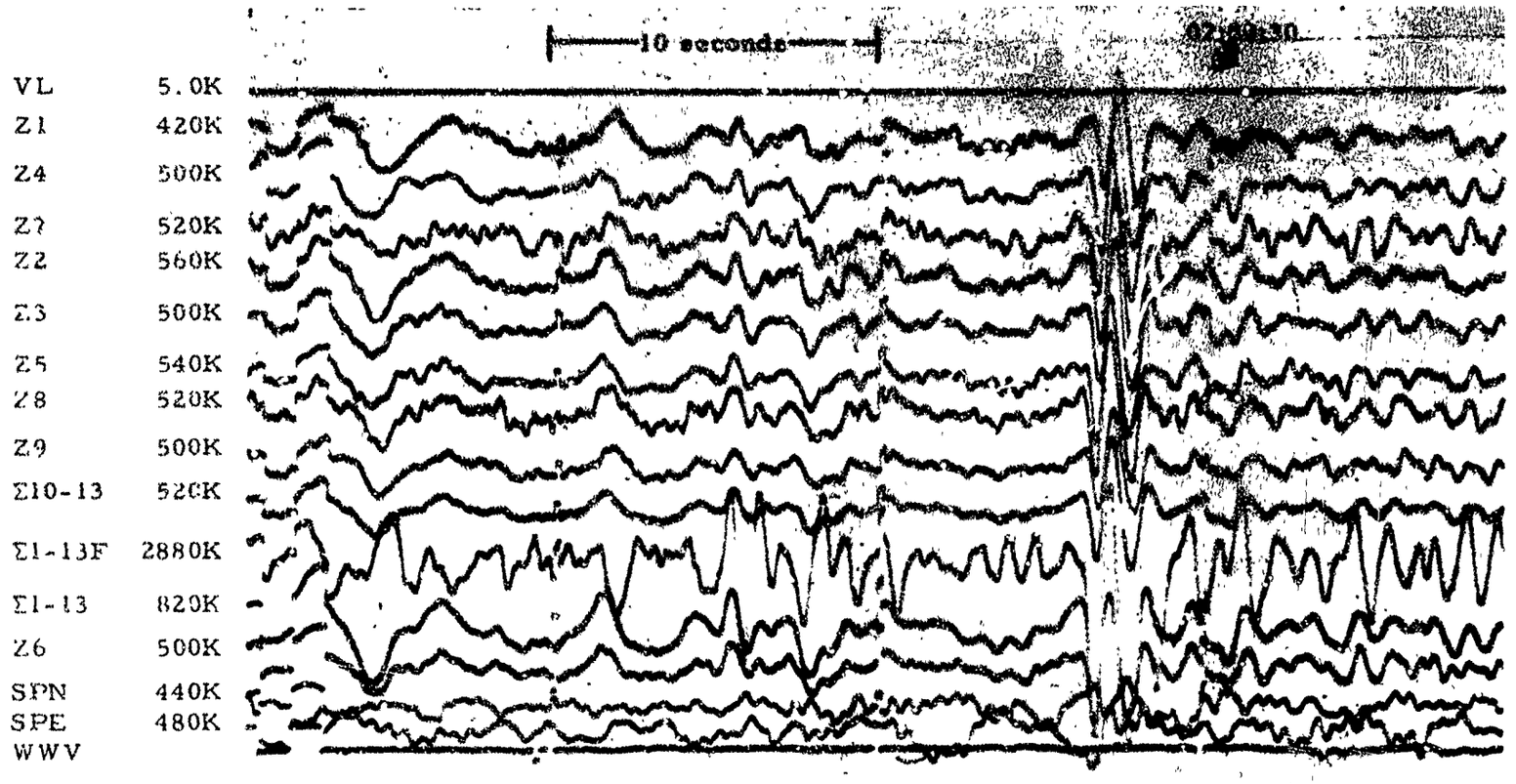

Figure 2-25. WMSO primary short-period seismogram illustrating $PKKP_1$ and $PKKP_2$ phase arrivals from the Sandwich Islands. Epicentral data: $\Delta \simeq 110^{\circ}$, $h \simeq 110$ km, azimuth $\simeq 147^{\circ}$, no magnitude data available. (X10 enlargement of 16-mm film)

WMSO
Run 344
10 Dec 1963
Data Group 311

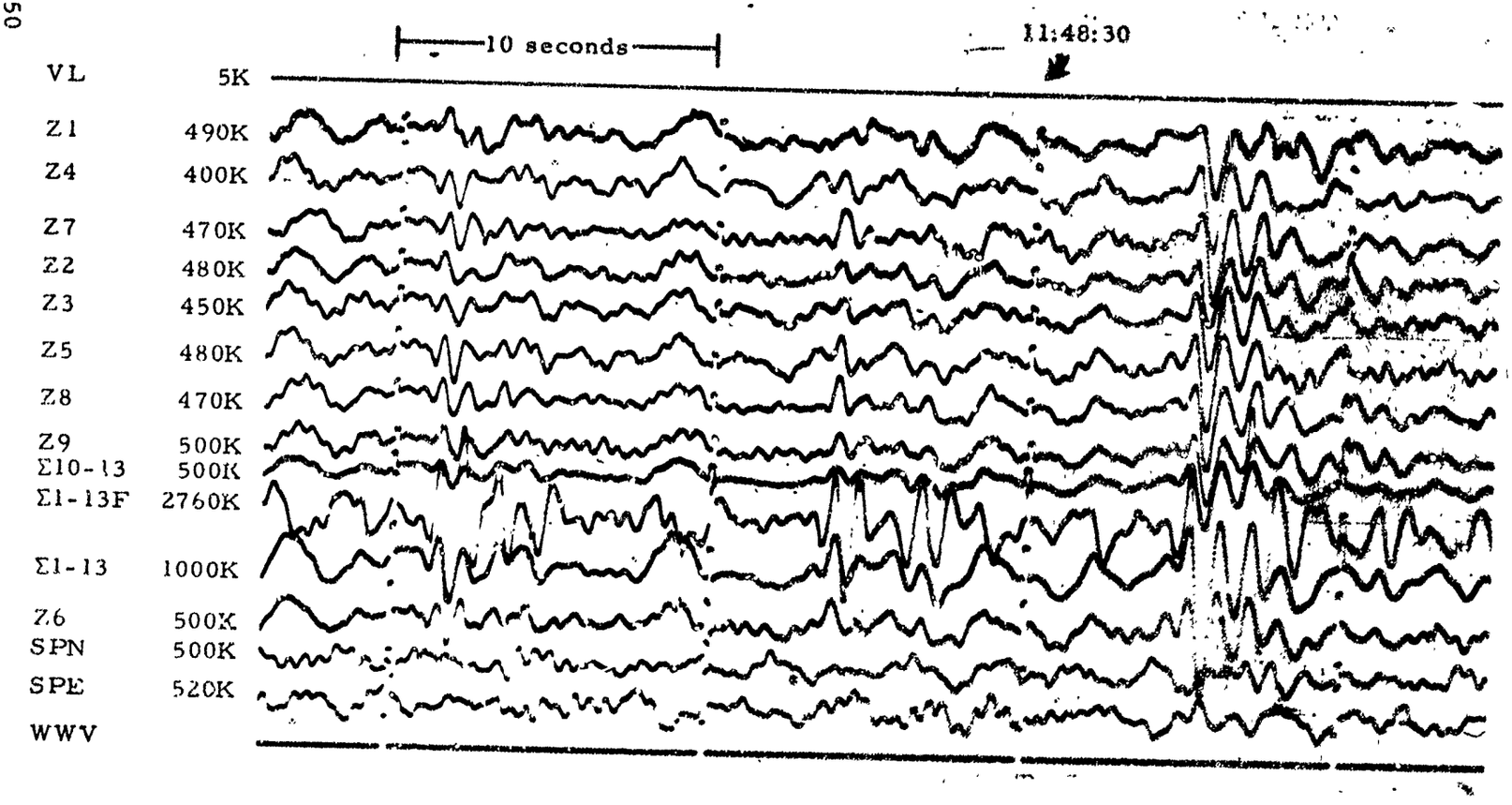

Figure 2-26. $PKKP_1$-$PKKP_2$-$PKKP_3$ as recorded on the WMSO short-period seismogram. Epicenter: Santa Cruz Island region, $\Delta \simeq 101^{\circ}$, h ≃ 61 km, azimuth ≃ 262°, magnitude ≃ 5.5 (X10 enlargement of 16-mm film)

WMSO
Run 358
24 Dec 1963
Data Group 311

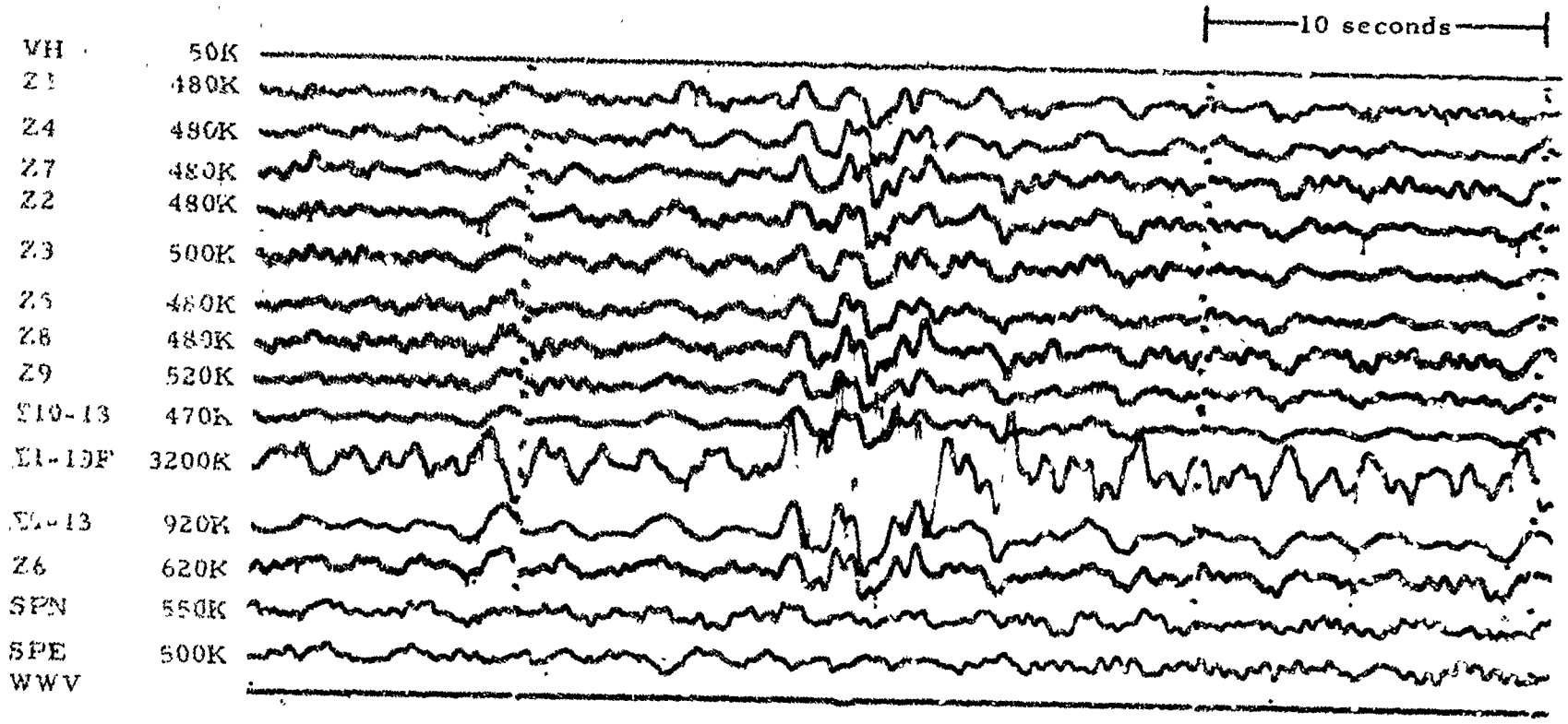

Figure 2-27. WMSO primary short-period seismogram illustrating an SKKP phase arrival. Epicenter: near north coast of Java, Δ = 142°, h = 323 km, azimuth = 314°, magnitude = 5.1 (X10 enlargement of 16-mm film)

WMSO
Run 326
22 Nov 1963
Data Group 311

WWV

Z1	540K
Z2	500K
Z3	500K
Z4	500K
Z5	520K
Z6	480K
Z7	460K
Z8	560K
Z9	460K
Σ10-13	440K
Σ1-13F	3360K
Σ1-13	[illegible]
SPN	480K
SPE	480K
LG 5	90K

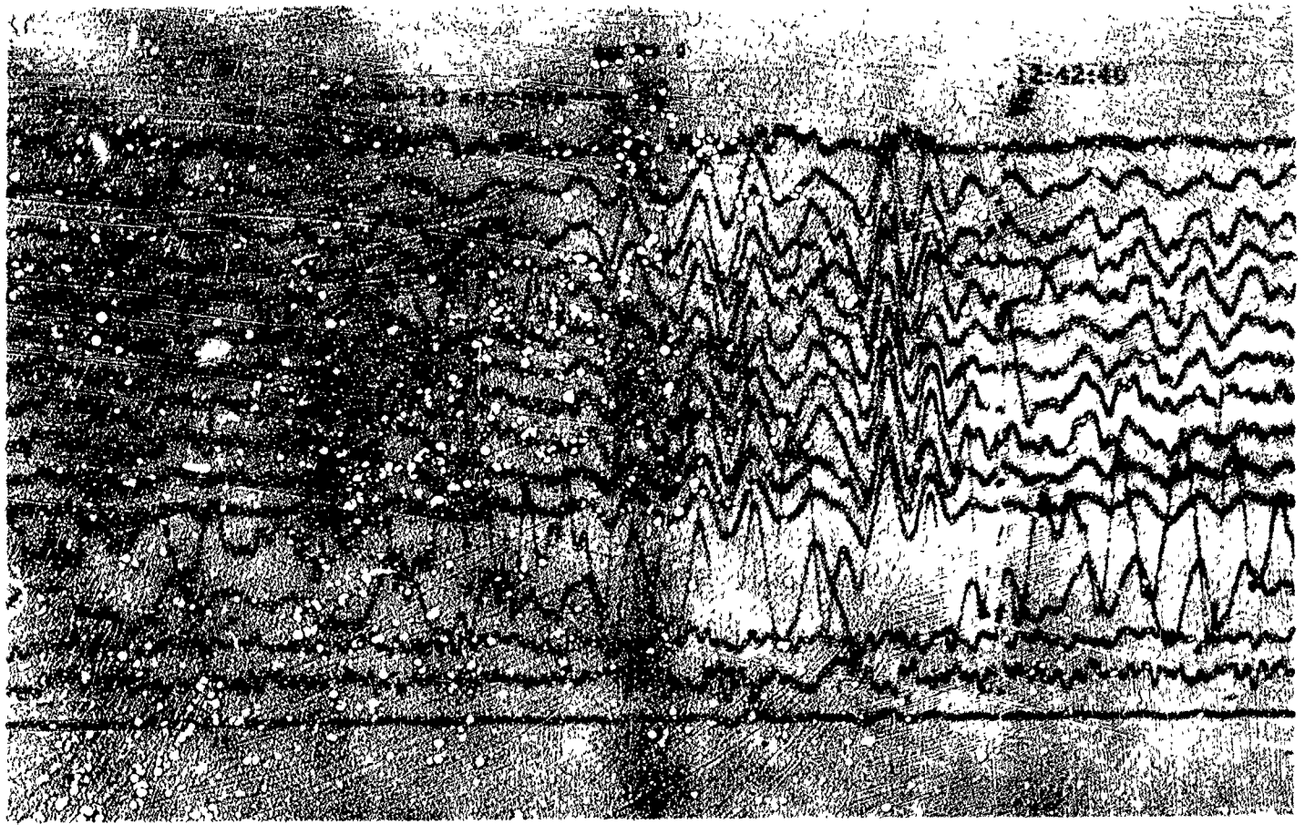

Figure 2-28. WMSO seismogram illustrating a PKPPKP (P'P') phase arrival. Epicenter: off the east coast of Kamchatka, $\Delta \approx 70^{\circ}$, h ≈ 33 km, azimuth ≈ 321°, magnitude ≈ 5.7 (X10 enlargement of 16-mm film)

WMSO
Run 301
28 Oct 1963

TR 64-50

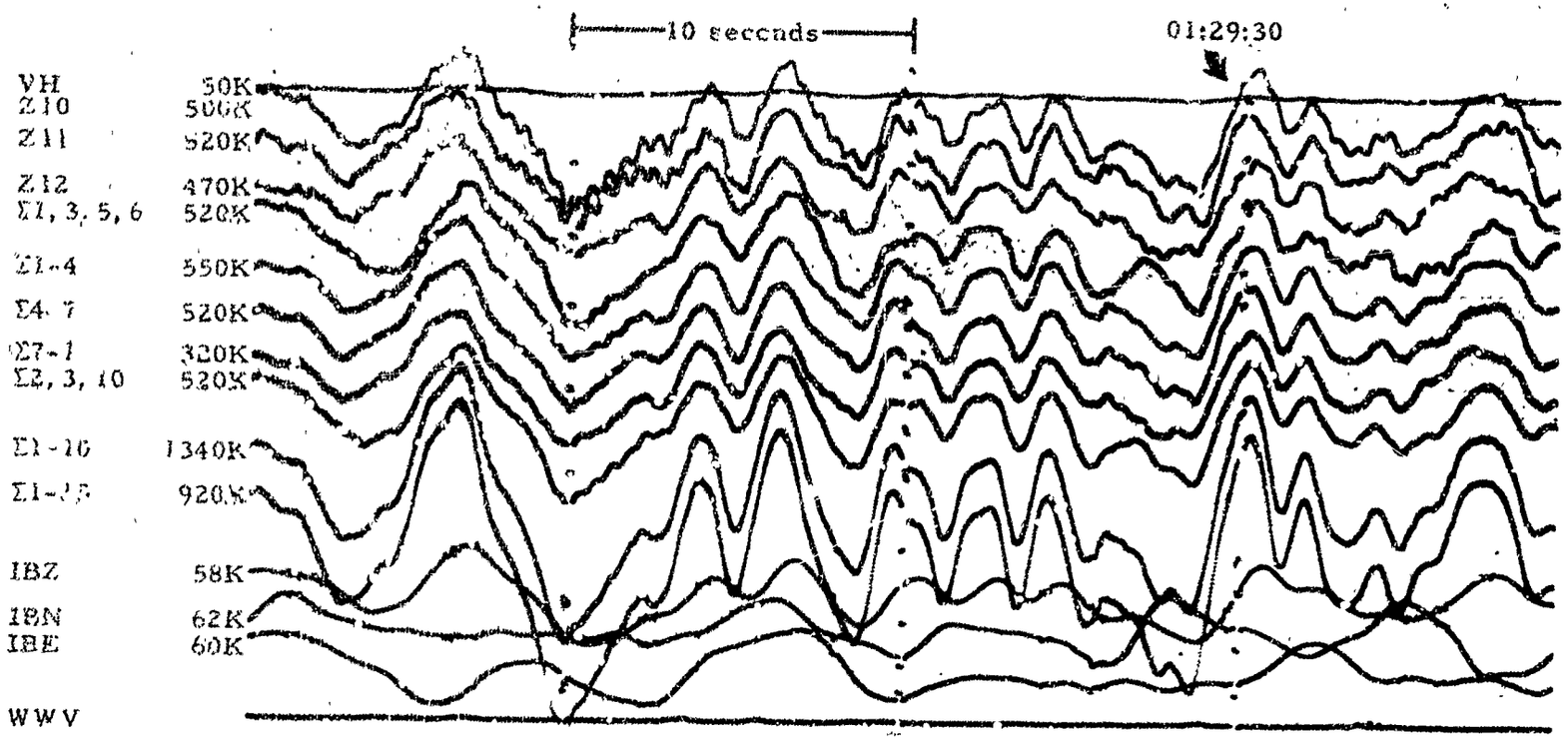

Figure 2-29. WMSO seismogram illustrating a PKPPKPPKP (P'P'P') phase arrival. Epicenter: Kermadec Islands, $\Delta \simeq 95^{\circ}$, $h \simeq 46$ km, azimuth $\simeq 243^{\circ}$, magnitude $\simeq 6.5$ (X10 enlargement of 16-mm film)

WMSO
Run 352
18 Dec 1963
Data Group 307

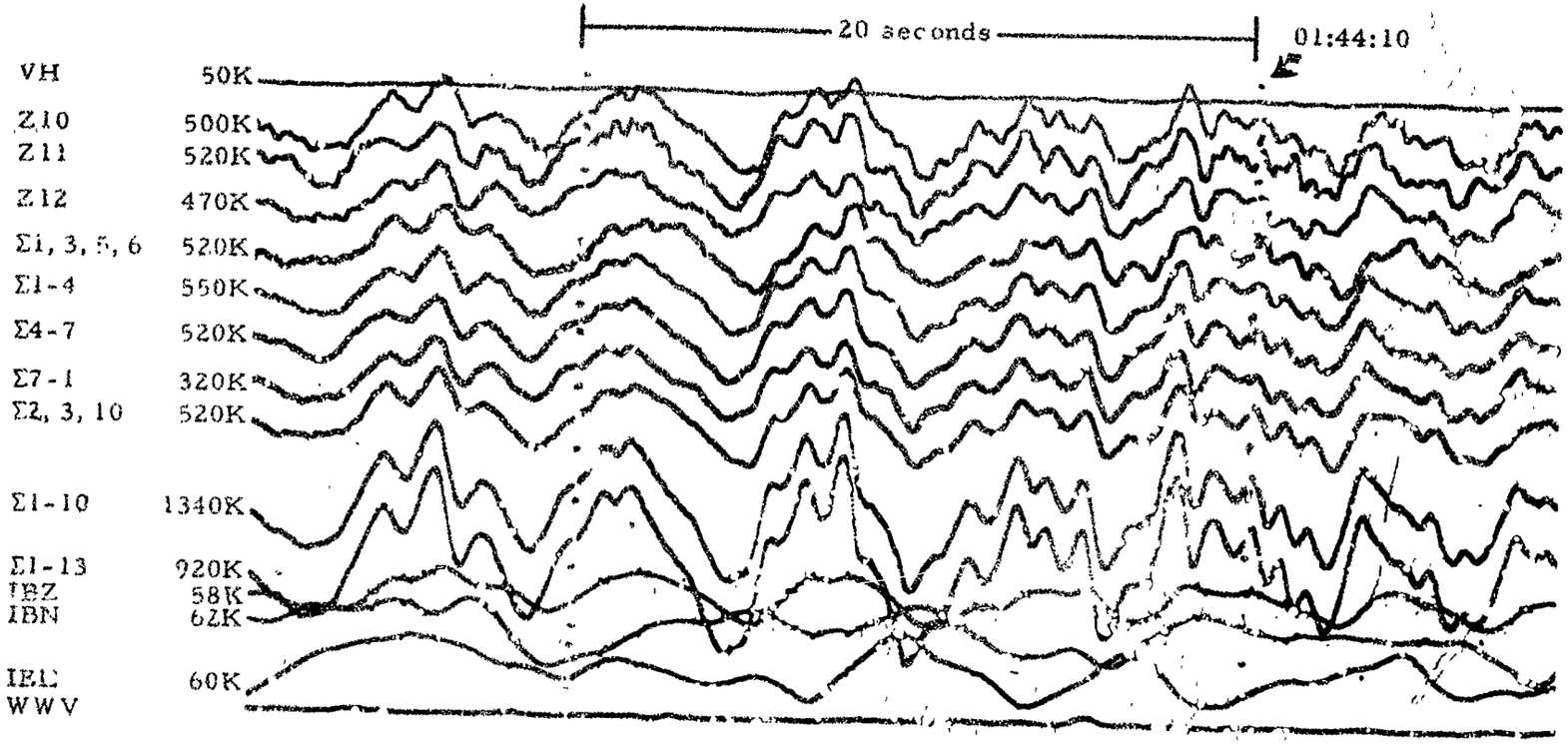

Figure 2-30. WMSO seismogram illustrating a PKPPKPPKP PKP (P'P'P'P') phase arrival. Epicenter: Kermadec Islands, Δ ≃ 95°, h [illegible] km, azimuth ≃ 243°, magnitude ≃ 6.5 (X10 enlargement of 16-mm film)

WMSO
Run 352
18 Dec 1963
Data Group 307

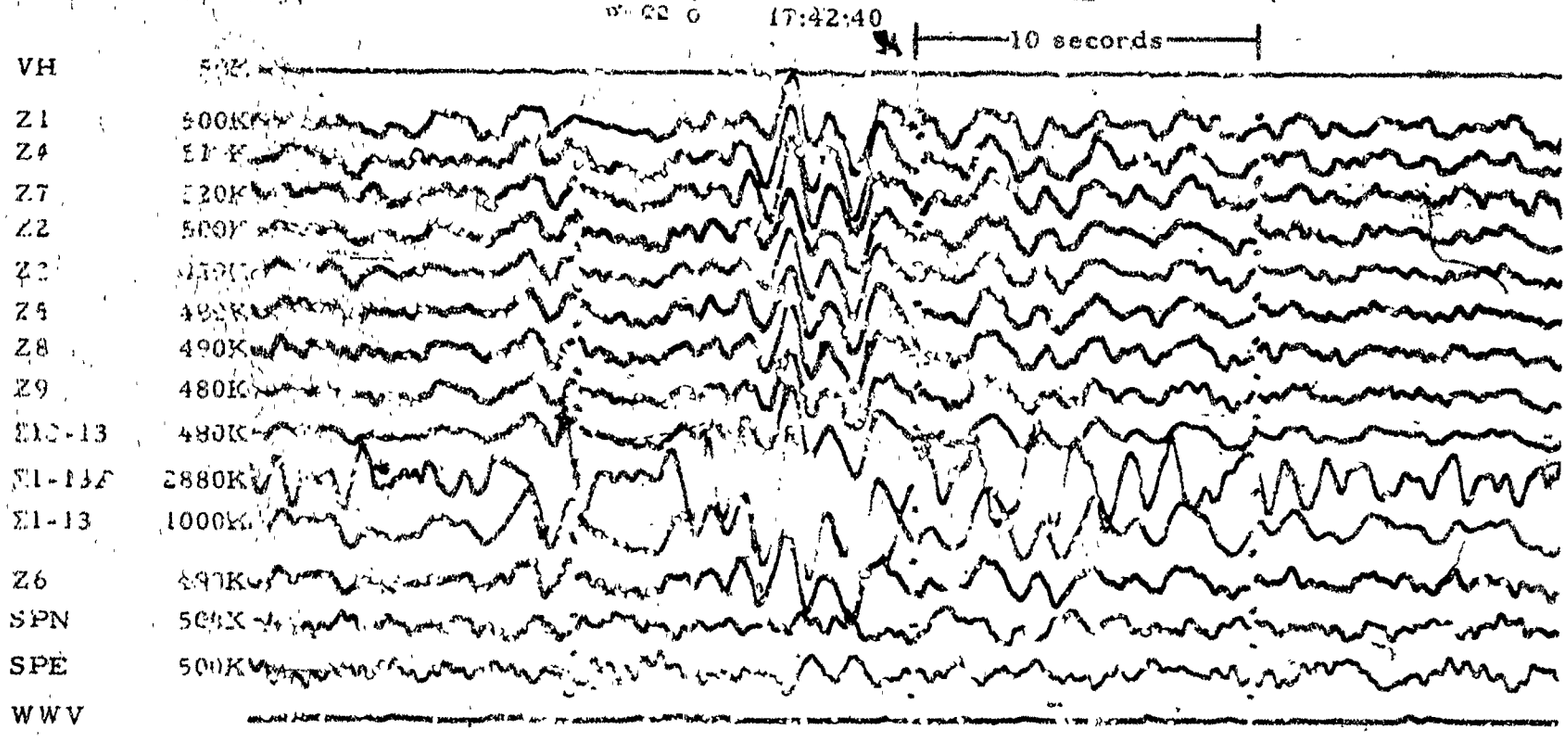

Figure 2-31. WMSO seismogram illustrating a PcPPKP phase arrival. Epicenter: Loyalty Islands region, $\Delta = 103^{\circ}$, $h = 111$ km, azimuth $= 254^{\circ}$, magnitude $= 6.7$ (X10 enlargement of 16-mm film)

WMSO
Run 020
20 Jan 1964
Data Group 311

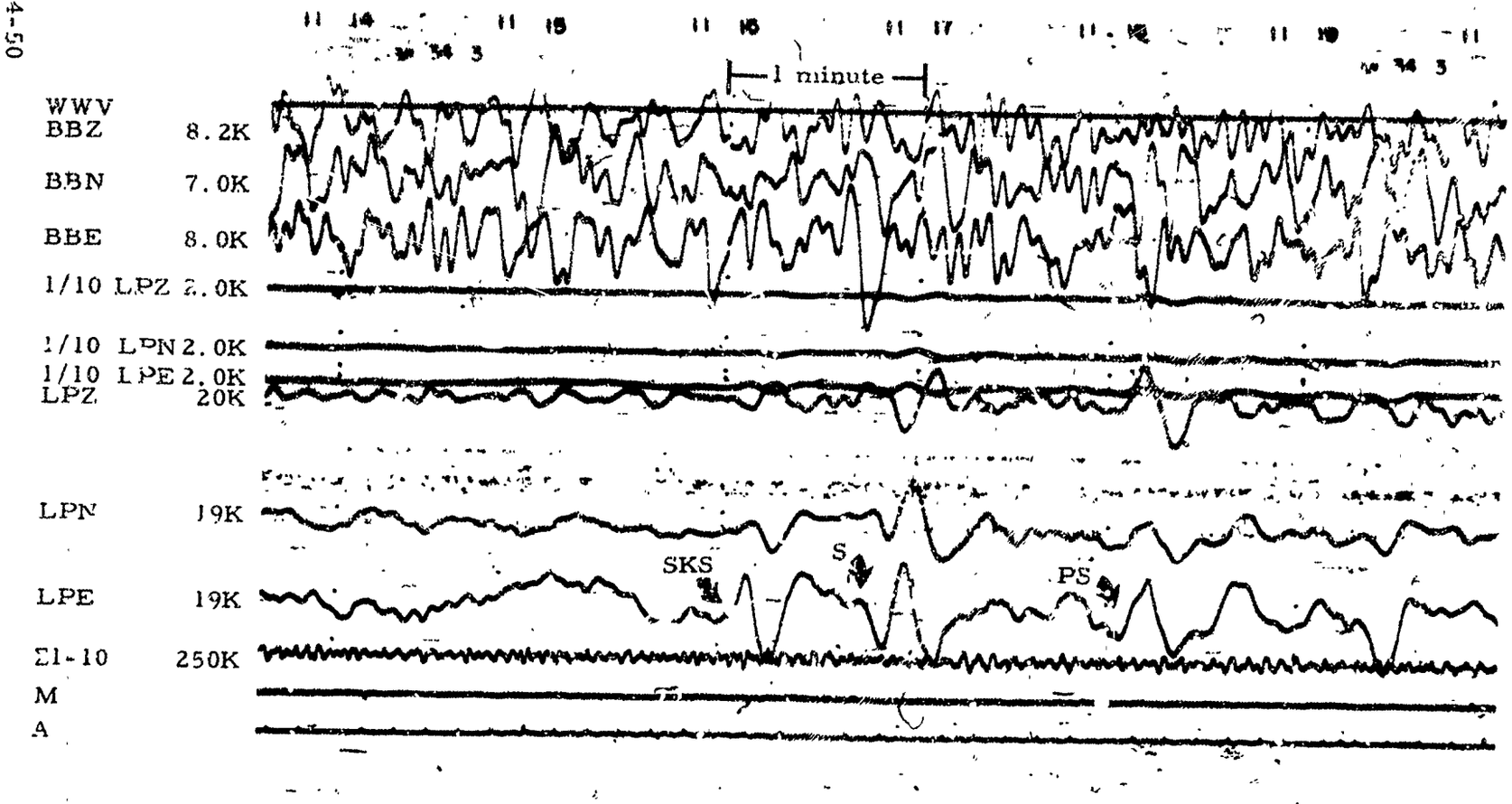

Figure 2-32. WMSO seismogram illustrating SKS, S, and PS phase arrivals from the Fiji Islands region. See figure 2-33 for the corresponding short-period recording of SKS. Epicentral data: $\Delta \simeq 94^{\circ}$, $h \simeq 435$ km, [illegible]th $\simeq 247^{\circ}$, magnitude $\simeq 5.0$ (X10 enlargement of 16-mm film)

WMSO
Run 343
9 Dec 1963
Data Group 204

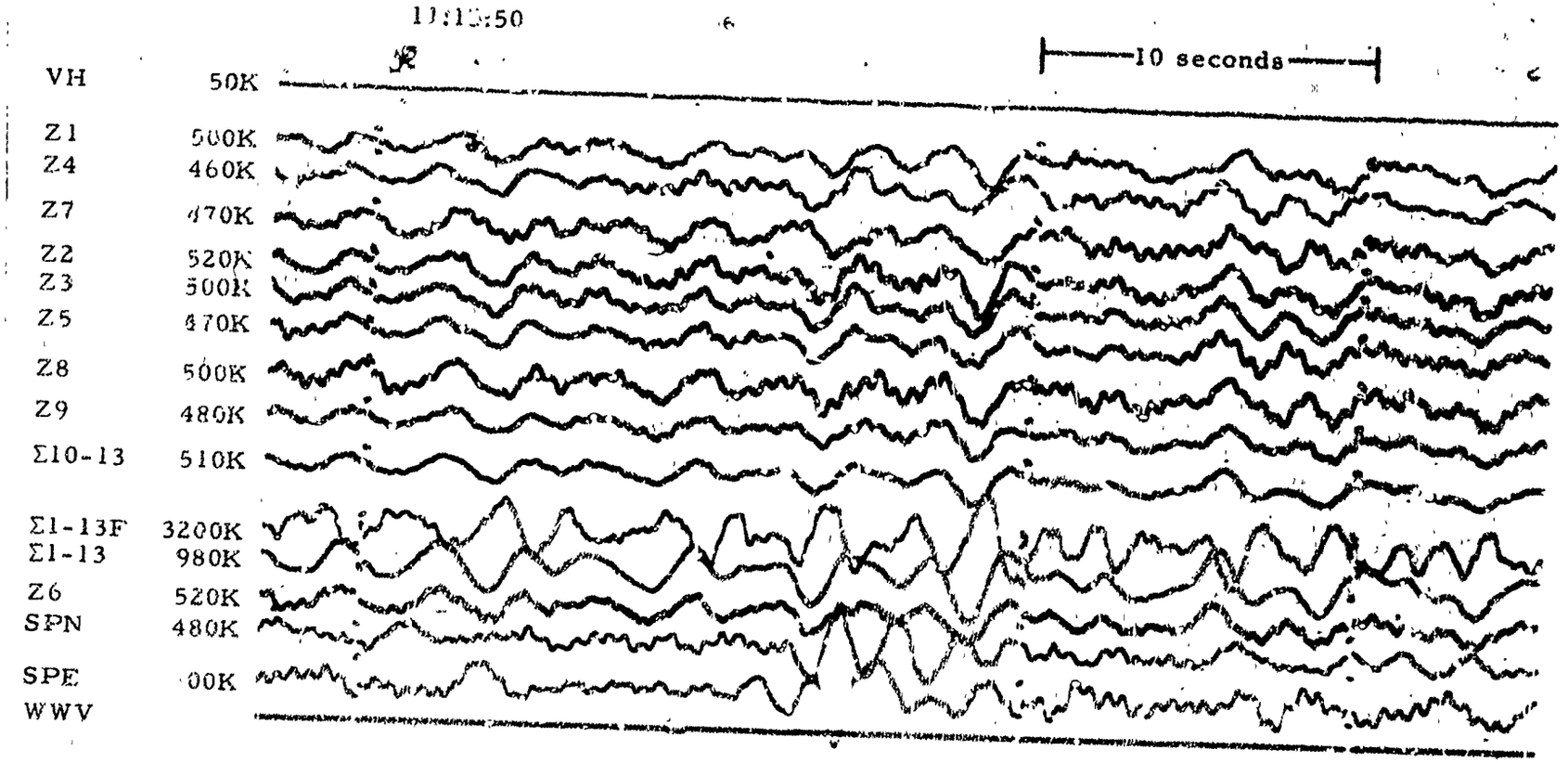

Figure 2-33. WMSO seismogram illustrating an SKS phase arrival from the Fiji Islands region. Epicentral data: $\Delta \approx 94°$, $h \approx 435$ km, azimuth $\approx 247°$, magnitude ≈ 5.0 (X10 enlargement of 16-mm film)

WMSO
Run 342
9 Dec 1963
Data Group 311

TR 64-50

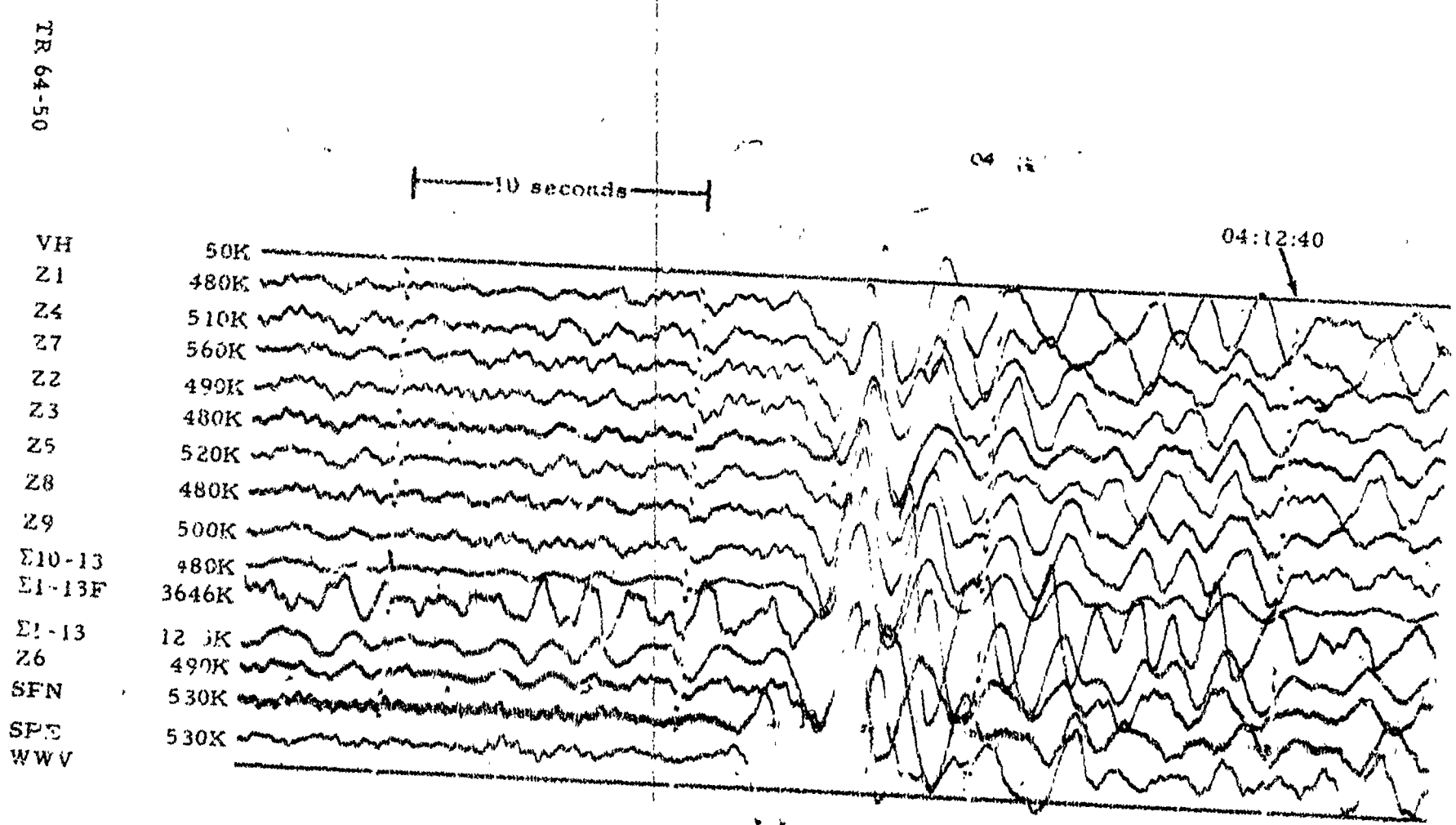

WMSO
Run 203
21 July 1964
Data Group 3003

Figure 2-33a. WMSO seismogram illustrating an SKS phase arrival from the Fiji Islands region. Epicentral data: $\Delta = 96^{\circ}$, h = 222 km, azimuth = 243°, magnitude = 5.8 (X10 enlargement of 16-mm film)

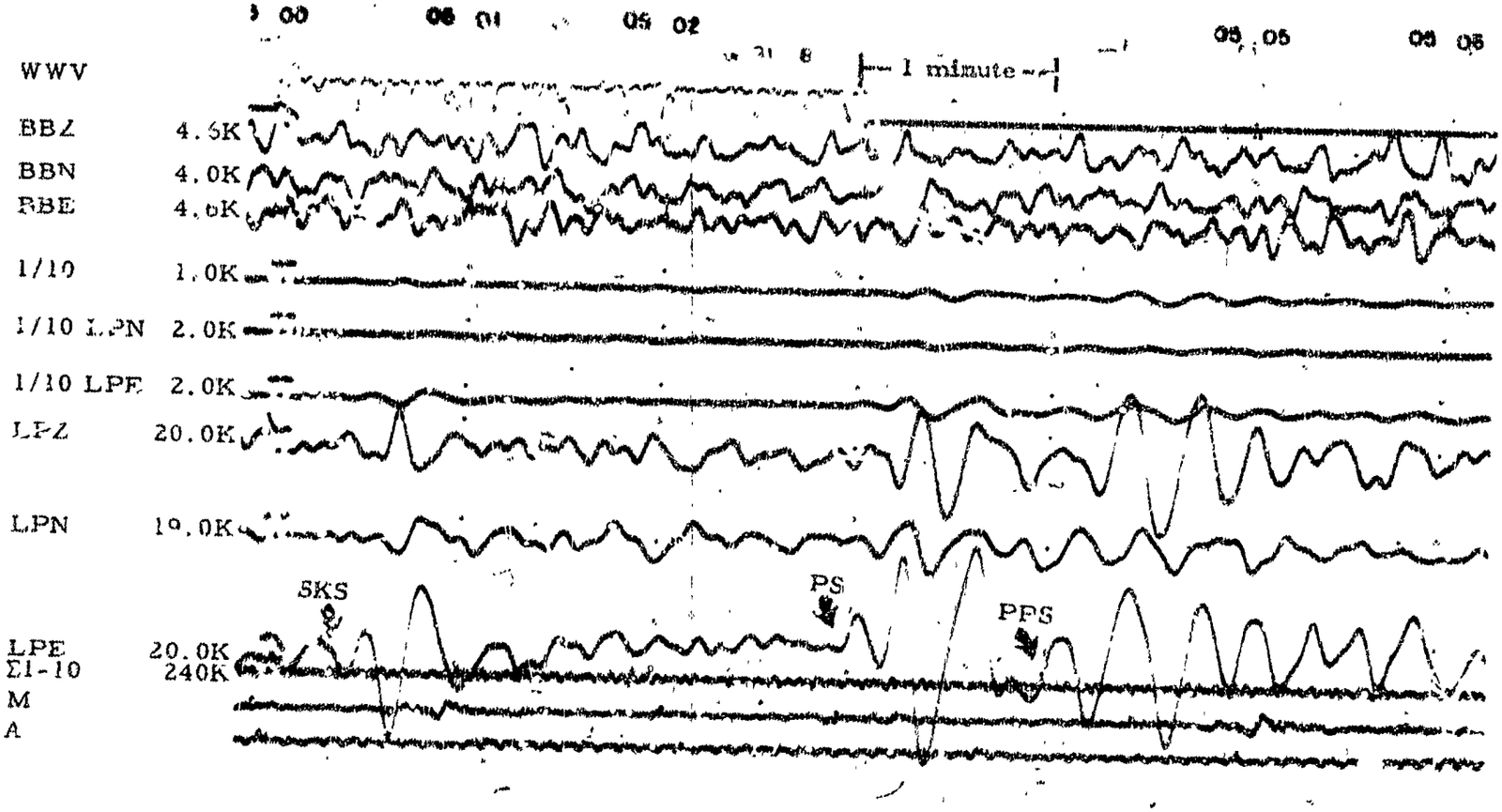

Figure 2-34. WMSO seismogram illustrating SKS, PS, and PPS phase arrivals from the New Hebrides Islands. Epicentral data: Δ = 103°, h = 33 km, azimuth = 257°, magnitude = 4.8 (2:10 enlargement of 16-mm film)

WMSO
Run 318
24 Nov 1963
Data Group 304

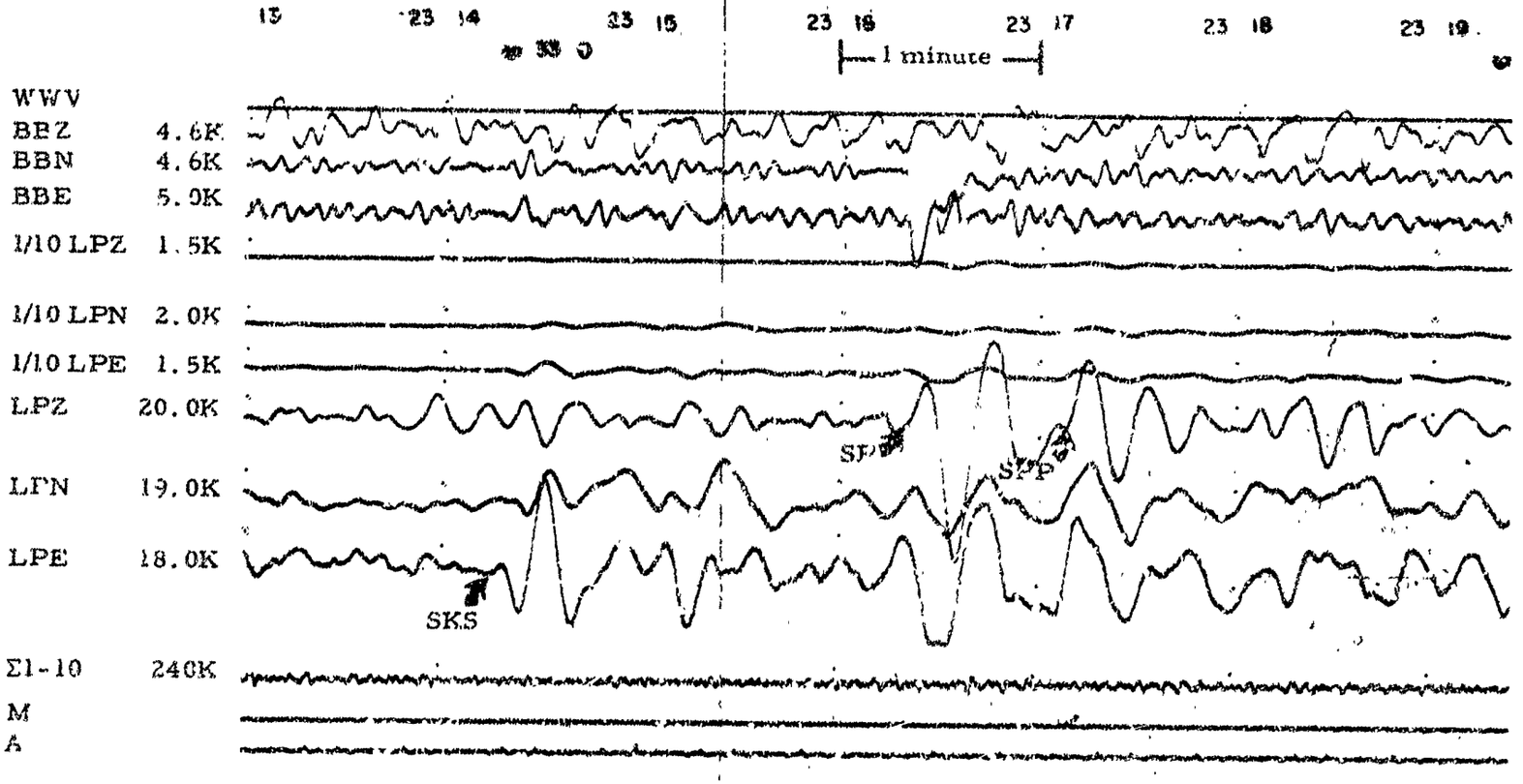

Figure 2-35. WMSO seismogram illustrating SKS, SP, and SPP phases from the Fiji Islands region. Epicentral data: $\Delta \approx 96^{\circ}$, h ≈ 33 km, azimuth ≈ 254°, magnitude ≈ 5.3 (X10 enlargement of 16-mm film)

WMSO
Run 326
26 Nov 63
Data Group 304

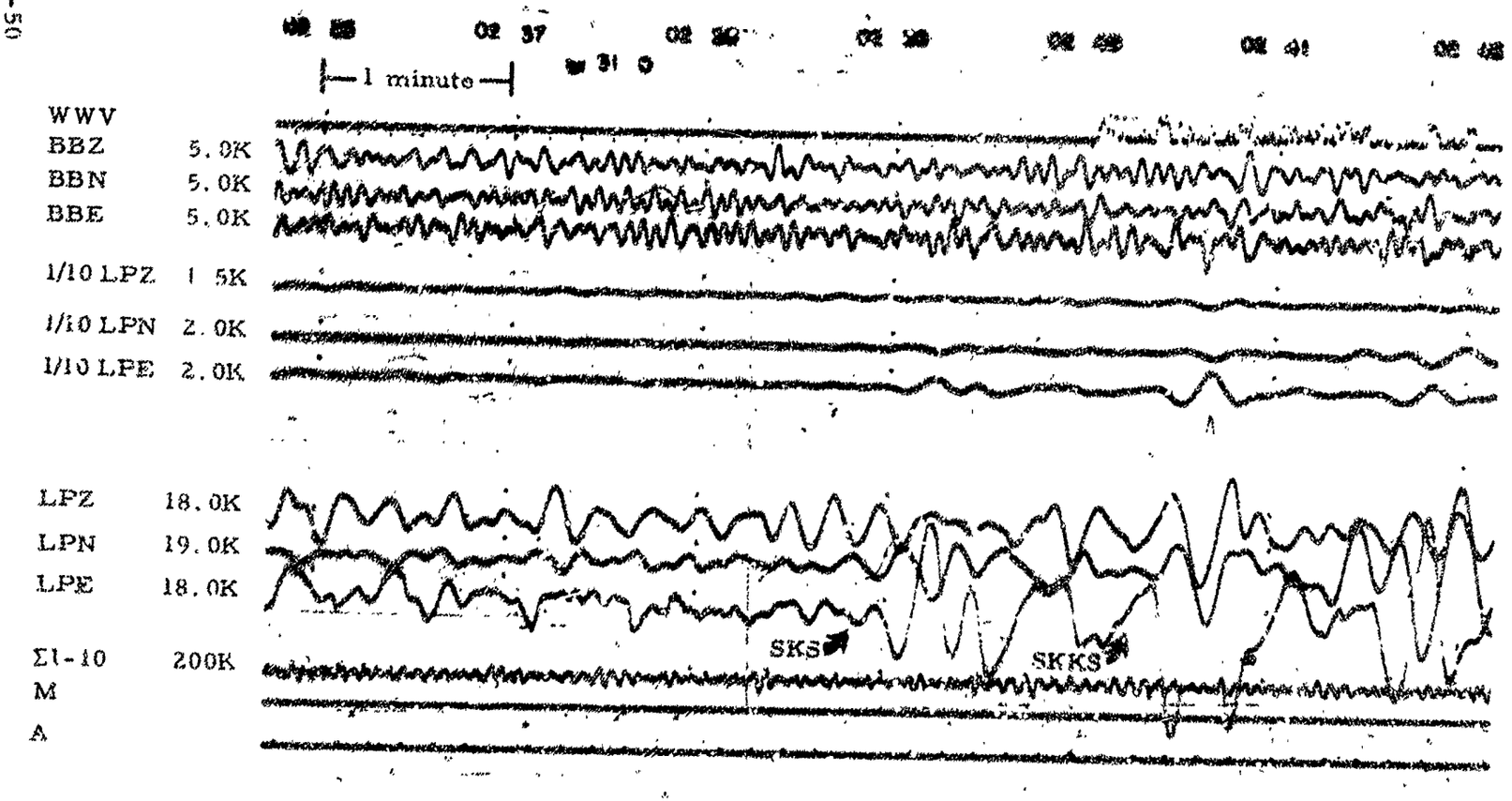

Figure 2-36. WMSO seismogram illustrating SKS and SKKS phase arrivals from Western New Guinea. Epicentral data: $\Delta \approx 118^{\circ}$, $h \approx 33$ km, azimuth $\approx 288^{\circ}$, magnitude ≈ 5.7 (X10 enlargement of 16-mm film)

WMSO
Run 310
6 Nov 1963
Data Group 304

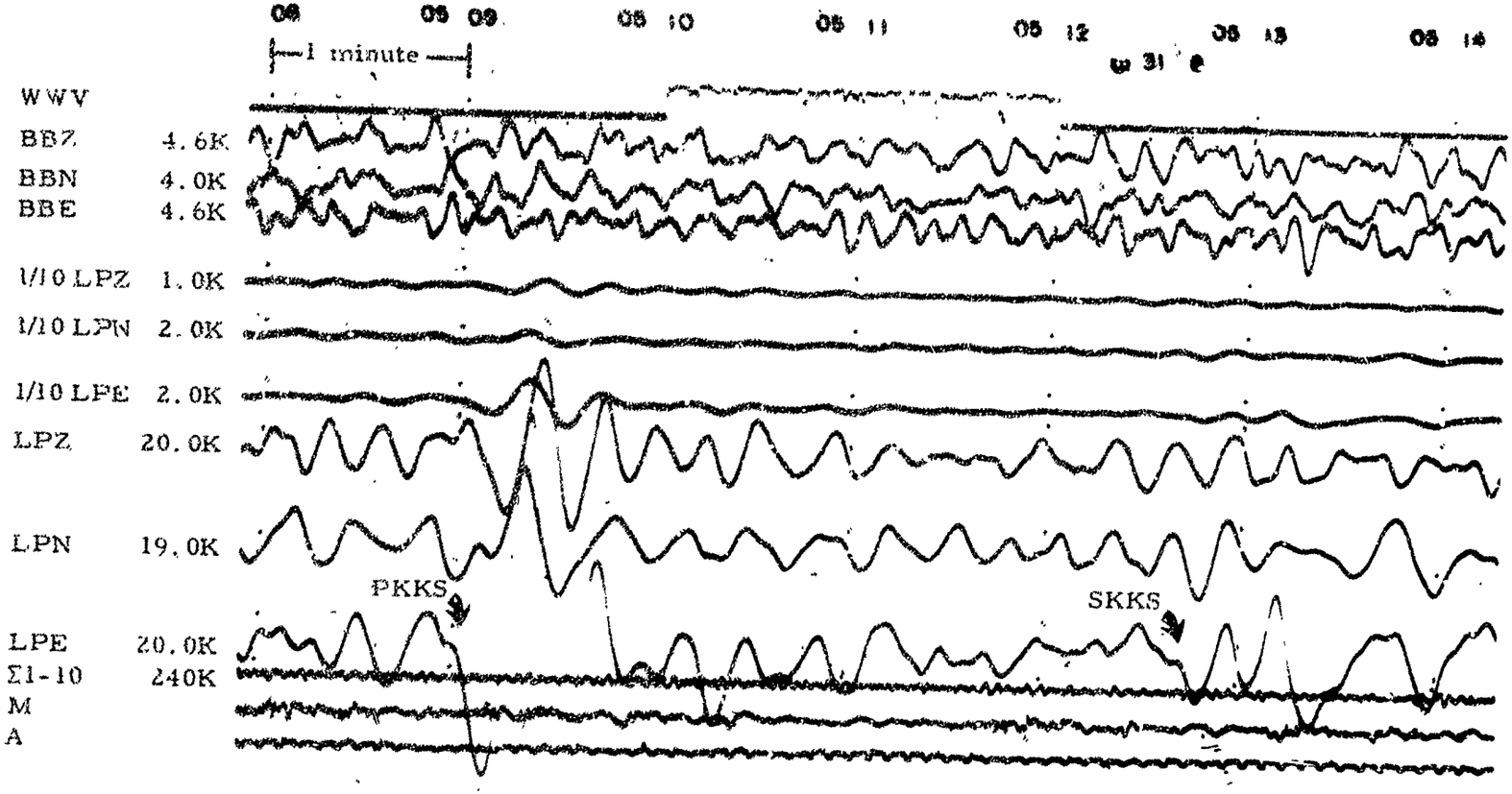

Figure 2-37. WMSO seismogram illustrating PKKS and SKKS phase arrivals from the New Hebrides Islands. Epicentral data: $\Delta \simeq 103^{\circ}$, h ≃ 33 km, azimuth ≃ 257°, magnitude ≃ 4.8 (X10 enlargement of 16-mm film)

WMSO
Run 318
14 Nov 1963
Data Group 304

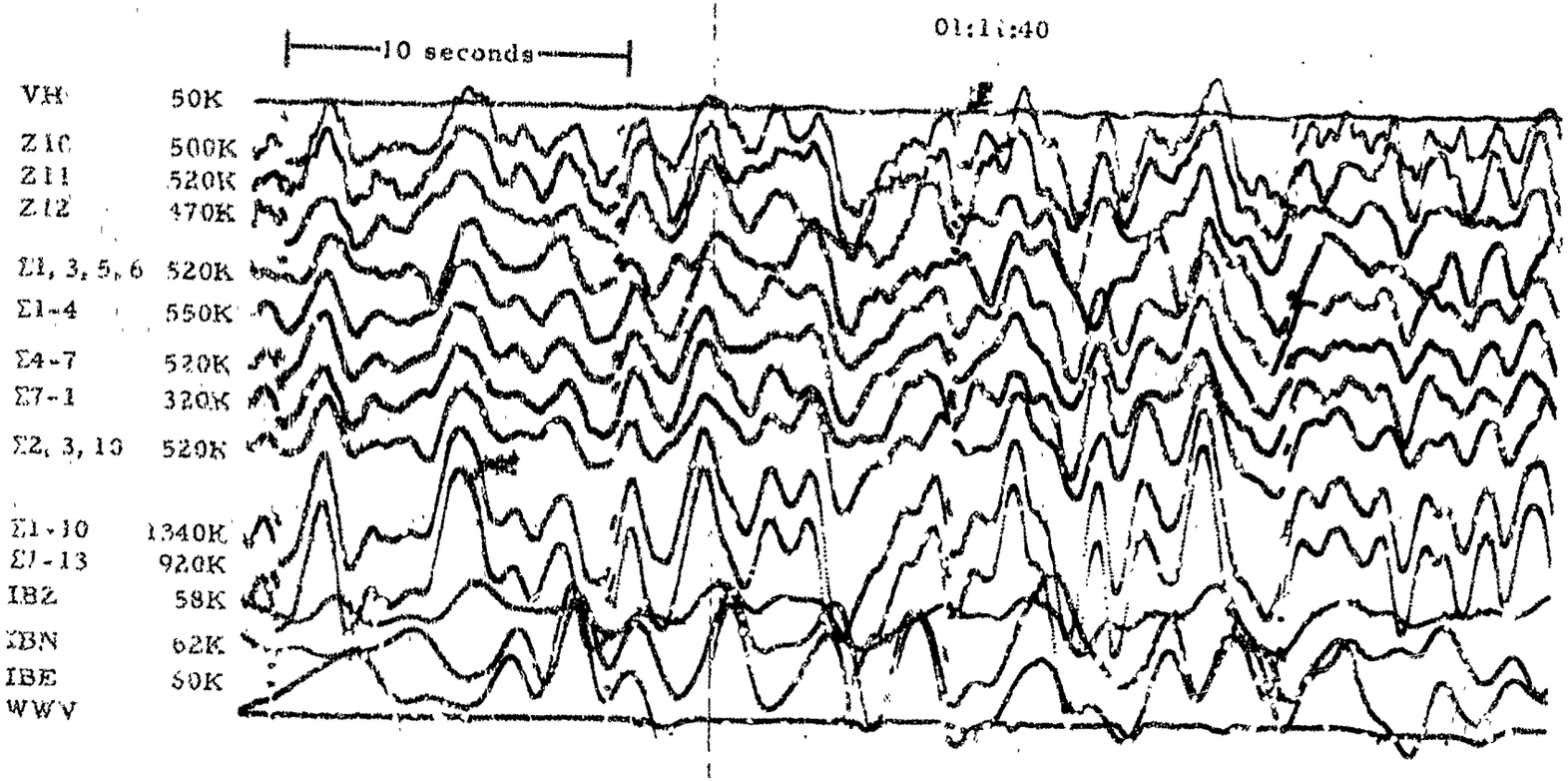

Figure 2-38. WMSO seismogram illustrating a PKPPKS phase arrival from the Kermadec Islands. Epicentral data: $\Delta \simeq 95^{\circ}$, $h \simeq 46$ km, azimuth $\simeq 240^{\circ}$, magnitude $\simeq 6.5$ (X10 enlargement of 16-mm film)

WMSO
Run 352
18 Dec 1963
Data Group 307

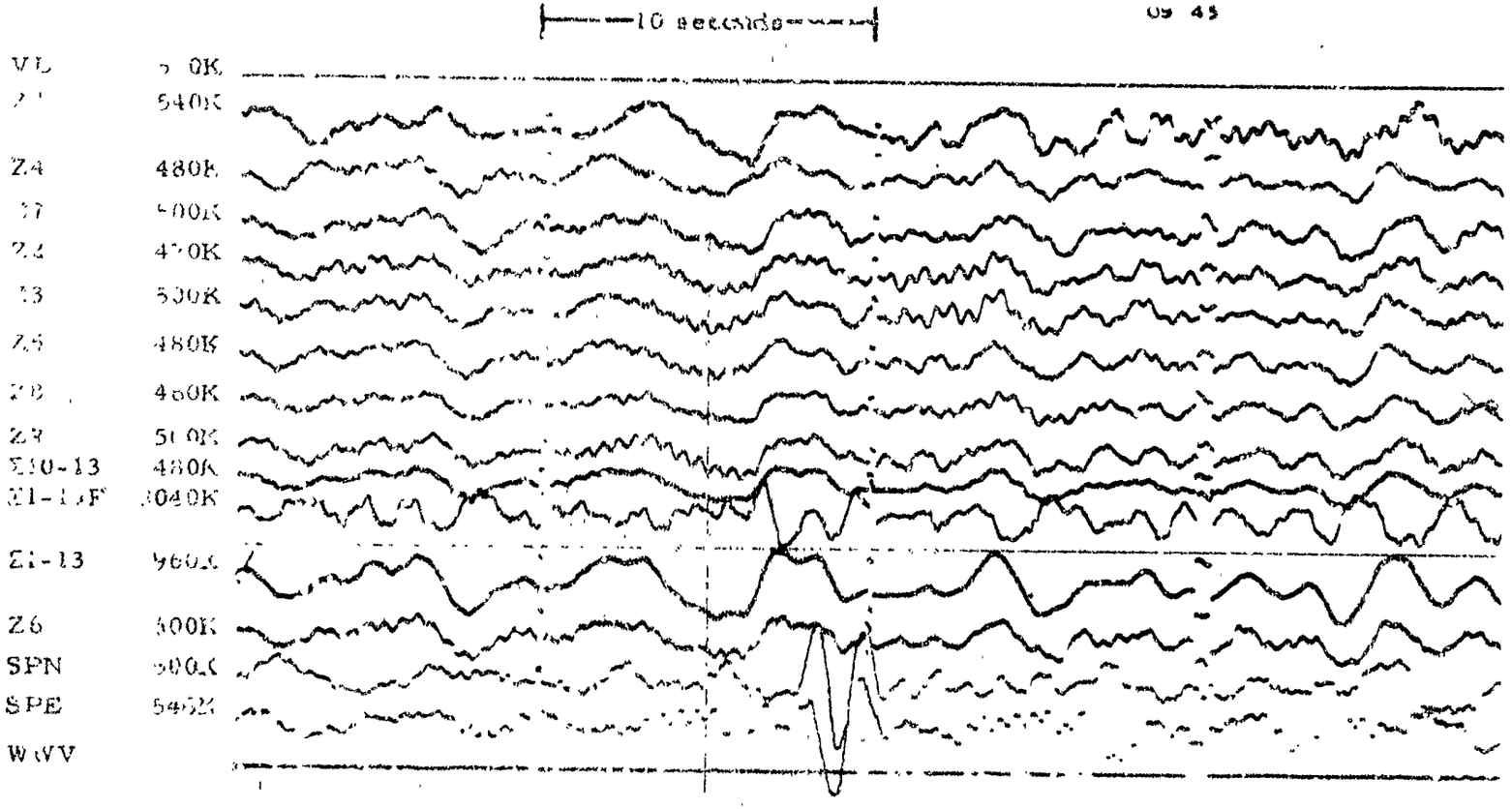

Figure 2-39. SKKKS as recorded on the WMSO short-period seismogram. Epicenter: Kermadec Islands, Δ = 101°, h = 33 km, azimuth = 238°, magnitude = 5.8 (X10 enlargement of 16-mm film)

WMSO
Run 362
28 Dec 1963
Data Group 211

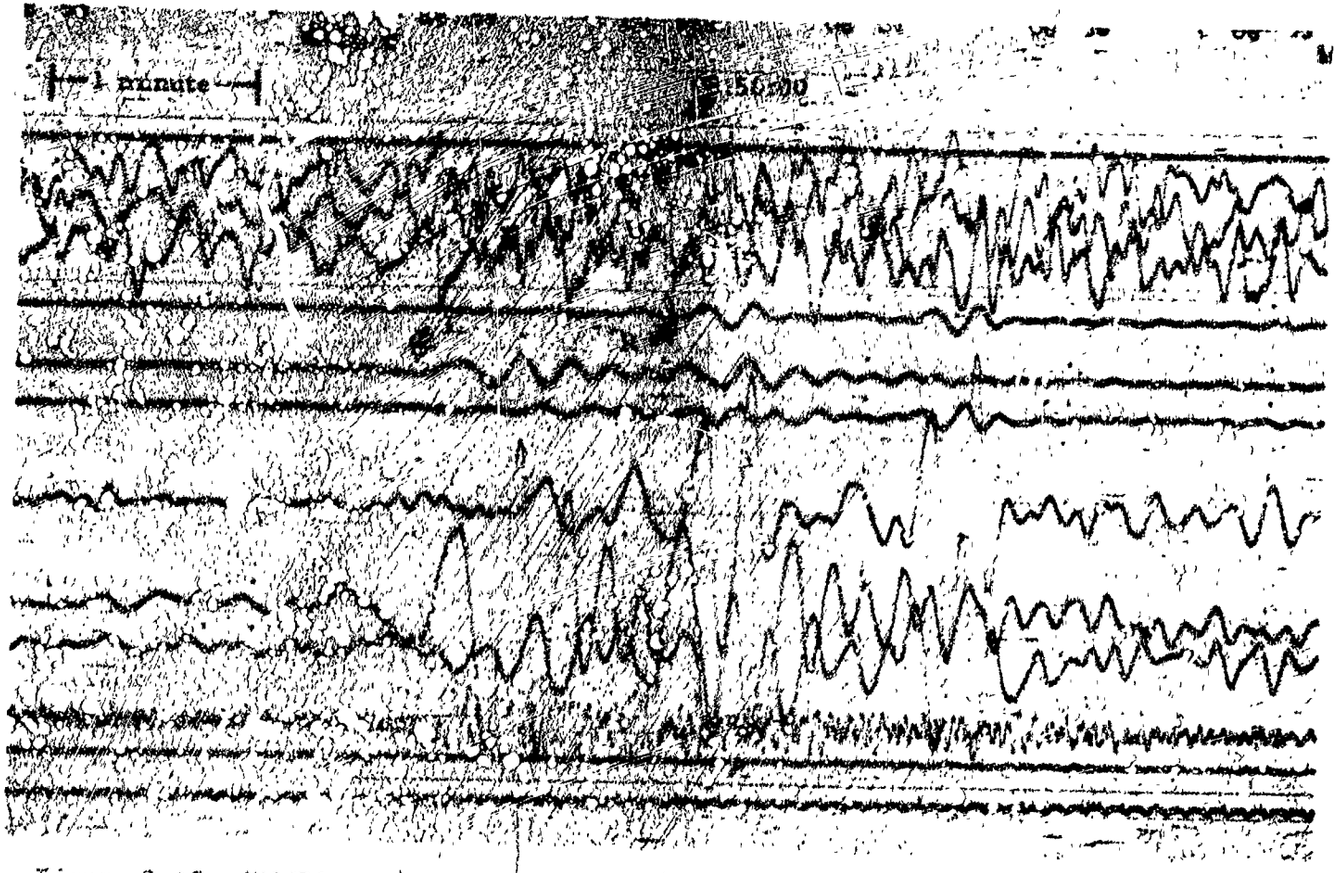

Figure 2-40. WMSO seismogram illustrating Love and Rayleigh phase arrivals from Sonora, Mexico. Epicentral data: $\Delta \approx 13^{\circ}$, $h \approx 14$ km, azimuth $\approx 300^{\circ}$, magnitude = 4.7 (X10 enlargement of 16-mm film)

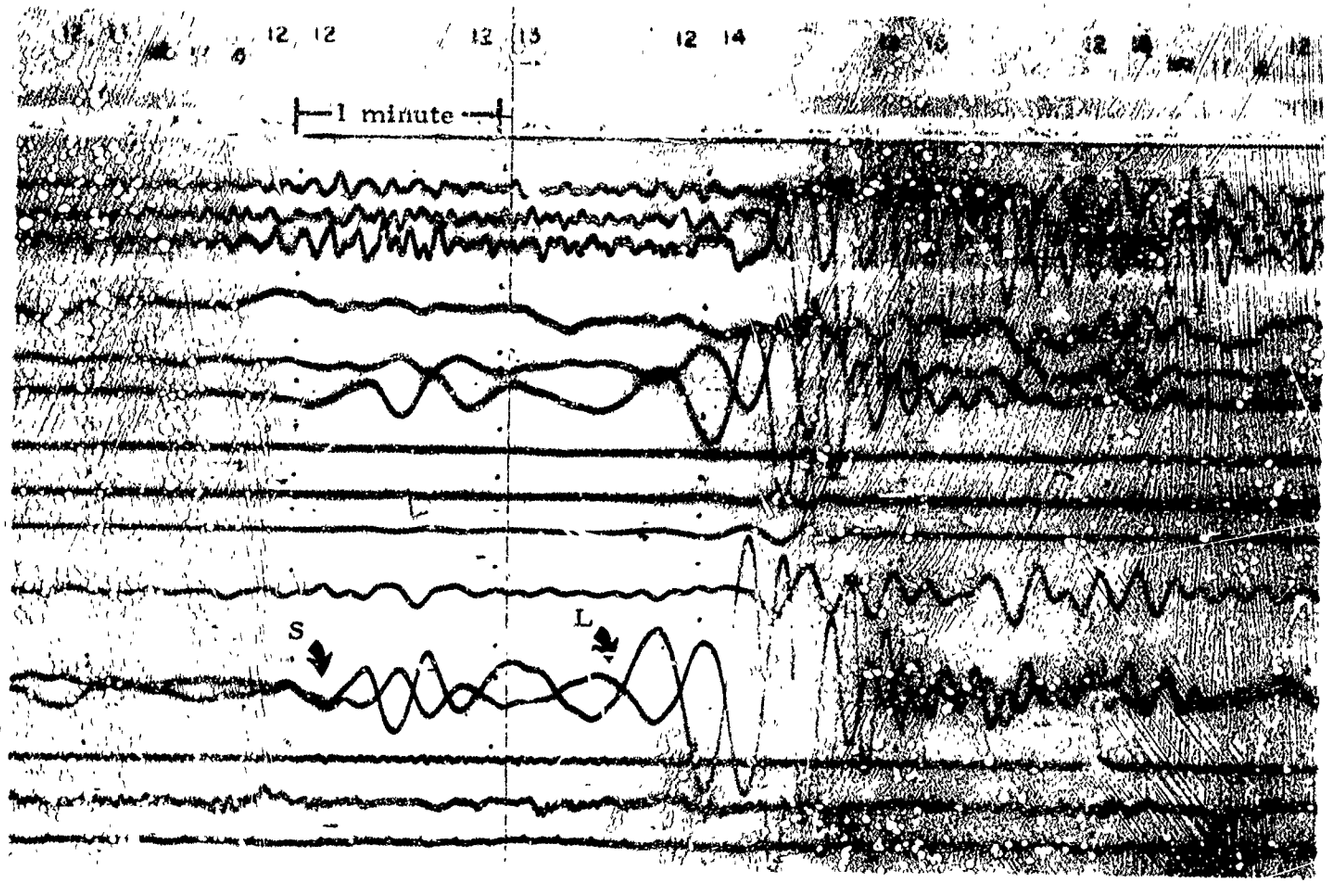

Figure 2-41. WMSO seismogram illustrating the broad-band system response to surface waves. Epicenter: off the coast of Central Mexico, $\Delta \simeq 16^{\circ}$, $h \simeq 33$ km, azimuth $\simeq 214^{\circ}$, magnitude $\simeq 3.9$ (X10 enlargement of 16-mm film)

WMSO
Run 174
23 Jun 1963

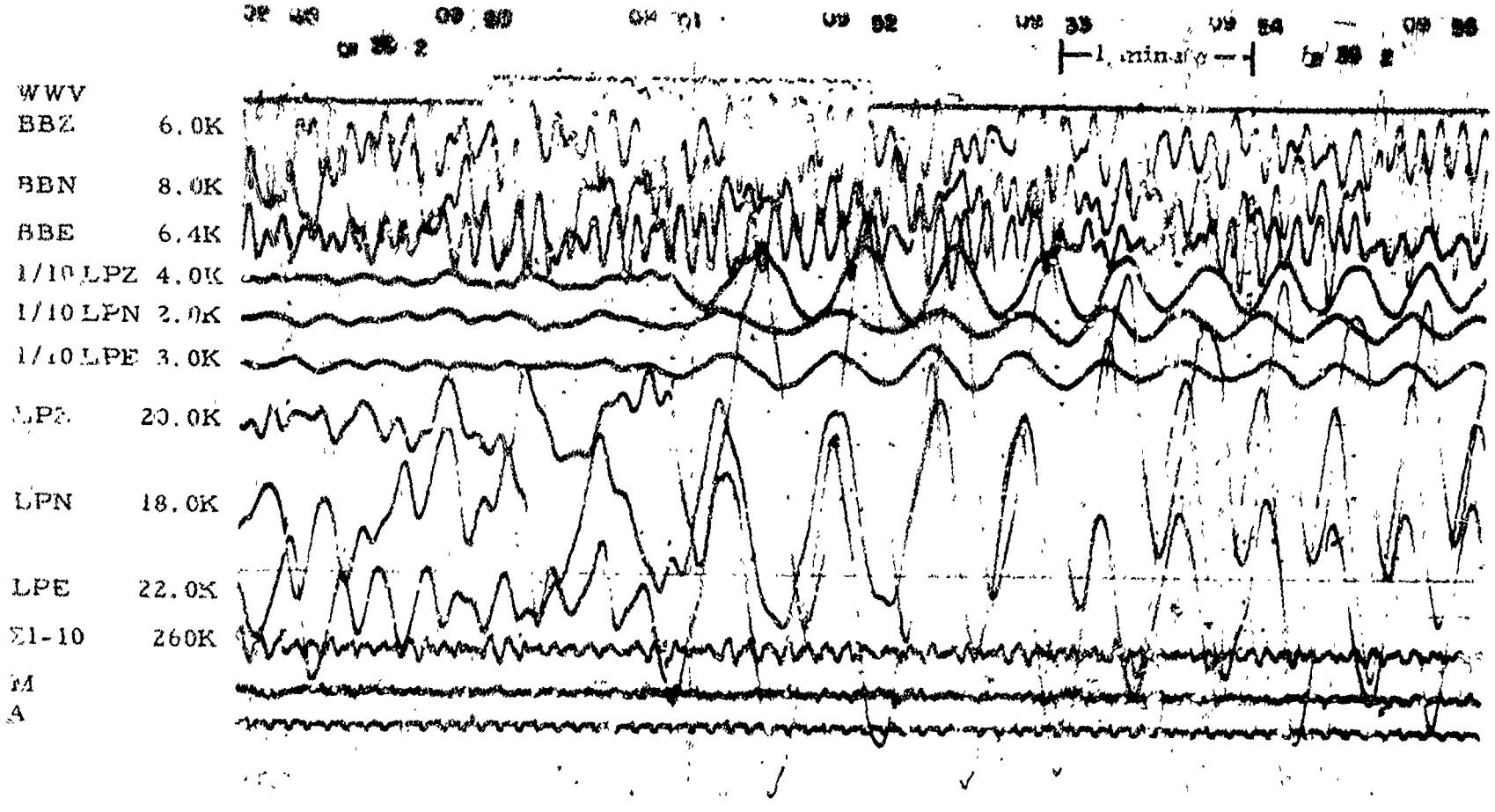

Figure 2-42. WMSO seismogram illustrating a $Rayleigh_1$ phase arrival. See figure 2-43 for $Rayleigh_2$ arrival from the same event. Epicenter: Kermadec Islands, $\Delta \simeq 101^{\circ}$, $h \simeq 33$ km, azimuth $\simeq 238^{\circ}$, magnitude ~ 5.8 (X10 enlargement of 16-mm film)

WMSO
Run 362
28 Dec 1963
Data Group 304

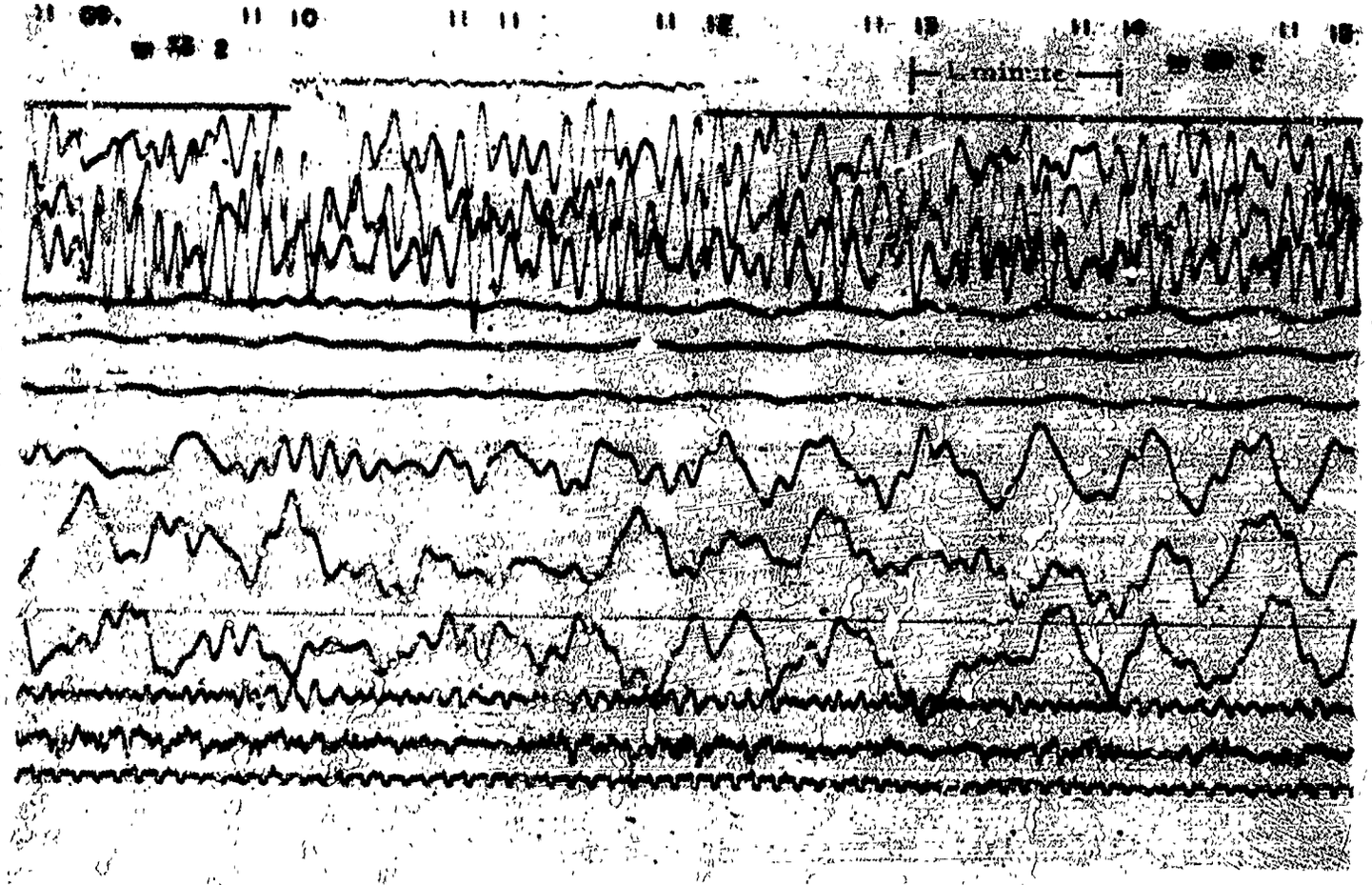

WMSO
Run 362
23 Dec 1963
Data Group 304

Figure 2-43. WMSO seismogram illustrating a Rayleigh$_2$ phase arrival. Epicenter: Kermadec Islands, $\Delta \simeq 101^{\circ}$, $h \simeq 33$ km, azimuth $\simeq 238^{\circ}$, magnitude $\simeq 5.8$ (X10 enlargement of 16-mm film)

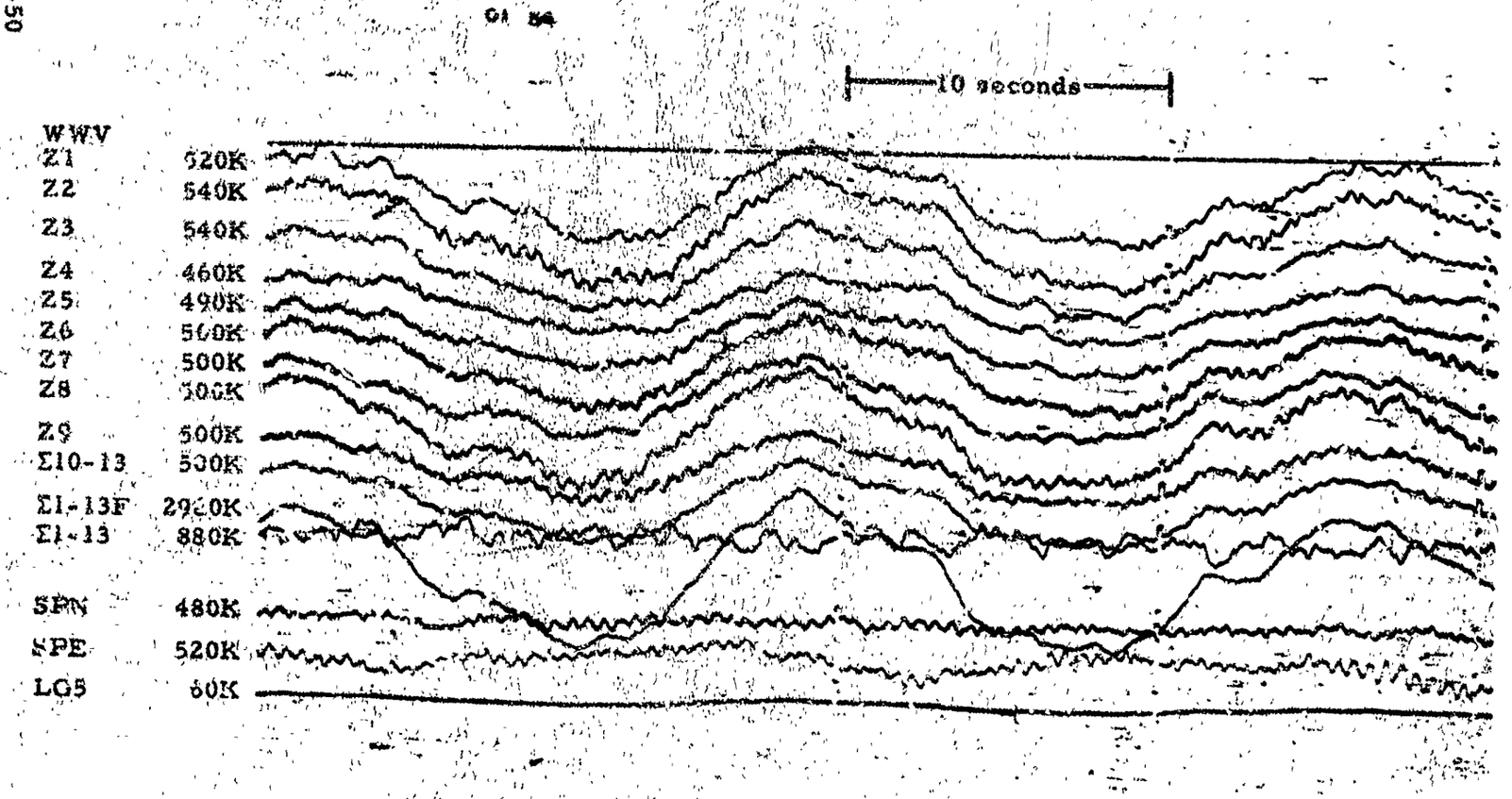

WMSO
Run 258
15 Sep 1963

Figure 2-44. Rayleigh waves as recorded on the WMSO short-period seismogram. Epicenter: Santa Cruz Island region, $\Delta \approx 101^{\circ}$, h ≈ 43 km, azimuth ≈ 265°, magnitude ≈ 6.3 (X10 enlargement of 16-mm film)

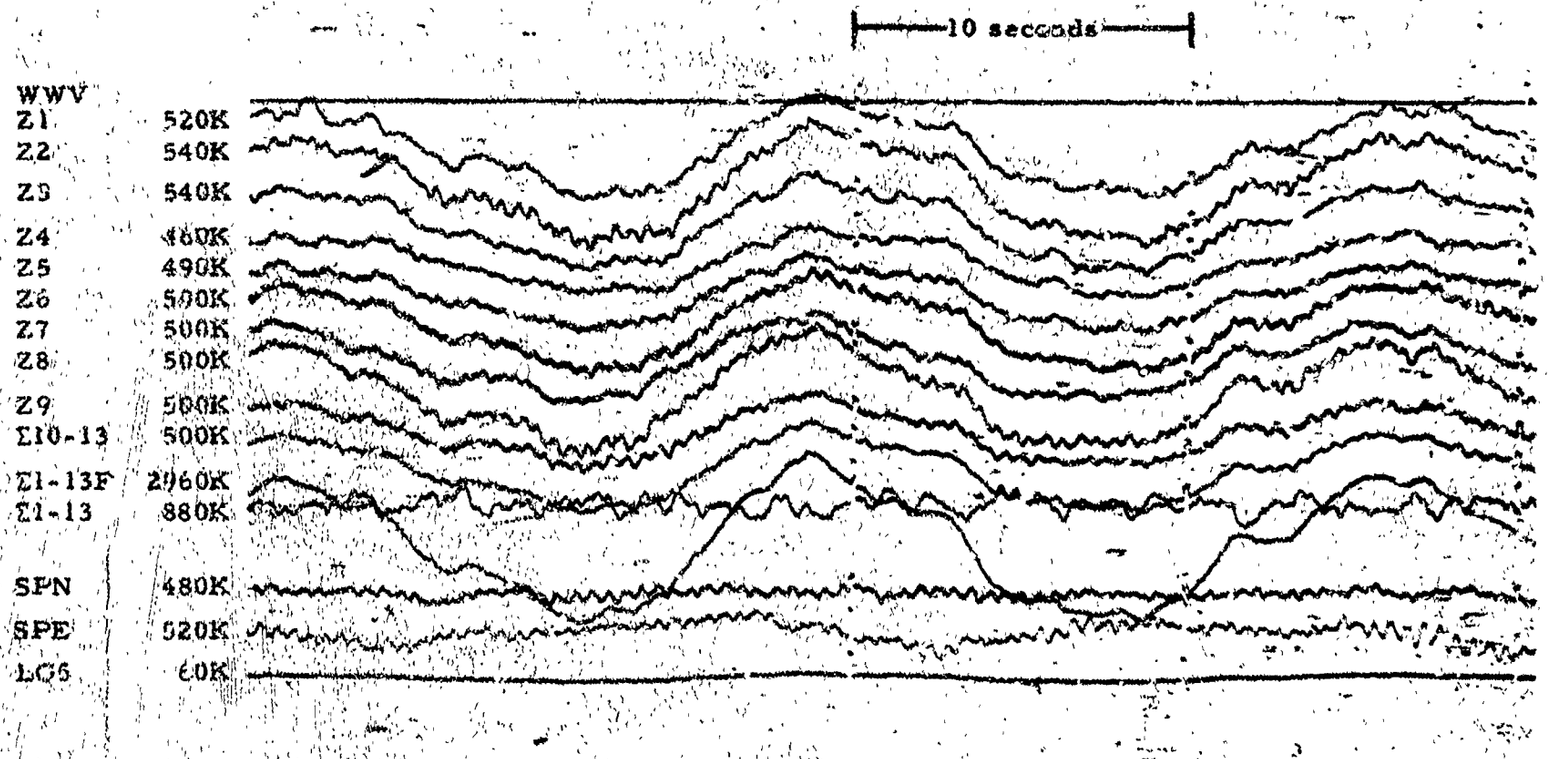

Figure 2-44. Rayleigh waves as recorded on the WMSO short-period seismogram. Epicenter: Santa Cruz Island region, Δ = 91°, h = 43 km, azimuth = 265°, magnitude = 6.3 (X10 enlargement of 16-mm film)

WMSO
Run 258
15 Sep 1963

3. P AND PKP PHASES FROM VARIOUS DISTANCES AND AZIMUTHS

3.1 DISTANCE = 0° to 16°

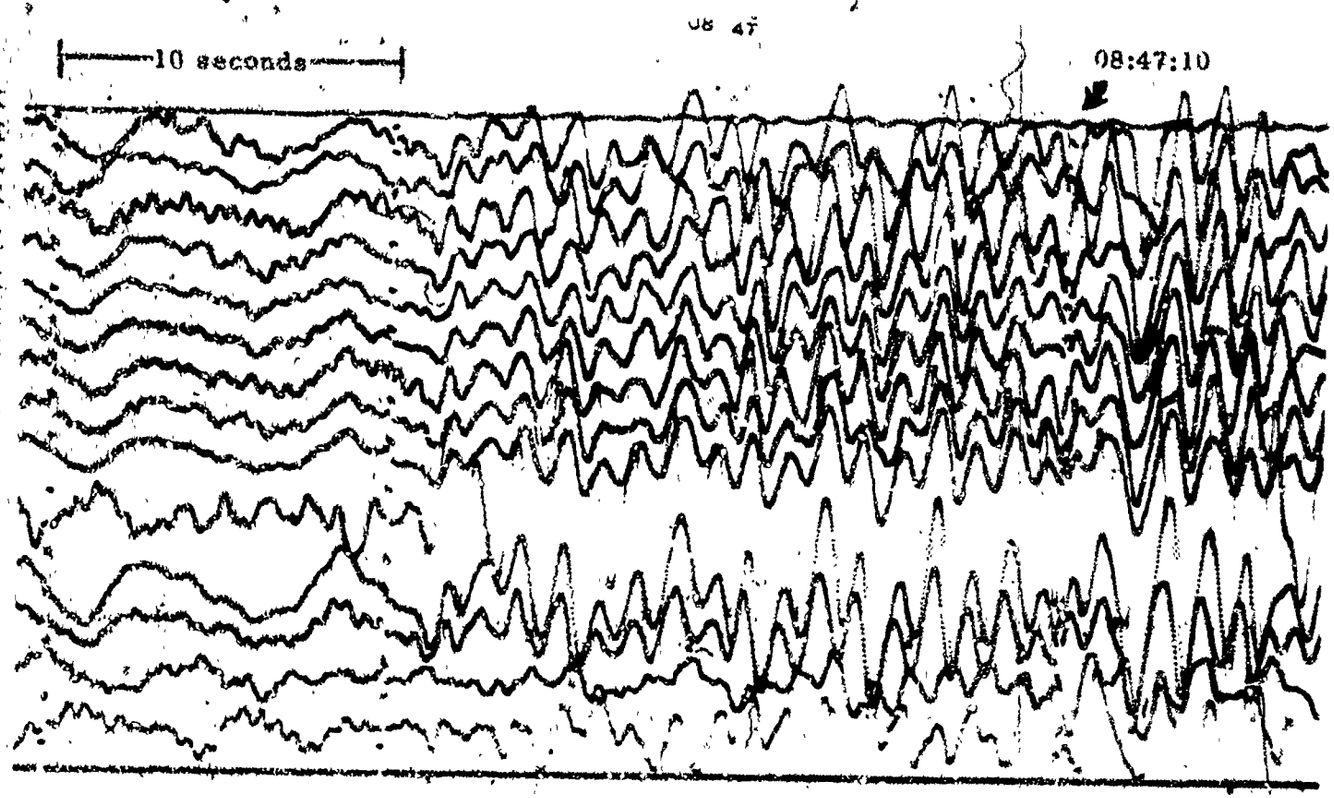

Figure 3-1. WMSO seismogram illustrating a P-phase arrival from the Gulf of California.
Epicentral data: $\delta \approx 14^{\circ}$, h = 14 km, azimuth = 261°, magnitude = 4.6
(X10 enlargement of 16-mm film)

WMSO
Run 034
3 Feb 1964
Data Group 311

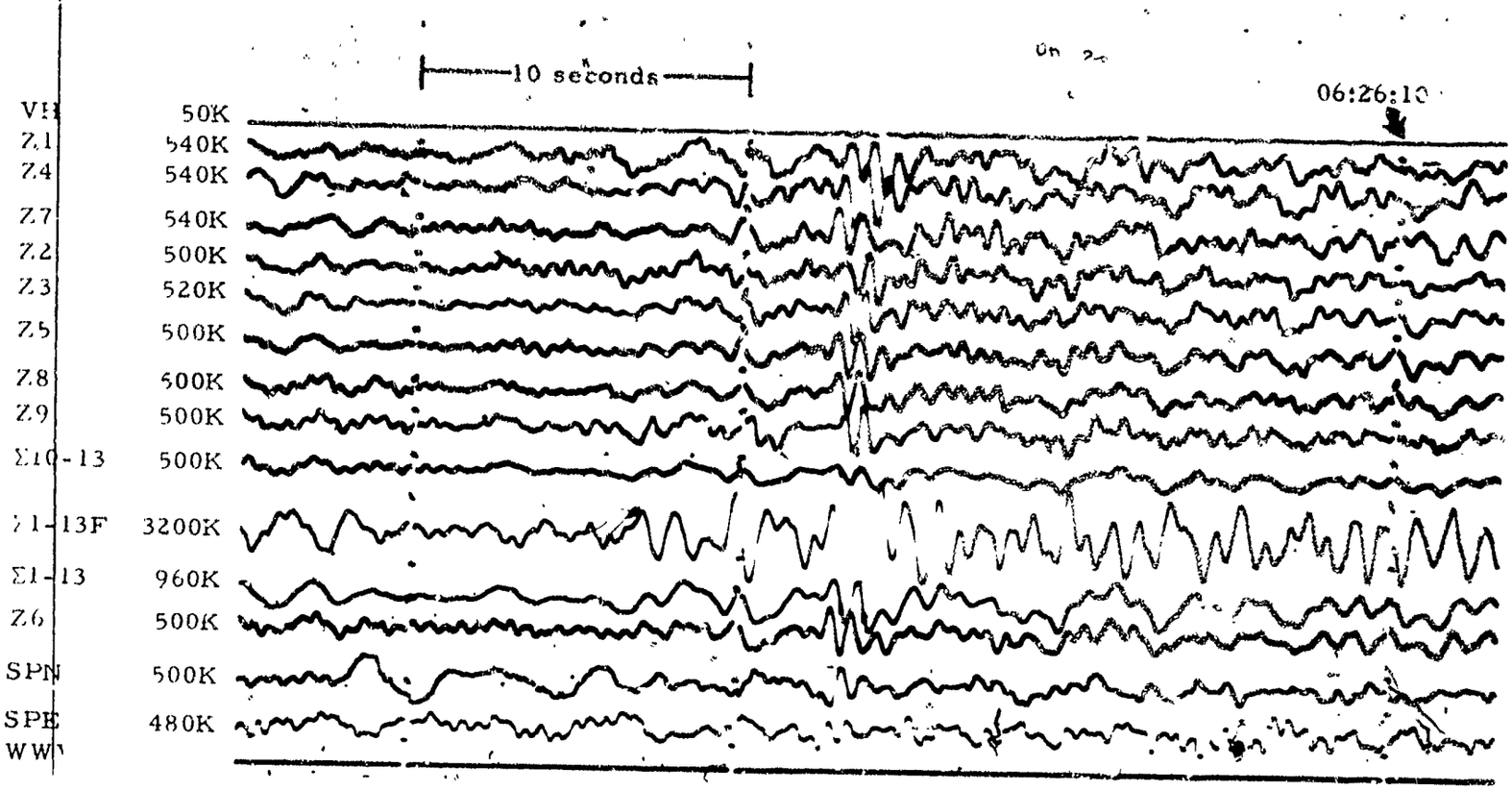

Figure 3-2. WMSO short-period seismogram illustrating a P-phase arrival from Central Idaho. Epicentral data: $\Delta \simeq 16^{\circ}$, $h \simeq 33$ km, azimuth $\simeq 313^{\circ}$, magnitude $\simeq 4.3$ (X10 enlargement of 16-mm film)

WMSO
Run 039
8 Feb 1964
Data Group 311

3.2 DISTANCE = 17° to 40°

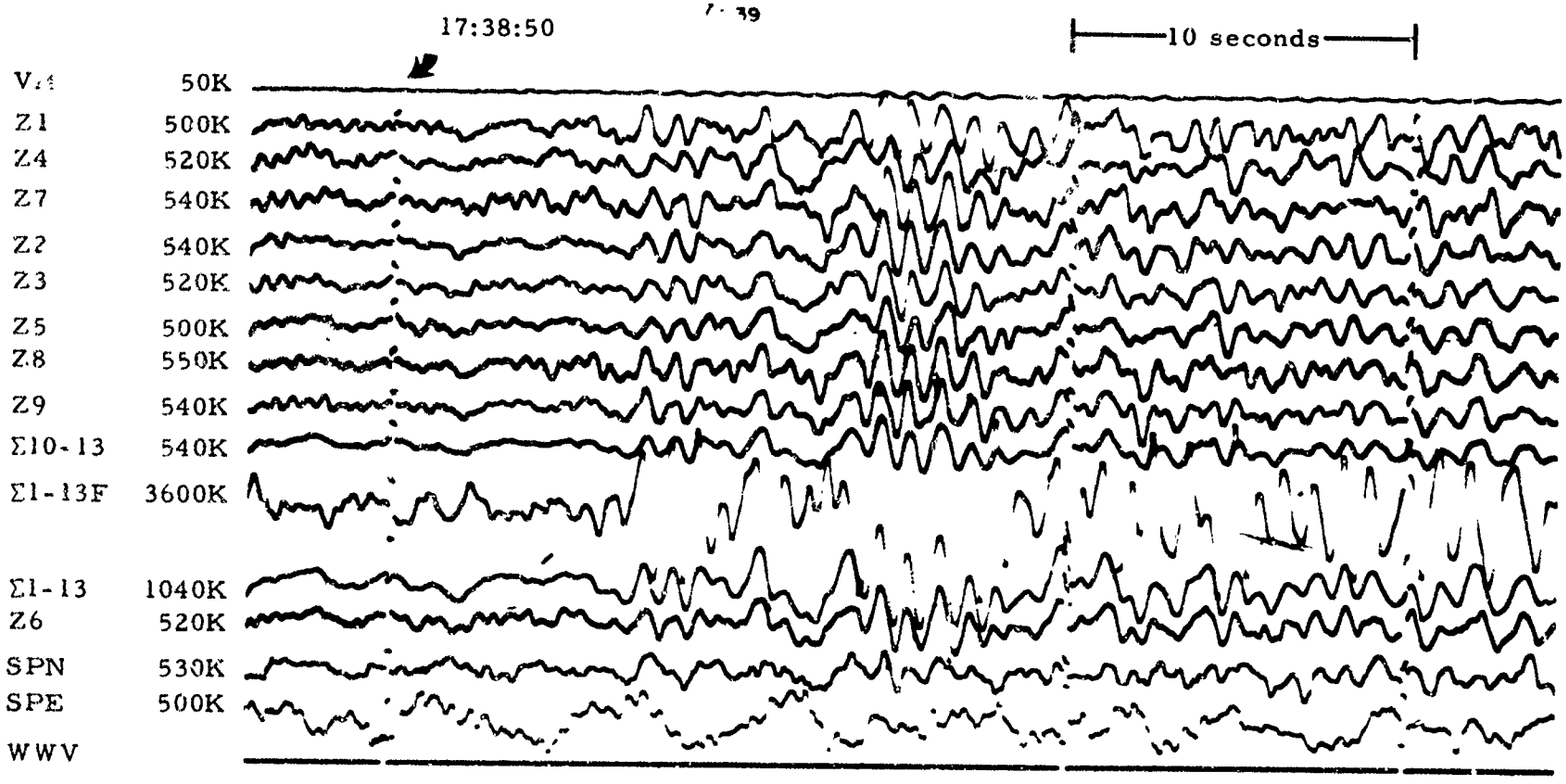

Figure 3-3. WMSO seismogram illustrating a P-phase arrival from Guerrero, Mexico. Epicentral data: $\Delta \simeq 17^{\circ}$, h ≃ 33 km, azimuth ≃ 181°, magnitude ≃ 4.1 (X10 enlargement of 16-mm film)

WMSO
Run 034
3 Feb 1964
Data Group 3003

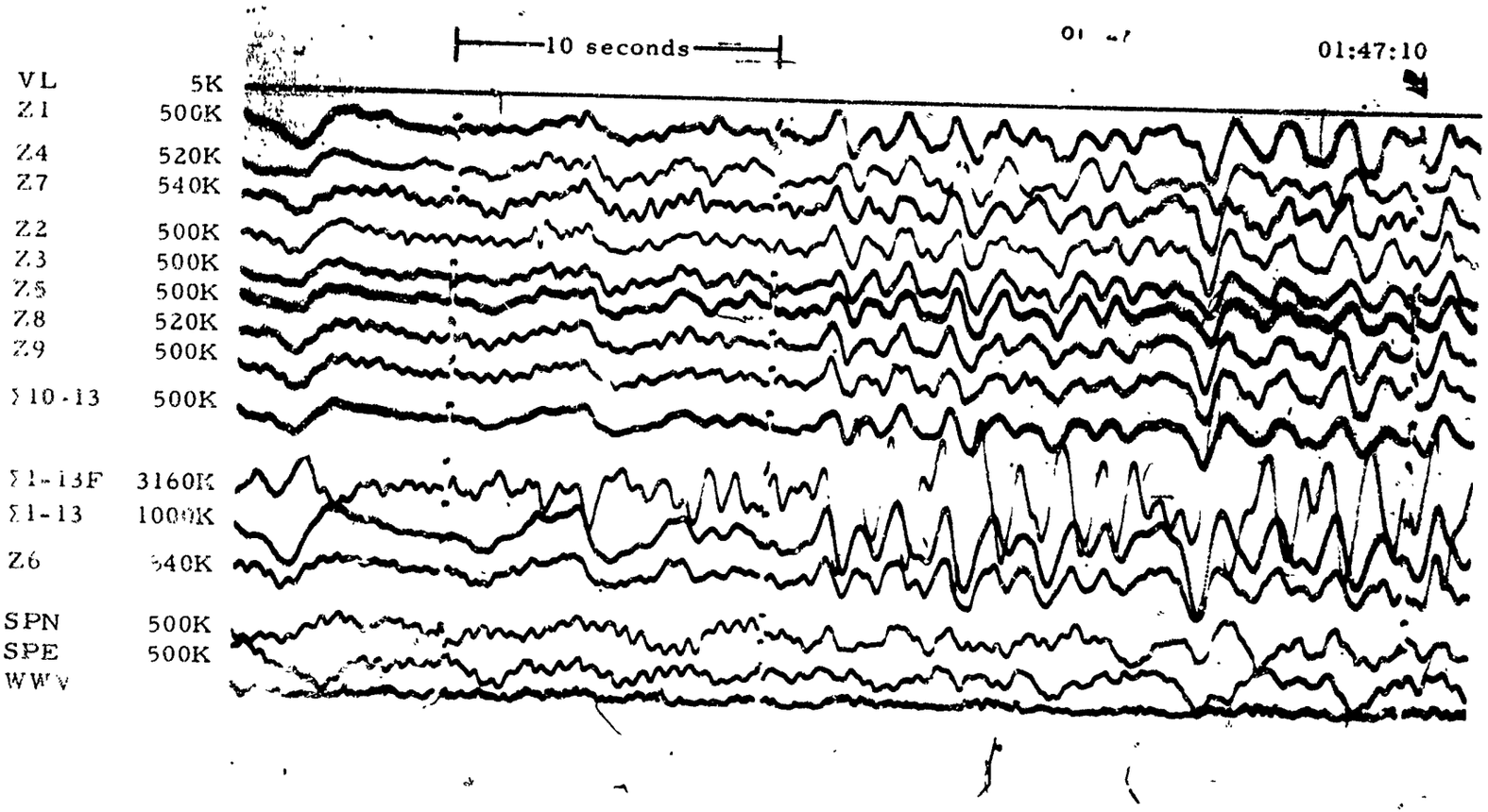

Figure 3-4. WMSO seismogram illustrating a P-phase arrival from the Revilla Gigedo Island region. Epicentral data: $\Delta \simeq 18^{\circ}$, h ≃ 33 km, azimuth ≃ 208°, magnitude ≃ 3.8 (X10 enlargement of 16-mm film)

WMSO
Run 023
23 Jan 1964
Data Group 3-1

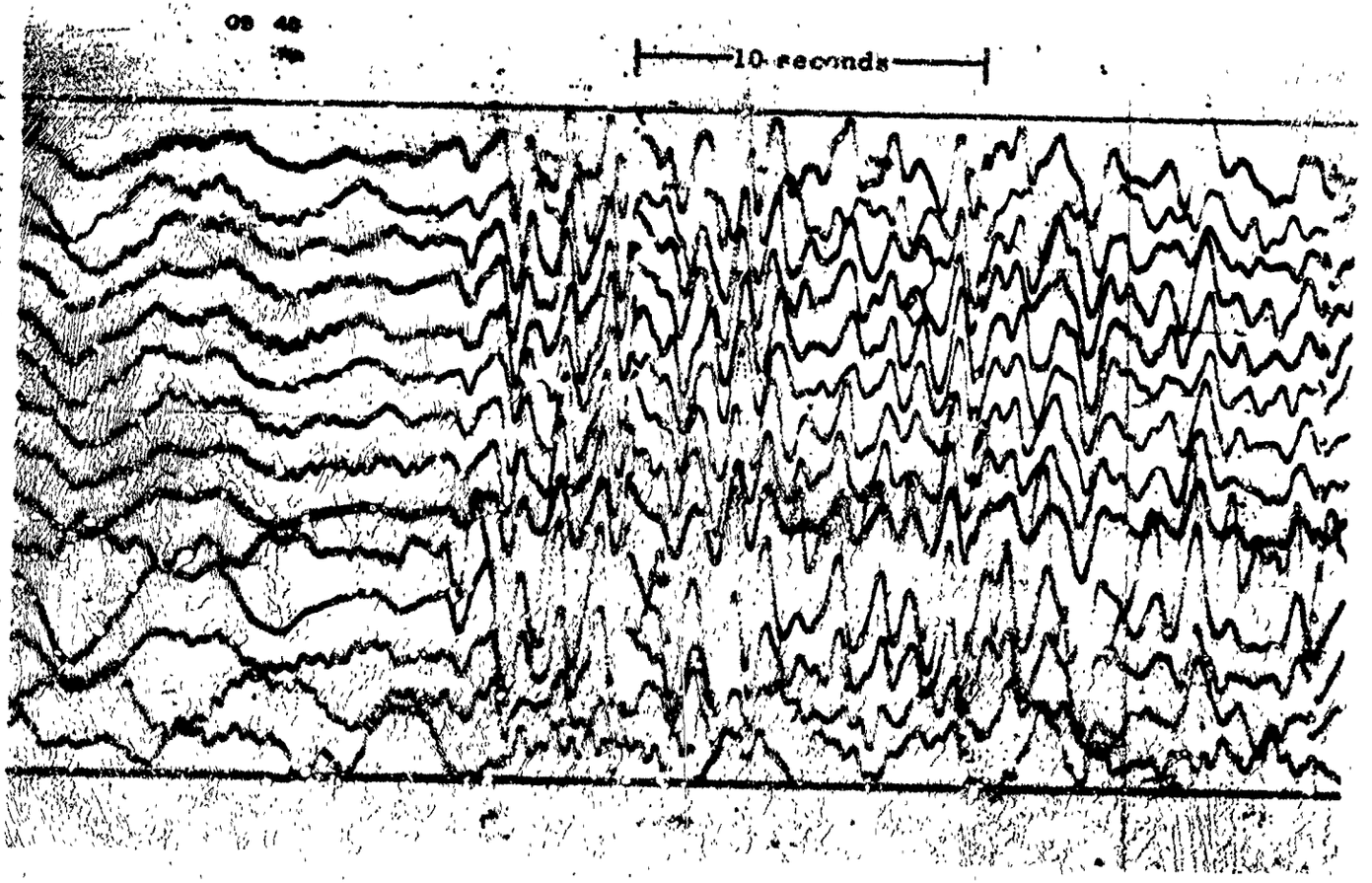

WMSO
Run 001
1 Jan 1964
Data Group 311

Figure 3-5. WMSO short-period seismogram illustrating a P-phase arrival. Epicenter: Jalisco, Mexico, $\Delta \simeq 18^{\circ}$, h ≃ 33 km, azimuth ≃ 204°, magnitude ≃ 4.4 (X10 enlargement of 16-mm film)

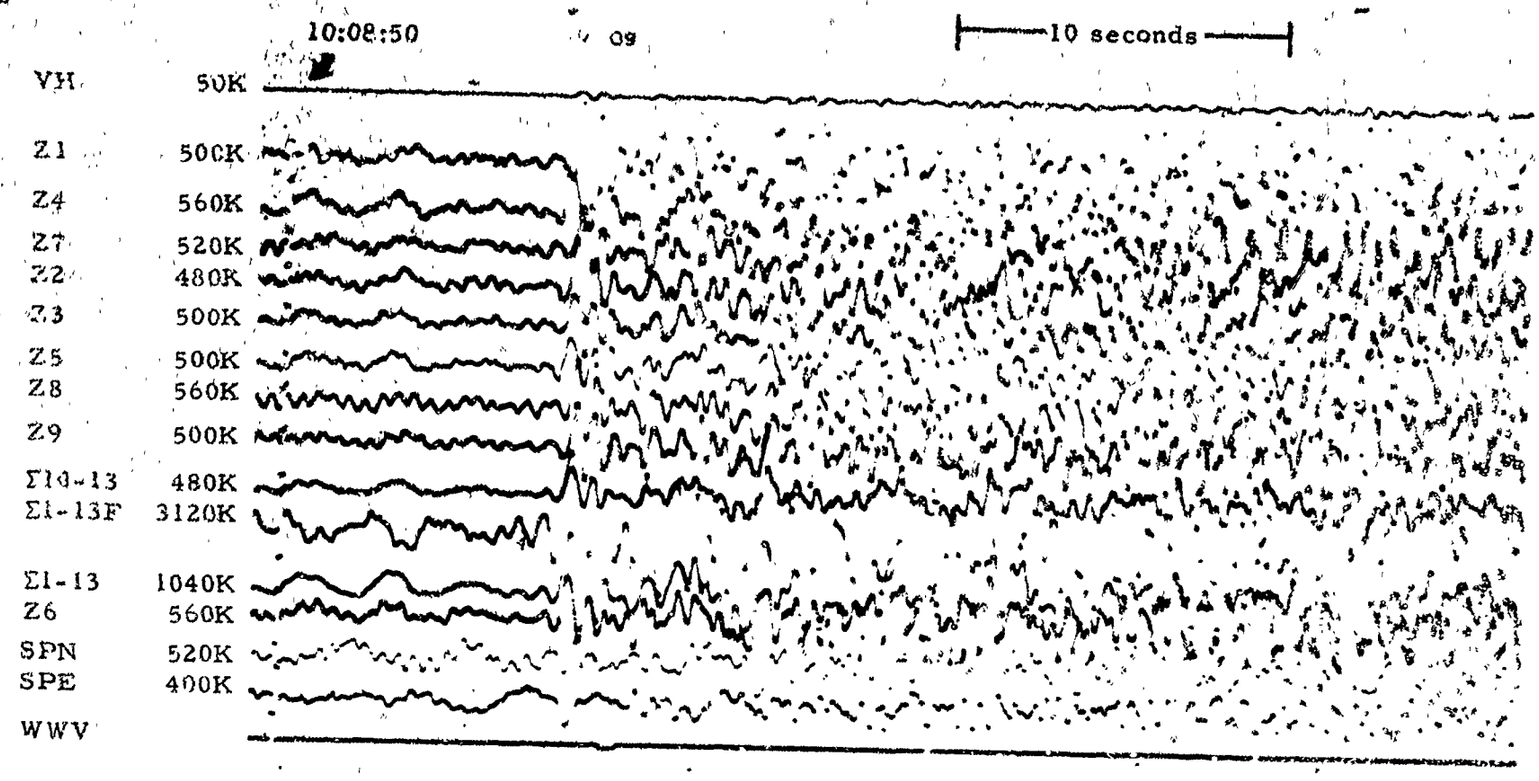

Figure 3-6. WMSO short-period seismogram illustrating a P-phase arrival from the Ontario-Quebec border. Epicentral data: $\Delta \approx 20^{\circ}$, h ≈ 33 km, azimuth ≈ 48°, magnitude ≈ 3.8 (X10 enlargement of 16-mm film)

WMSO
Run 008
8 Jan 1964
Data Group 311

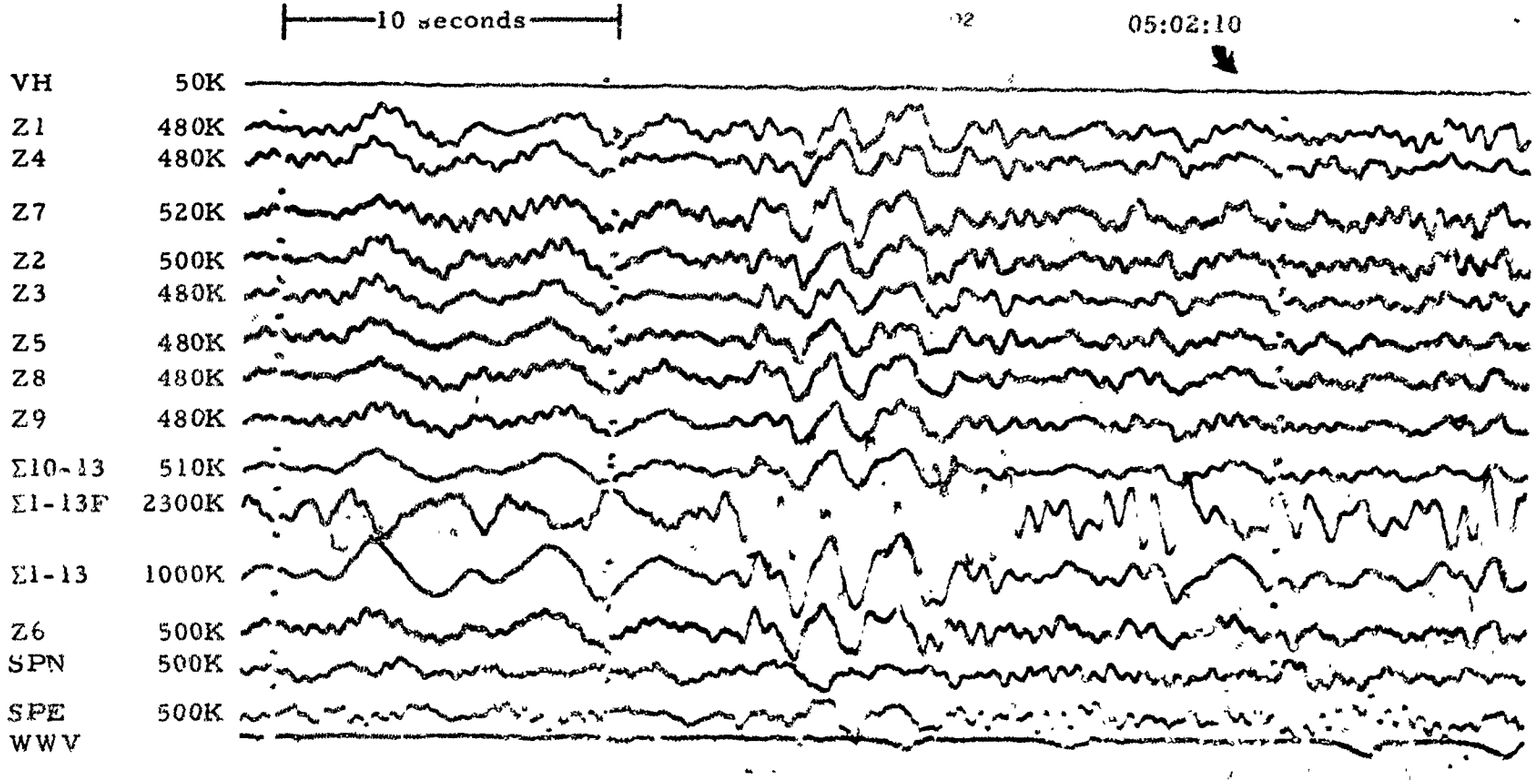

Figure 3-7. WMSO seismogram illustrating a P-phase arrival from off the coast of Oregon. Epicentral data: $\Delta \approx 23^{\circ}$, h ≈ 17 km, azimuth ≈ 300°, magnitude ≈ 4.5 (X10 enlargement of 16-mm film)

WMSO
Run 028
28 Jan 1964
Data Group 311

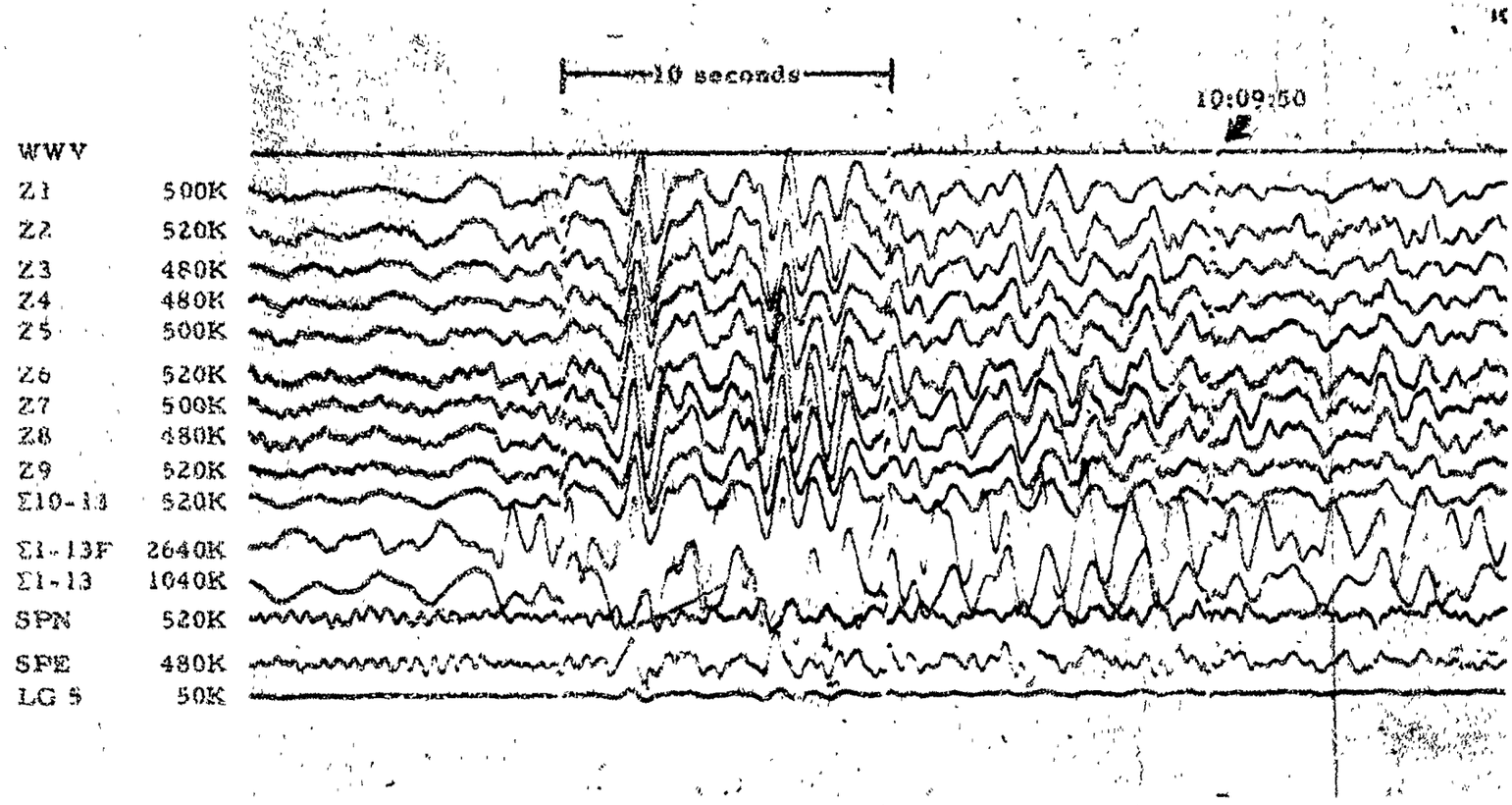

Figure 3-8. WMSO seismogram illustrating a P-phase arrival from off the coast of Oregon. Epicentral data: $\Delta \approx 26^{\circ}$, h = 33 km, azimuth = 302°, magnitude = 3.7 (X10 enlargement of 16-mm film)

WMSO
Run 271
28 Sep 1963

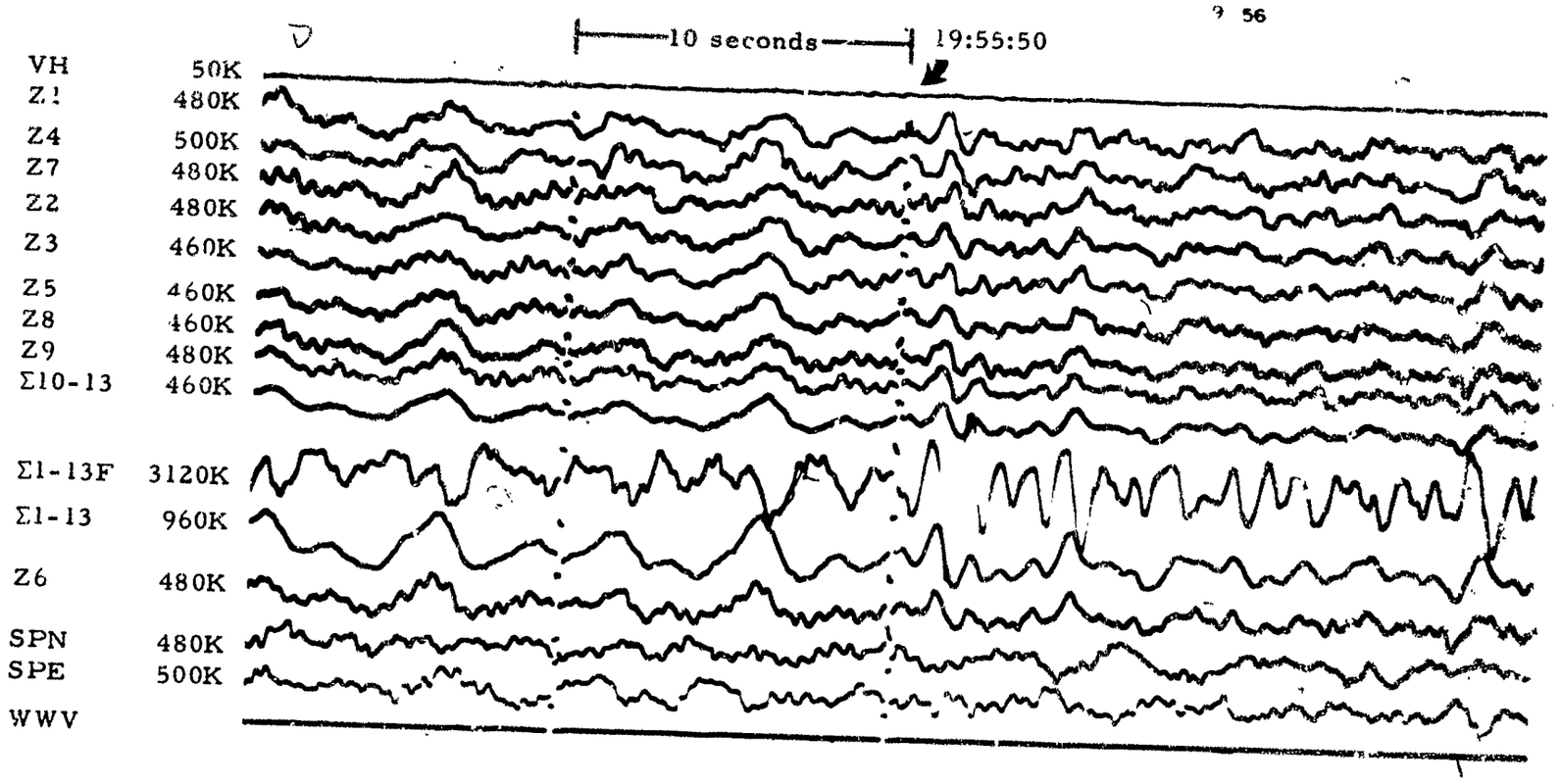

Figure 3-9. WMSO short-period seismogram illustrating a P-phase arrival. Epicenter: near the north coast of Venezuela, $\Delta \simeq 36^{\circ}$, h ≃ 41 km, azimuth ≃ 126°, magnitude ≃ 4.5 (X10 enlargement of 16-mm film)

WMSO
Run 025
25 Jan 1964
Data Group 311

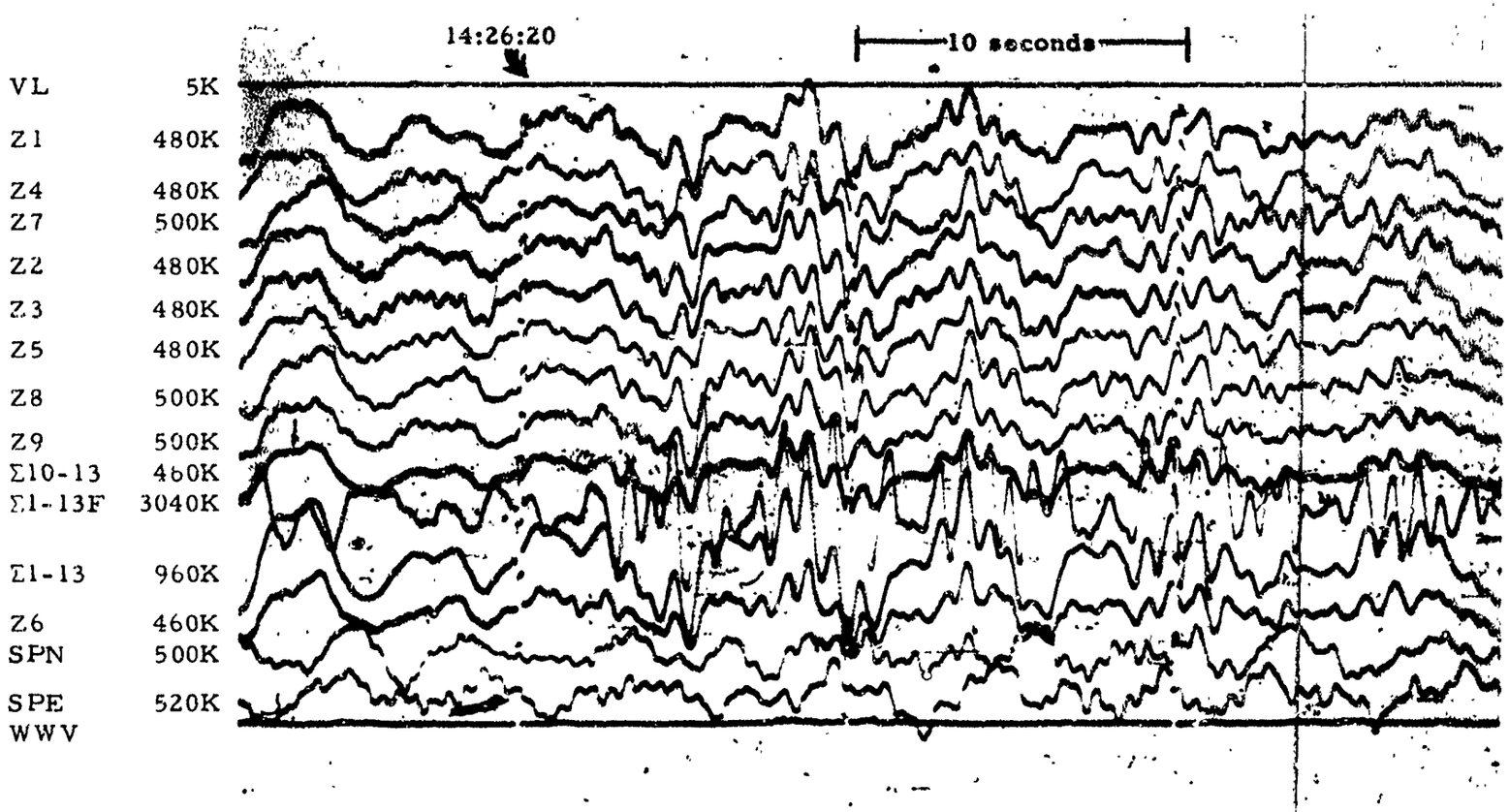

Figure 3-10. WMSO seismogram illustrating a P-phase arrival from the Galapagos Islands. Epicentral data: $\Delta \simeq 39^{\circ}$, h ≃ 33 km, azimuth ≃ 192°, magnitude ≃ 4.6 (X10 enlargement of 16-mm film)

WMSO
Run 001
1 Jan 1964
Data Group 311

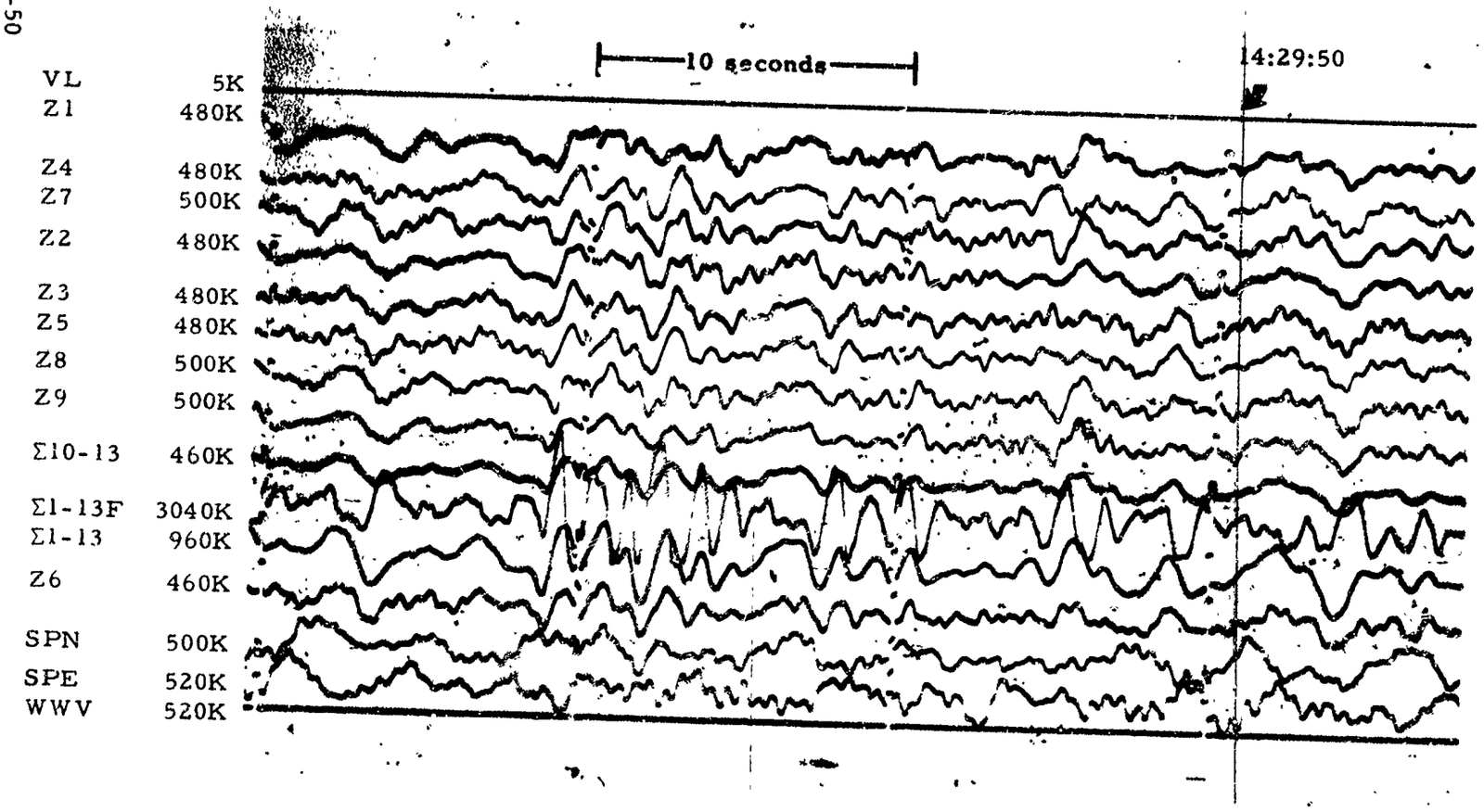

Figure 3-11. WMSO seismogram illustrating a P-phase arrival. Epicenter: near the coast of Southern Chile, $\Delta \simeq 39^{\circ}$, $h \simeq 33$ km, azimuth $\simeq 162^{\circ}$, magnitude $\simeq 4.7$
(X10 enlargement of 16-mm film)

WMSO
Run 001
1 Jan 1964
Data Group 311

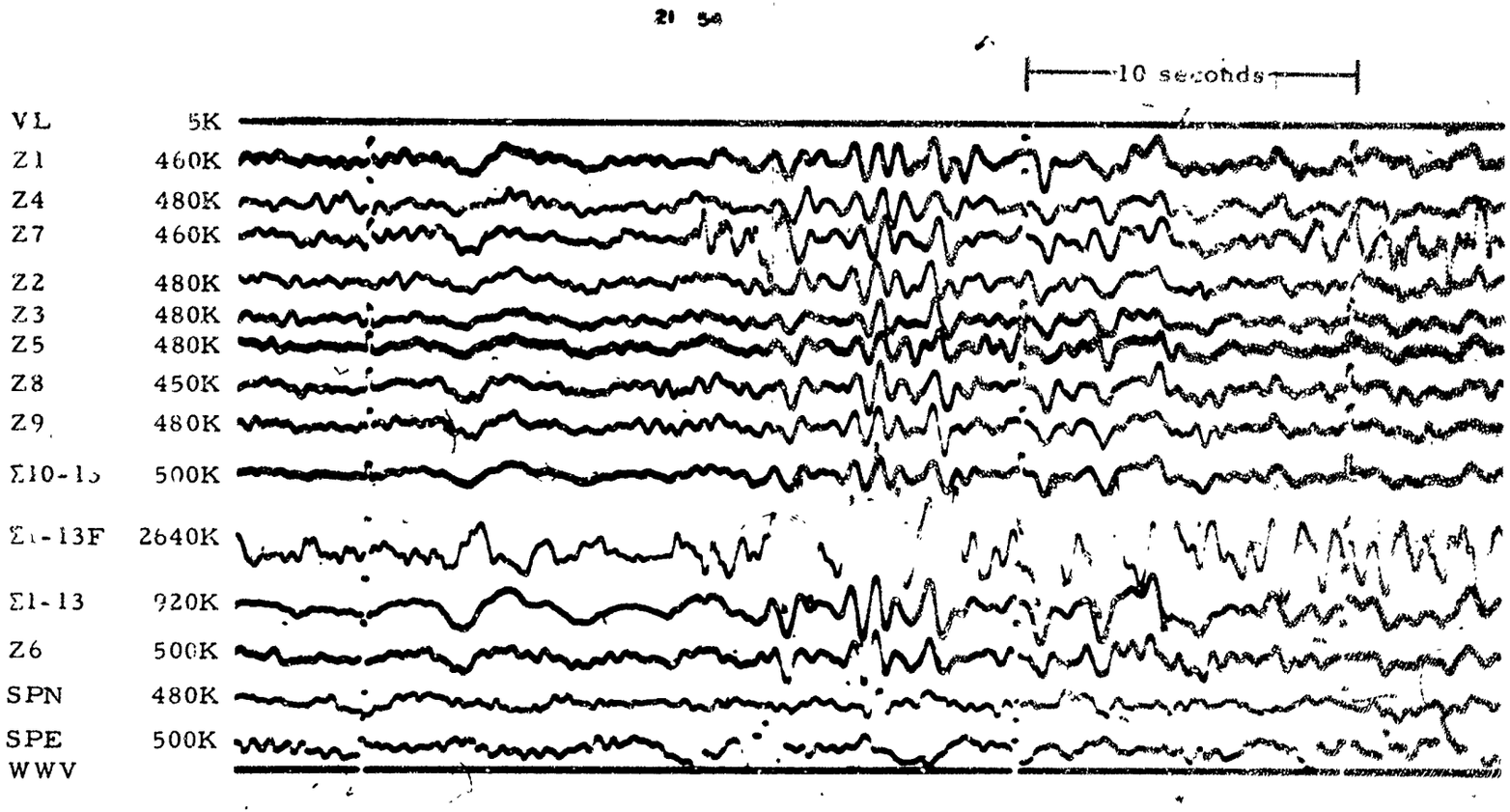

Figure 3-12. WMSO short-period seismogram illustrating a P-phase arrival from Ecuador. Epicentral data: $\Delta \simeq 40^{\circ}$, h ≃ 33 km, azimuth ≃ 147°, magnitude ≃ 4.6 (X10 enlargement of 16-mm film)

WMSO
Run 031
31 Jan 1964
Data Group 311

3.3 DISTANCE = 41° to 60°

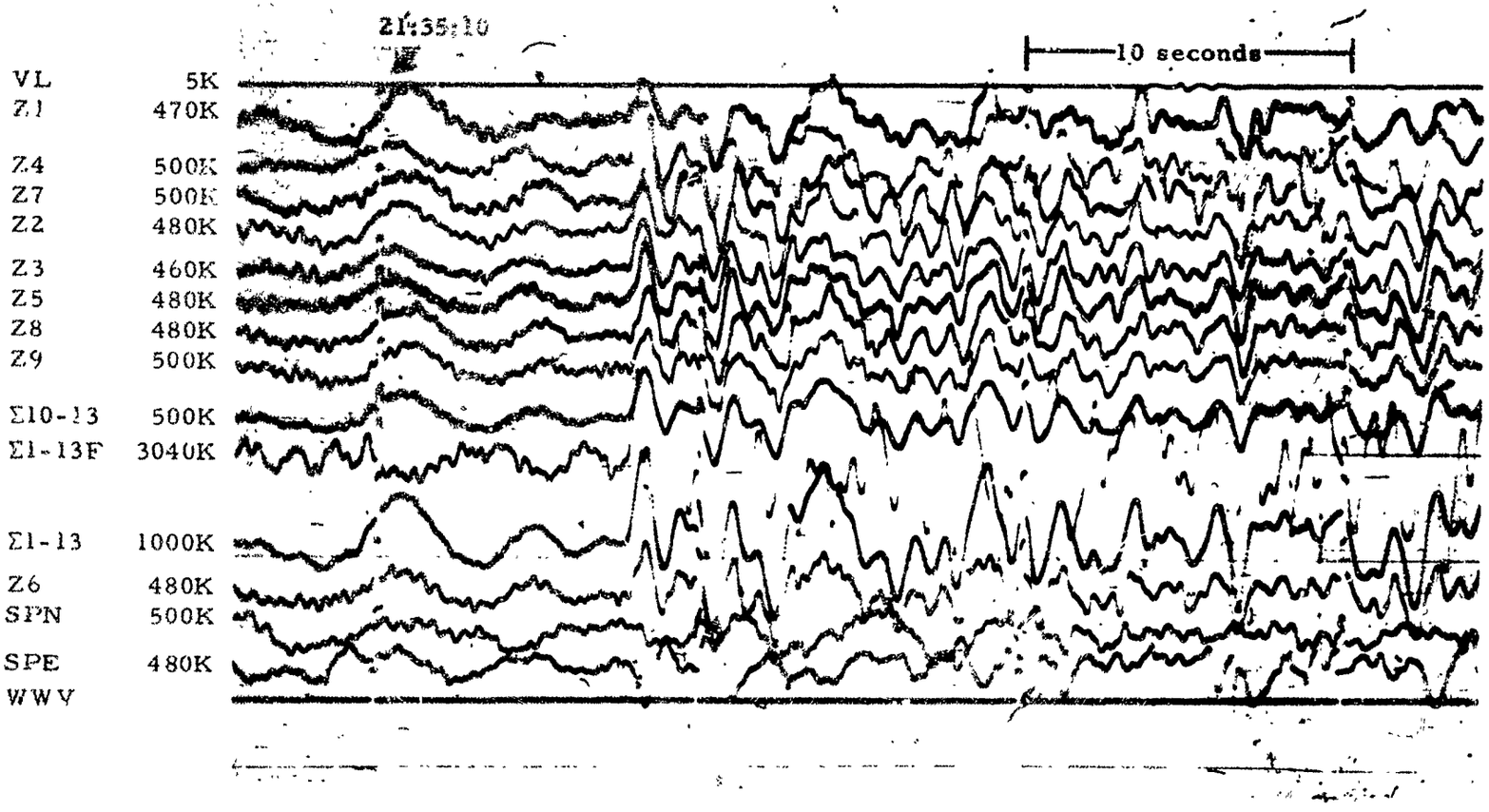

Figure 3-13. WMSO seismogram illustrating a P-phase arrival from the North Atlantic Ocean. Epicentral data: $\Delta \simeq 48^{\circ}$, h ≃ 33 km, azimuth ≃ 88°, magnitude ≃ 4.7 (X10 enlargement of 16-mm film)

WMSO
Run 015
15 Jan 1964
Data Group 311

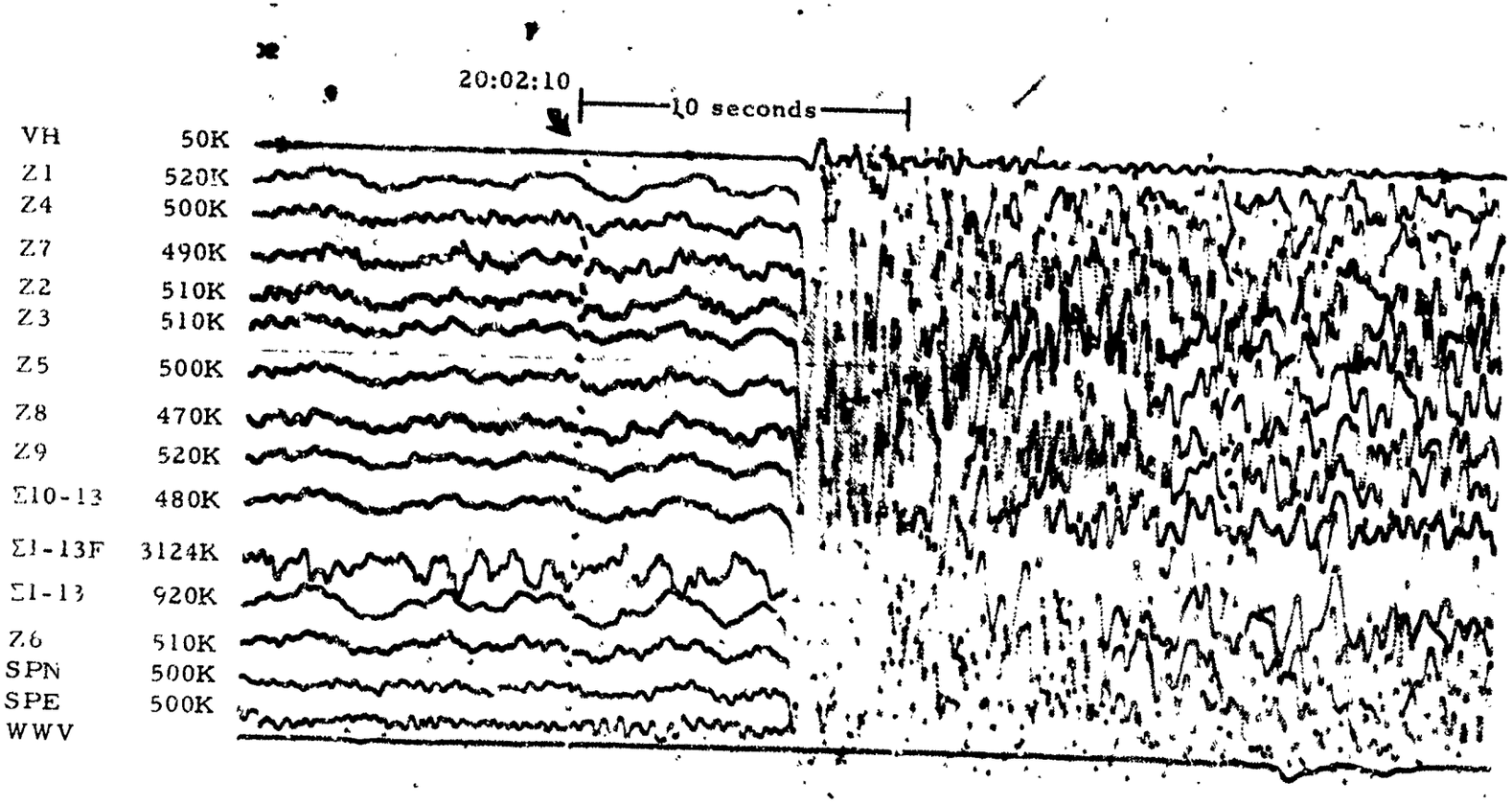

Figure 3-14. An event from Western Brazil as recorded at WMSO. Epicentral data: $\Delta \simeq 51^{\circ}$, h ≃ 585 km, azimuth ≃ 144°, magnitude ≃ 4.9 (X10 enlargement of 16-mm film)

WMSO
Run 315
1 Nov 1963
Data Group 302

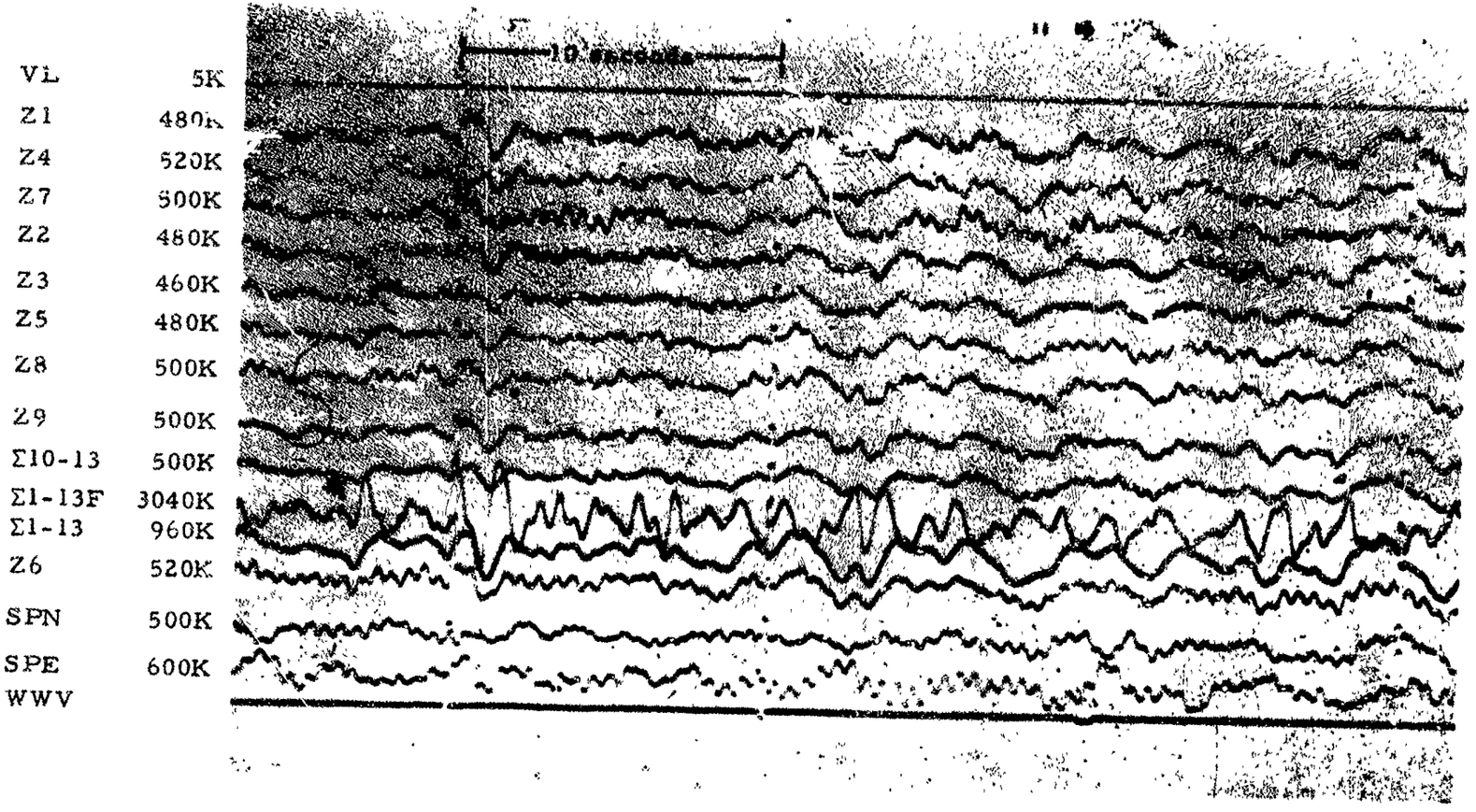

Figure 3-15. WMSO seismogram illustrating a P-phase arrival. Epicenter: south of Hawaii Island, $\Delta \simeq 53^{\circ}$, h ≃ 33 km, azimuth ≃ 268°, magnitude ≃ 4.4 (X10 enlargement of 16-mm film)

WMSO
Run 007
7 Jan 1964
Data Group 311

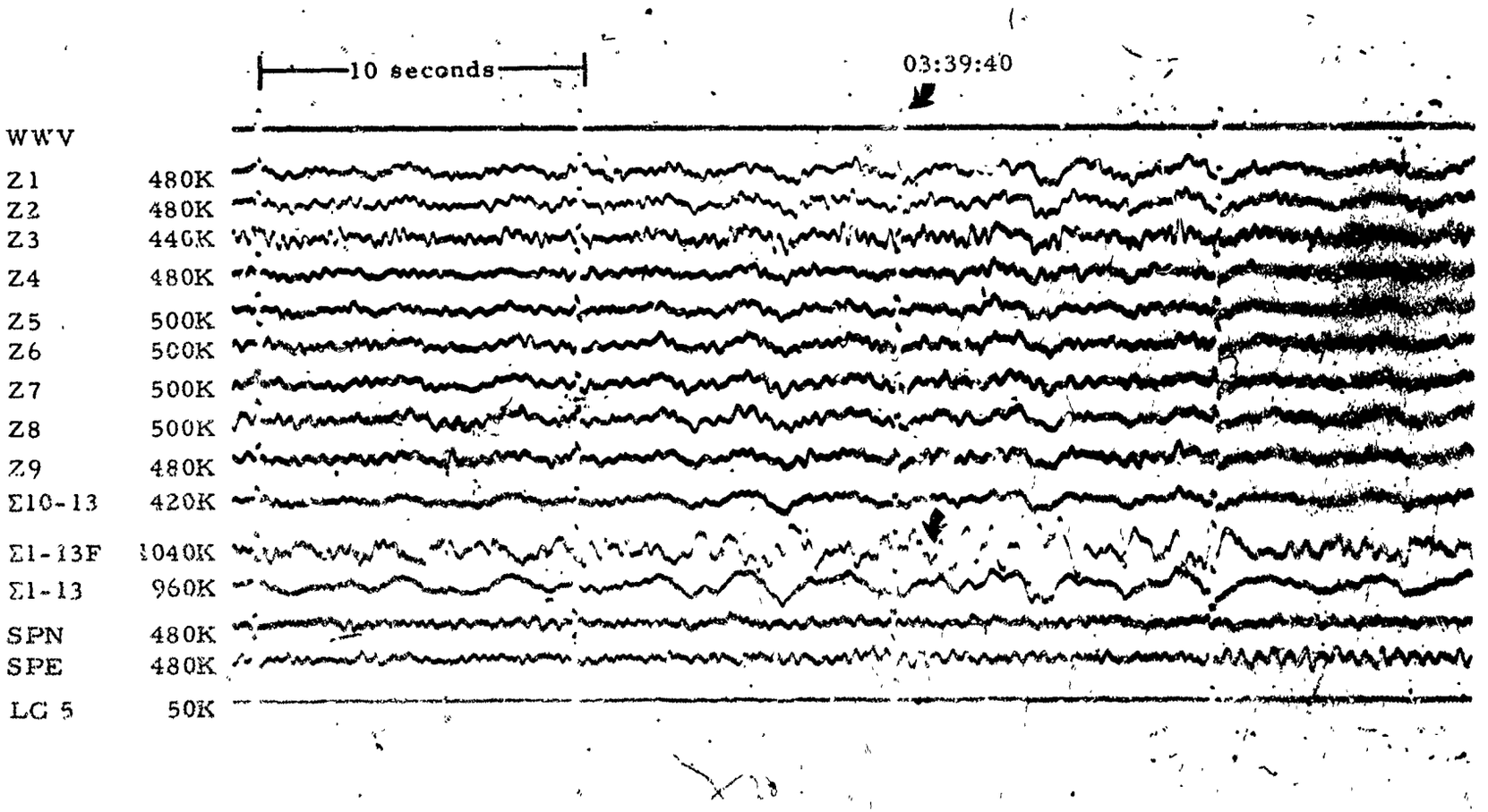

Figure 3-16. WMSO seismogram illustrating a P-phase arrival from the Andreanof Island region. Epicentral data: $\Delta \simeq 56^{\circ}$, h ≃ 33 km, azimuth ≃ 313°, magnitude ≃ 4.1 (X10 enlargement of 16-mm film)

WMSO
Run 247
4 Sep 1963

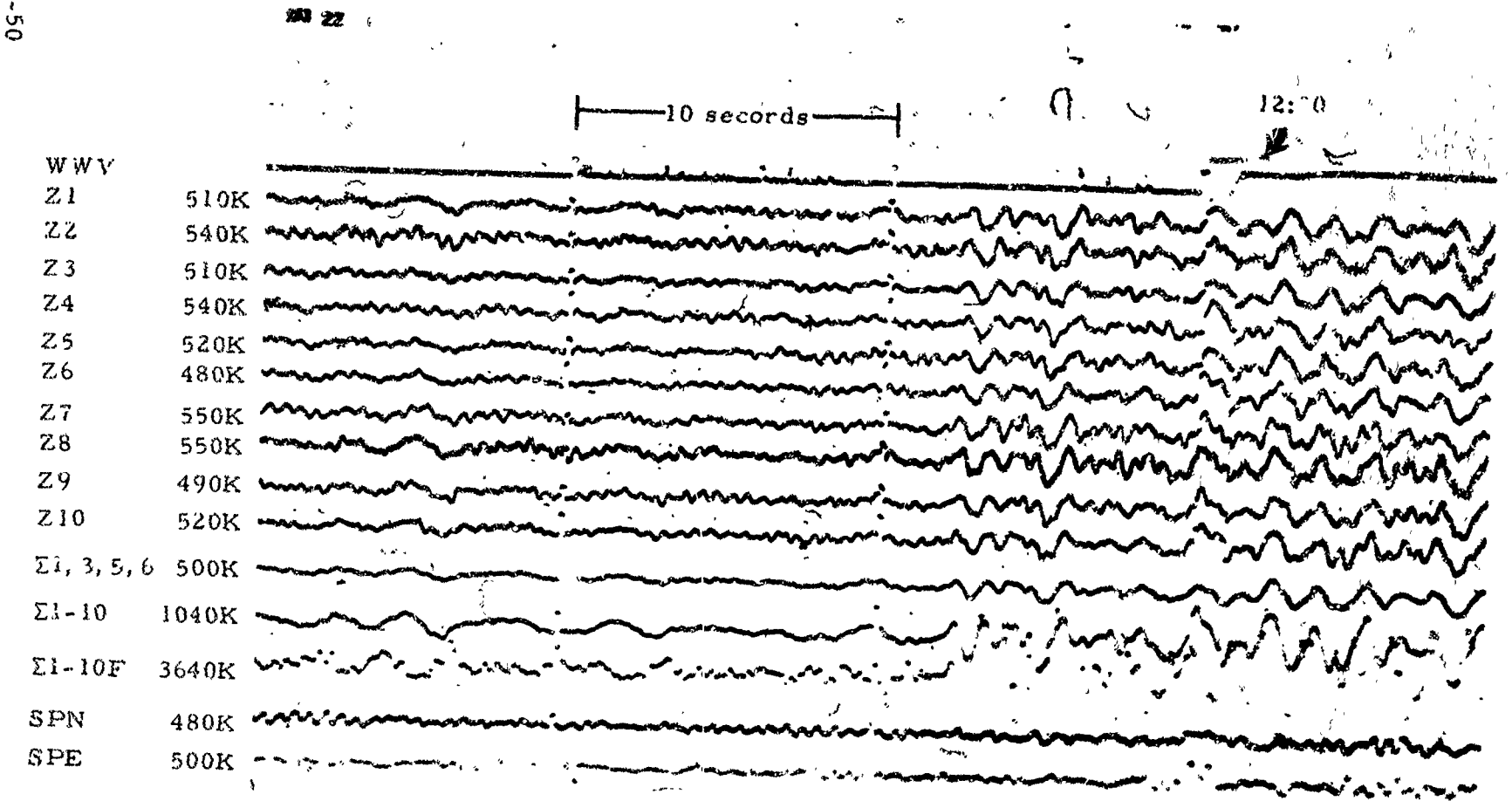

Figure 3-17. WMSO seismogram illustrating a P-phase arrival from the Andreanof Islands region. Epicentral data: $\Delta \simeq 58^{\circ}$, h ≃ 33 km, azimuth ≃ 314°, magnitude ≃ 4.5 (X10 enlargement of 16-mm film)

WMSO
Run 221
9 Aug 1963

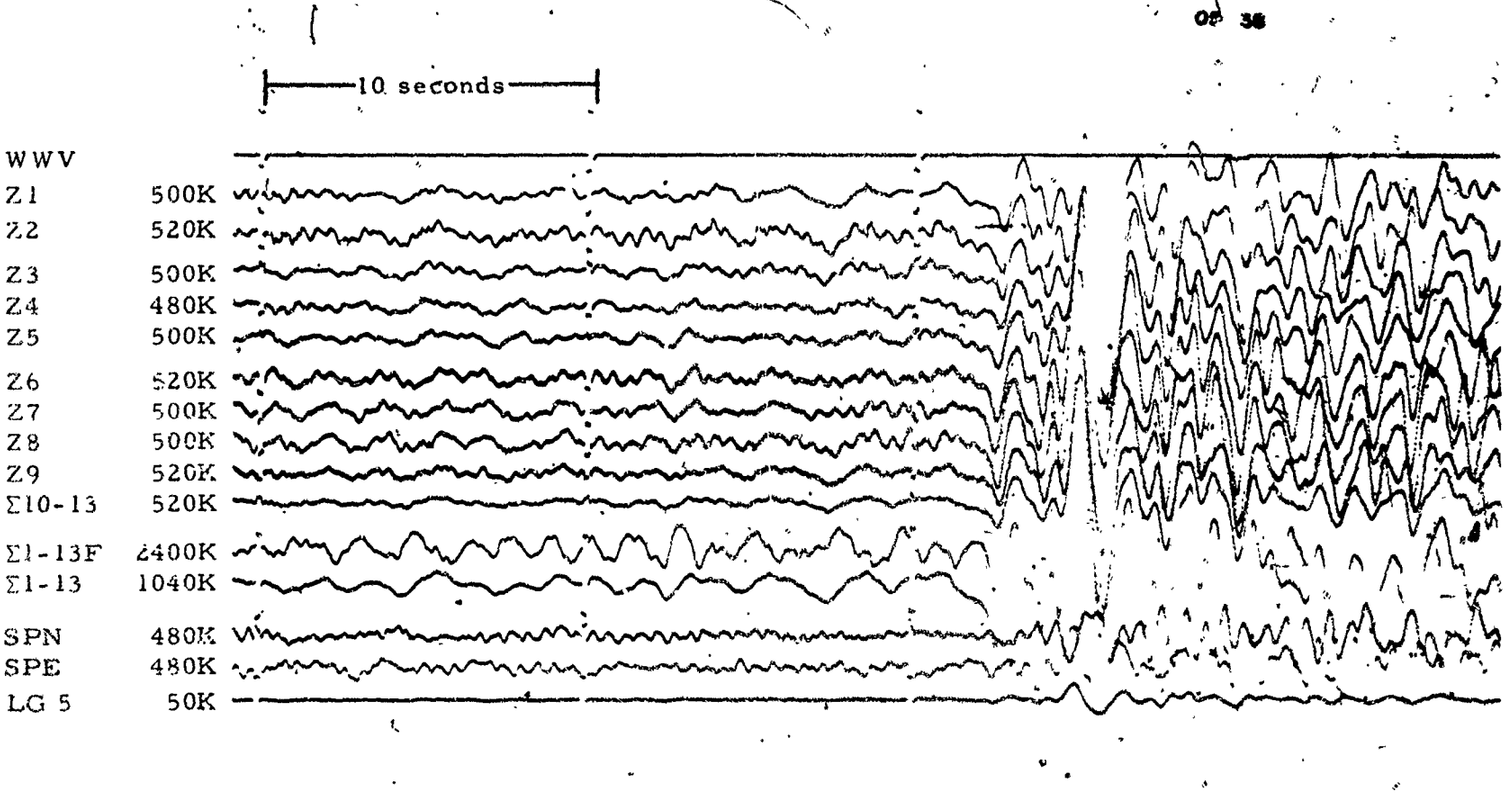

Figure 3-18. WMSO primary short-period seismogram illustrating a P-phase arrival from the Andreanof Islands region. Epicentral data: $\Delta \simeq 57^{\circ}$, $h \simeq 33$ km, azimuth $\simeq 312^{\circ}$, magnitude $\simeq 5.3$ (X10 enlargement of 16-mm film)

WMSO
Run 269
26 Sep 1963

3.4 DISTANCE = 61° to 80°

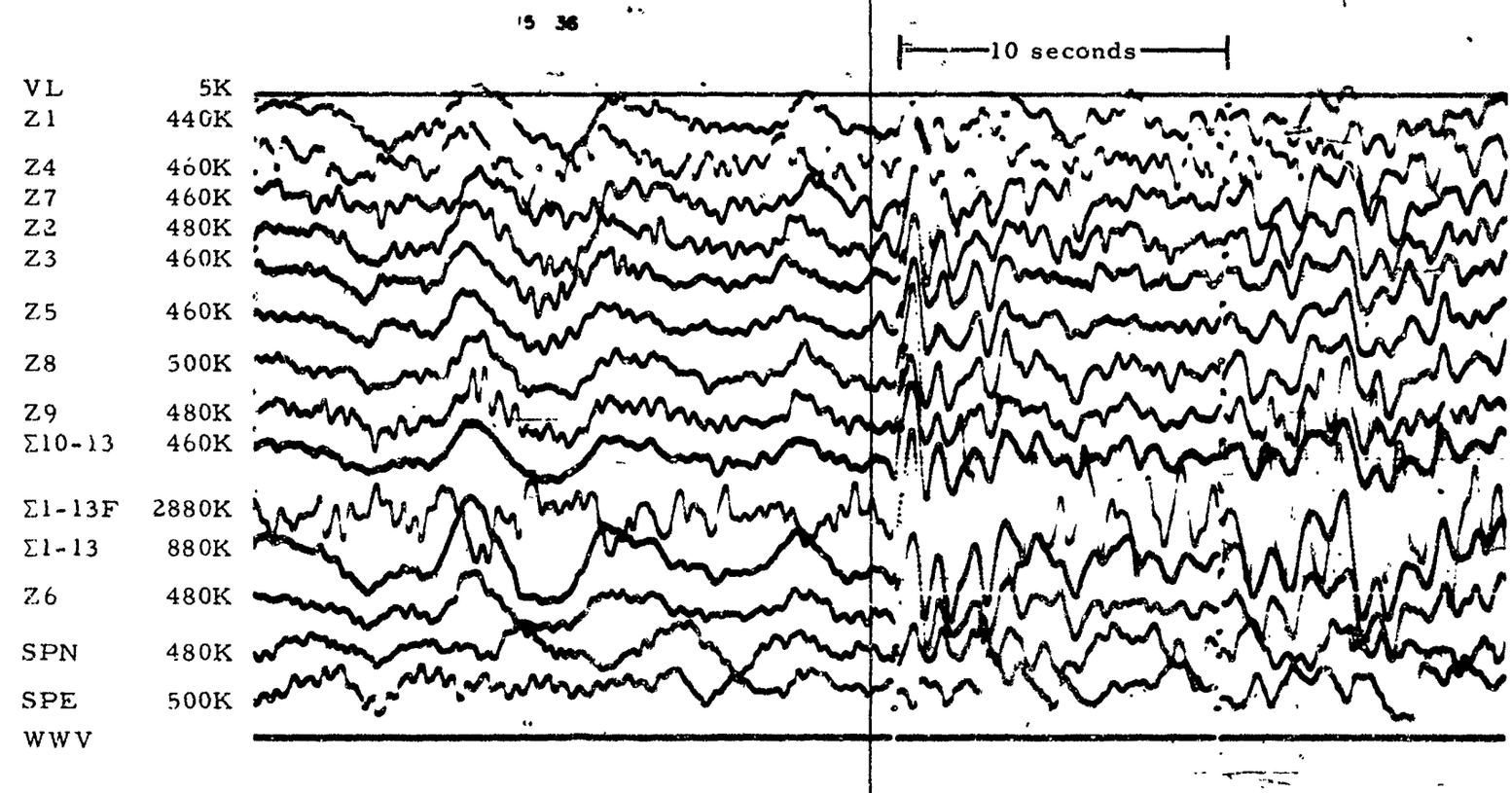

Figure 3-19. WMSO seismogram illustrating a P-phase arrival. Epicenter: near the coast of Northern Chile, $\Delta \simeq 62^{\circ}$, h = 30 km, azimuth $\simeq 150^{\circ}$, magnitude $\simeq 5.2$ (X10 enlargement of 16-mm film)

WMSO
Run 050
19 Feb 1964
Data Group 3003

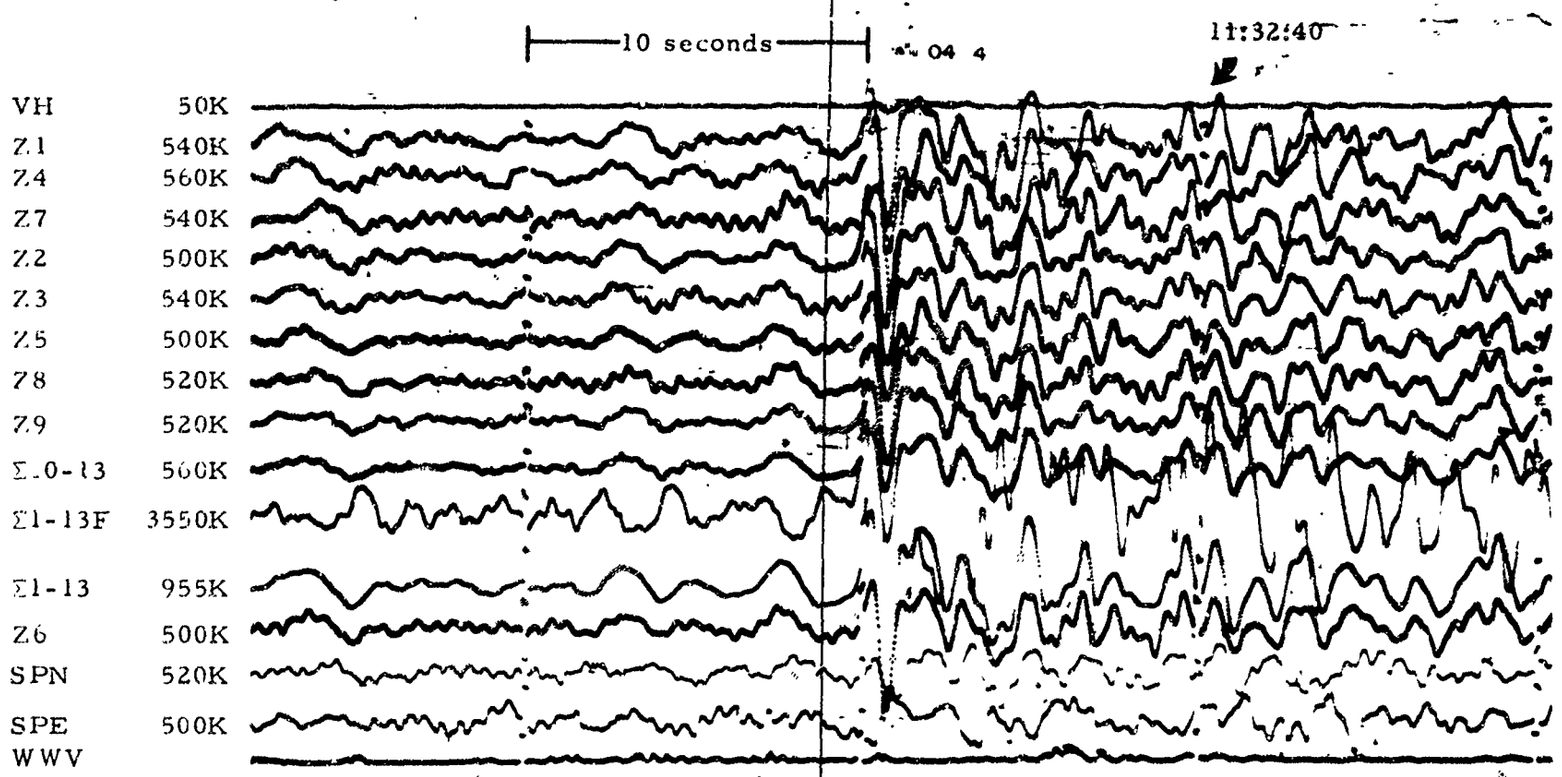

Figure 3-20. WMSO seismogram illustrating a P-phase arrival from the Bolivia-Brazil border. Epicentral data: $\Delta \simeq 66^{\circ}$, h ≃ 3? km, azimuth ≃ 136°, magnitude ≃ 5.3 (X10 enlargement of 16-mm film)

WMSO
Run 044
13 Feb 1964
Data Group 3003

TR 64-50

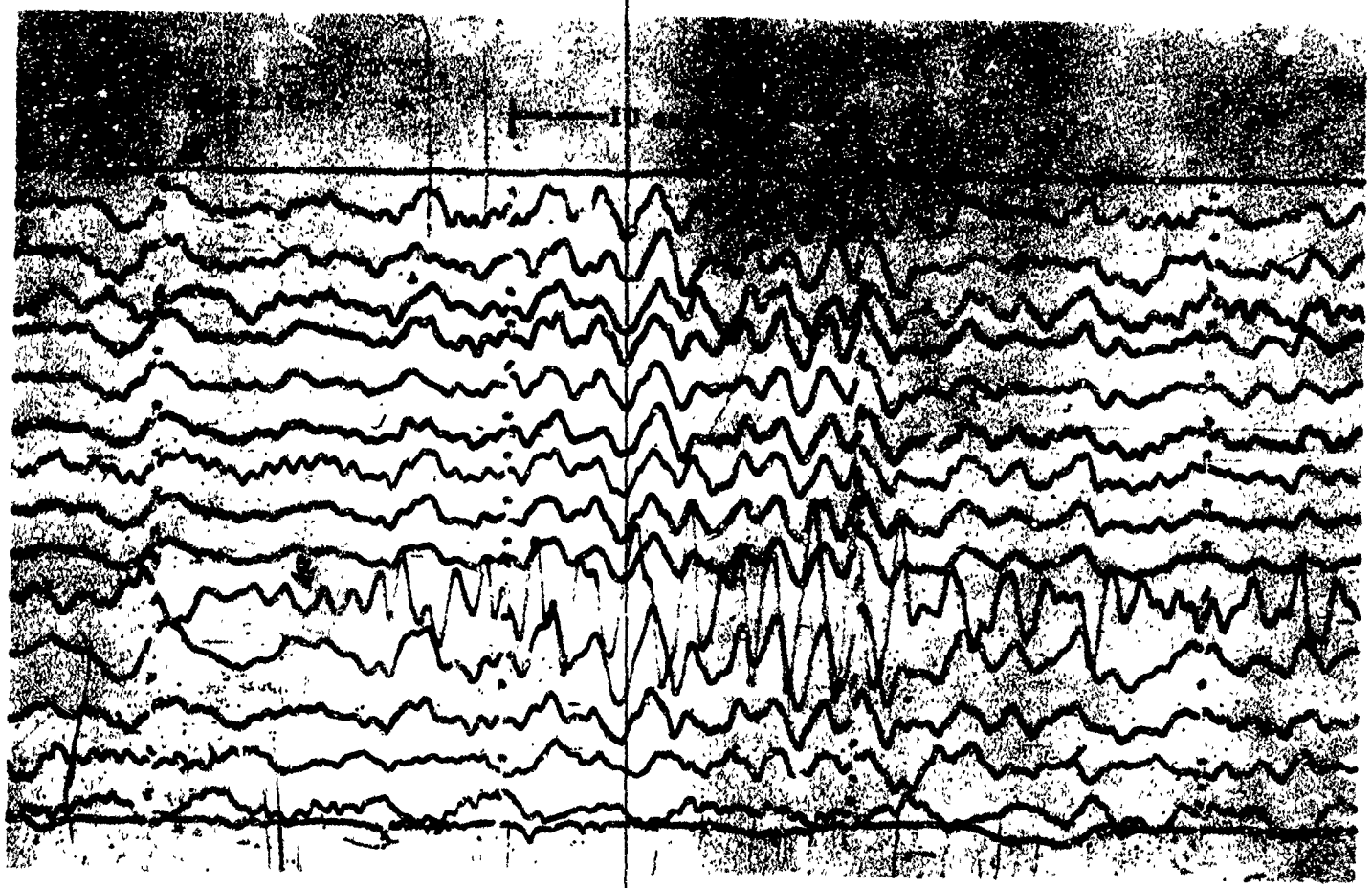

Figure 3-21. WMSO seismogram illustrating a P-phase arrival from the Easter Island region. Epicentral data: $\Delta \simeq 67^{\circ}$, $h \simeq 33$ km, azimuth $\simeq 186^{\circ}$, magnitude $\simeq 4.5$ (X10 enlargement of 16-mm film)

WMSO
Run 018
18 Jan 1964
Data Group 311

TR 64-50

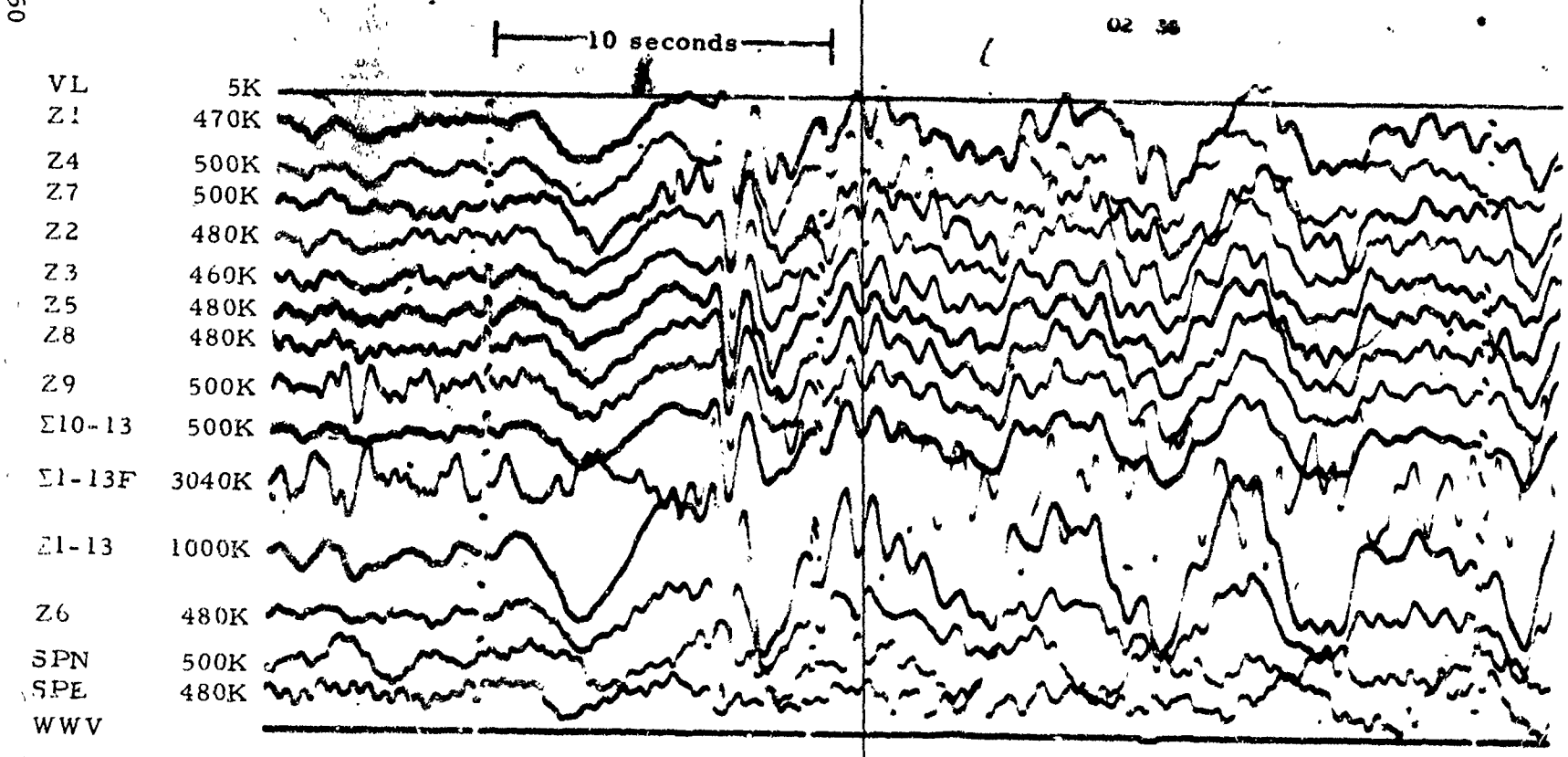

Figure 3-22. WMSO seismogram illustrating a P-phase arrival fromthe Kurile Islands.
Epicentral data: $\Delta \simeq 79^{\circ}$, h ≃ 45 km, azimuth ≃ 318°, magnitude ≃ 5.3
(X10 enlargement of 16-mm film)

WMSO
Run 015
15 Jan 1964
Data Group 311

3.5 DISTANCE = 81° to 100°

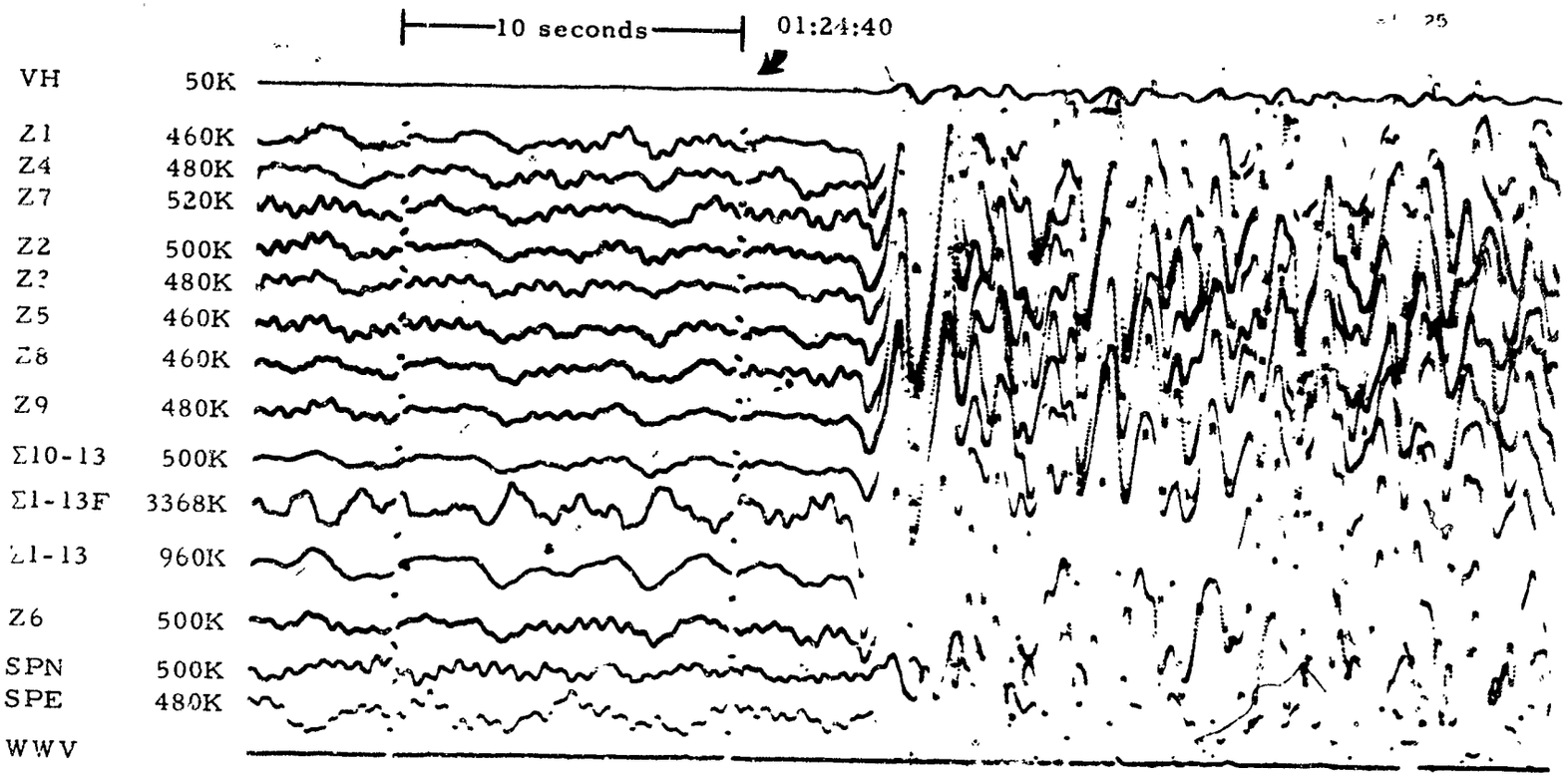

Figure 3-23. WMSO seismogram illustrating a P-phase arrival from the mid-Atlantic Ocean. Epicentral data: $\Delta \simeq 82^{o}$, h ≃ 33 km, azimuth ≃ 95°, magnitude ≃ 5.3 (X10 enlargement of 16-mm film)

WMSO
Run 027
27 Jan 1964
Data Group 311

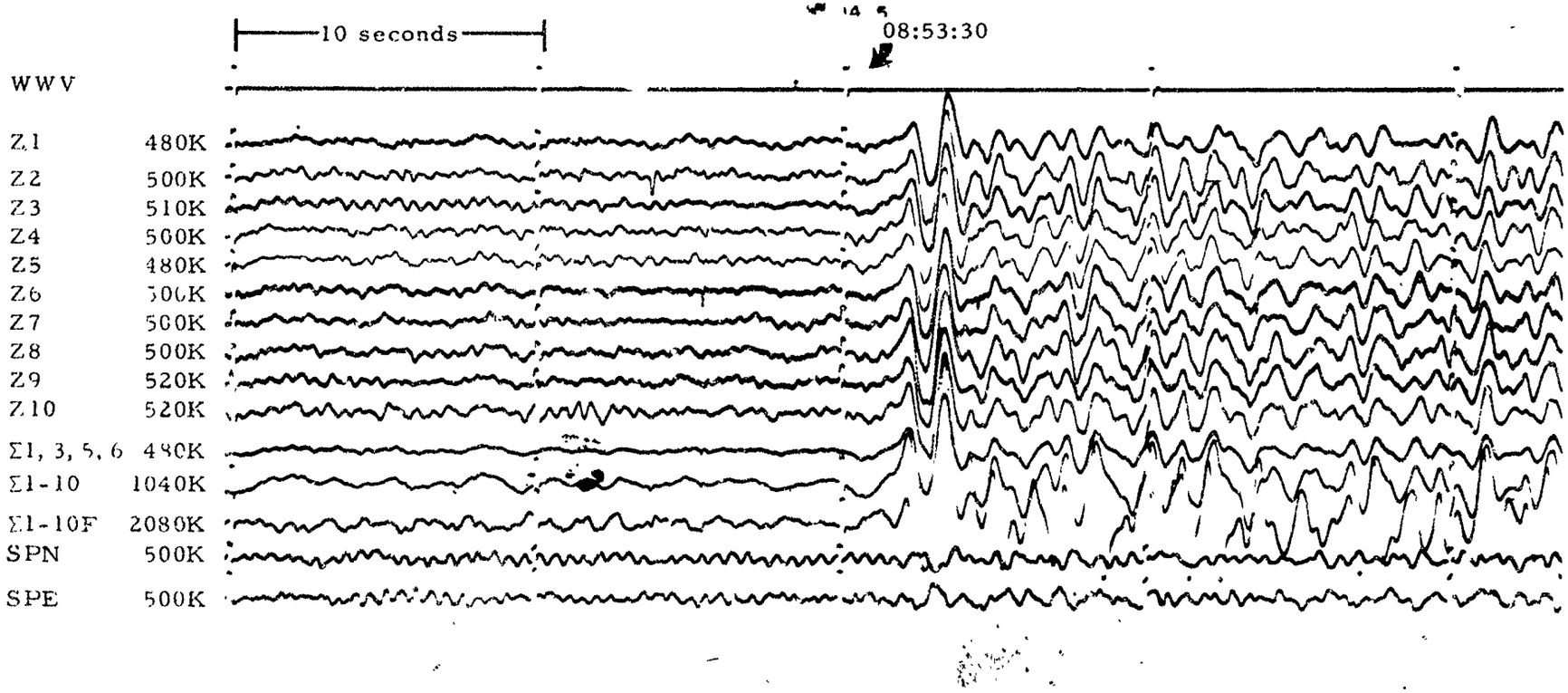

Figure 3-24. WMSO seismogram illustrating a P-phase arrival. Epicenter: near the east coast of Hokkaido, $\Delta \simeq 84^{\circ}$, h ≃ 80 km, azimuth ≃ 319°, magnitude ≃ 5.4 (X10 enlargement of 16-mm film)

WMSO
Run 145
25 May 1963

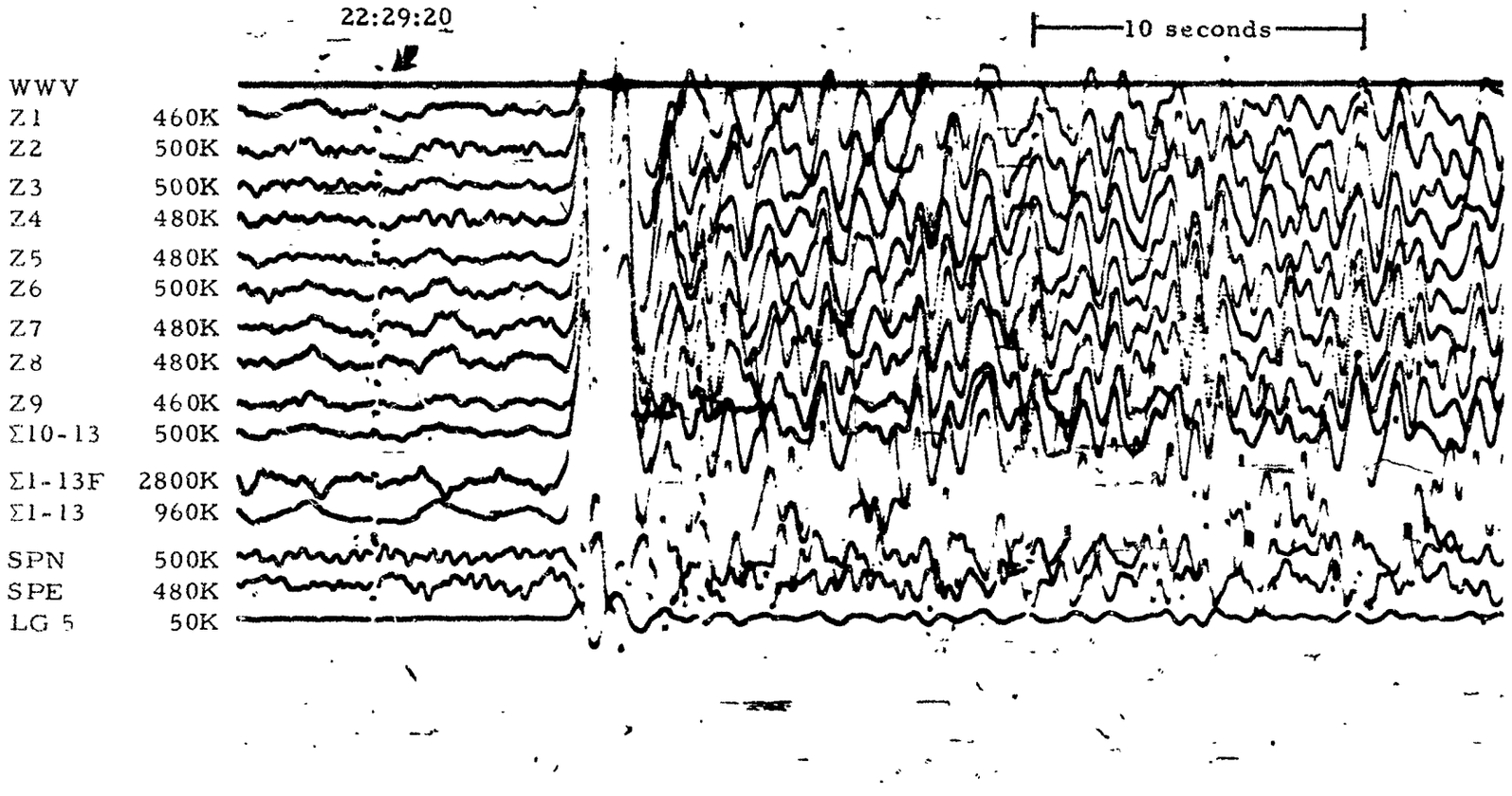

Figure 3-25. WMSO short-period seismogram illustrating a P-phase arrival from the Ionian Sea. Epicentral data: $\Delta \simeq 88^{\circ}$, $h \simeq 47$ km, azimuth $\simeq 46^{\circ}$, magnitude $\simeq 5.3$ (X10 enlargement of 16-mm film)

WMSO
Run 27
29 Sep 1963

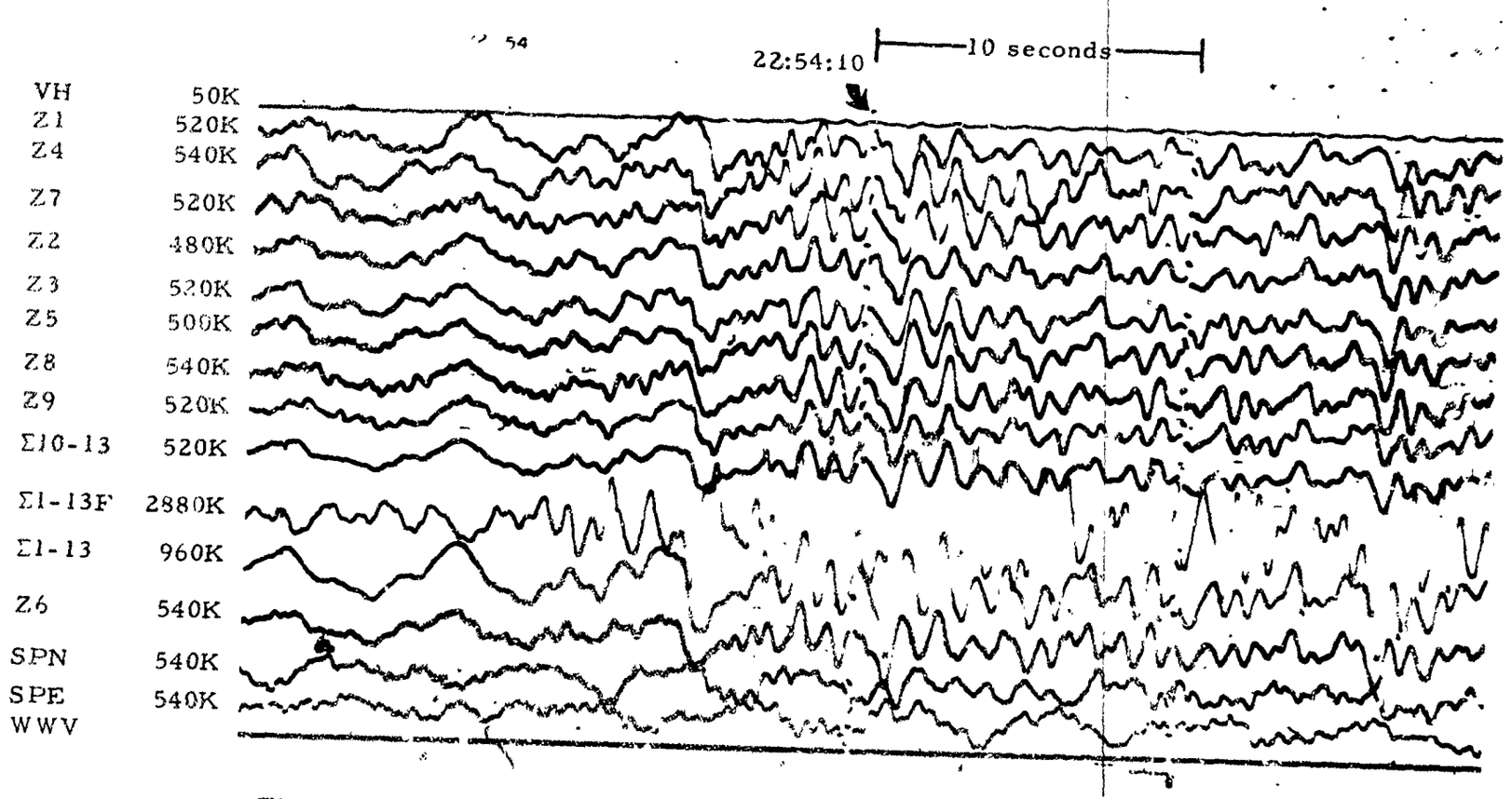

Figure 3-26. WMSO short-period seismogram illustrating a P-phase arrival from the Aegean Sea. Epicentral data: $\Delta \approx 89^{\circ}$, $h \approx 33$ km, azimuth $\approx 41^{\circ}$, magnitude ≈ 4.5 (X10 enlargement of 16-mm film)

WMSO
Run 054
23 Feb 1964
Data Group 3003

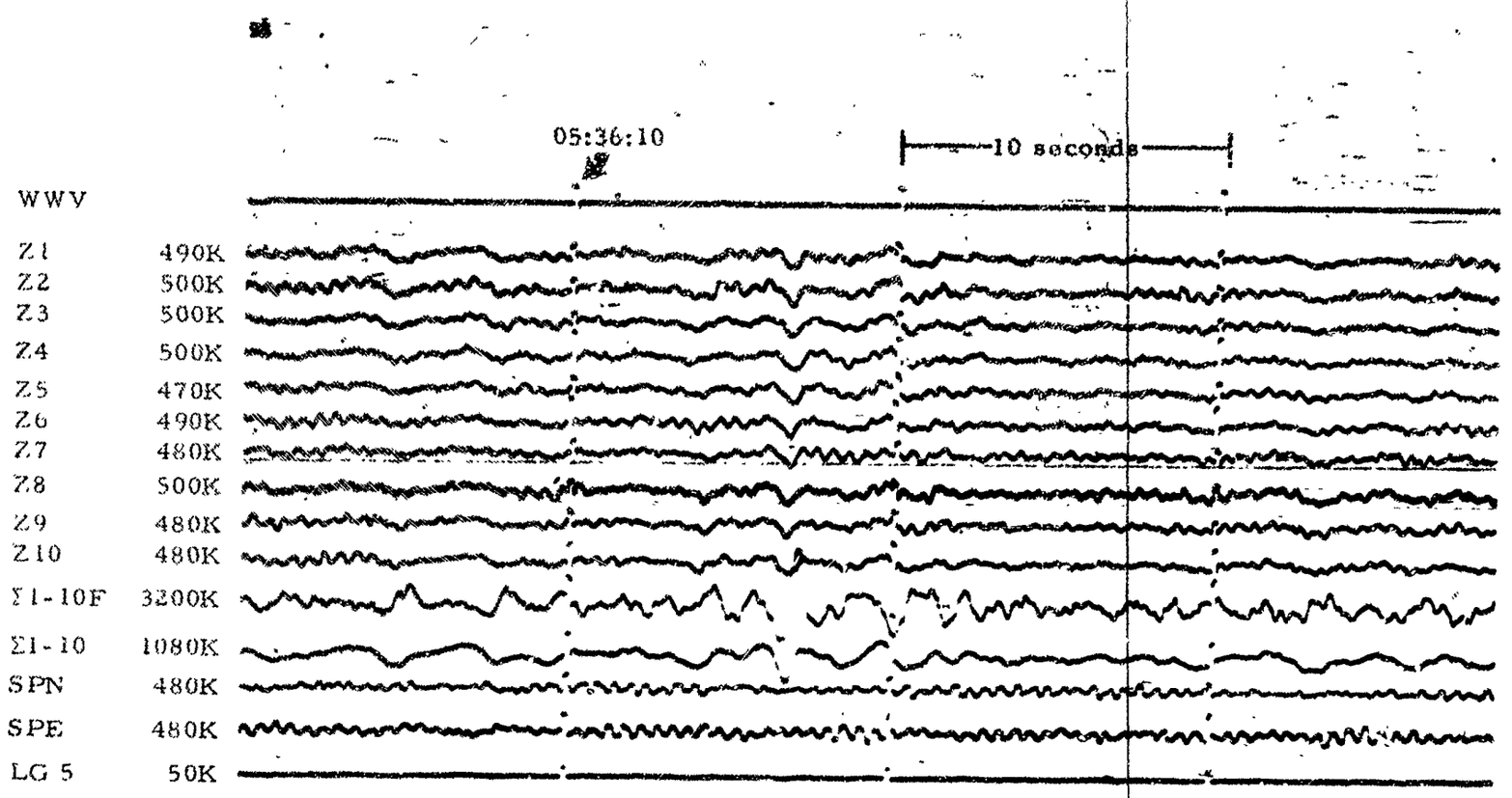

Figure 3-27. WMSO seismogram illustrating a P-phase arrival from the Fiji Islands.
Epicentral data: $\Delta \simeq 92^{\circ}$, h ≃ 509 km, azimuth ≃ 250°, magnitude ≃ 4.1
(X10 enlargement of 16-mm film)

WMSO
Run 223
11 Aug 1963

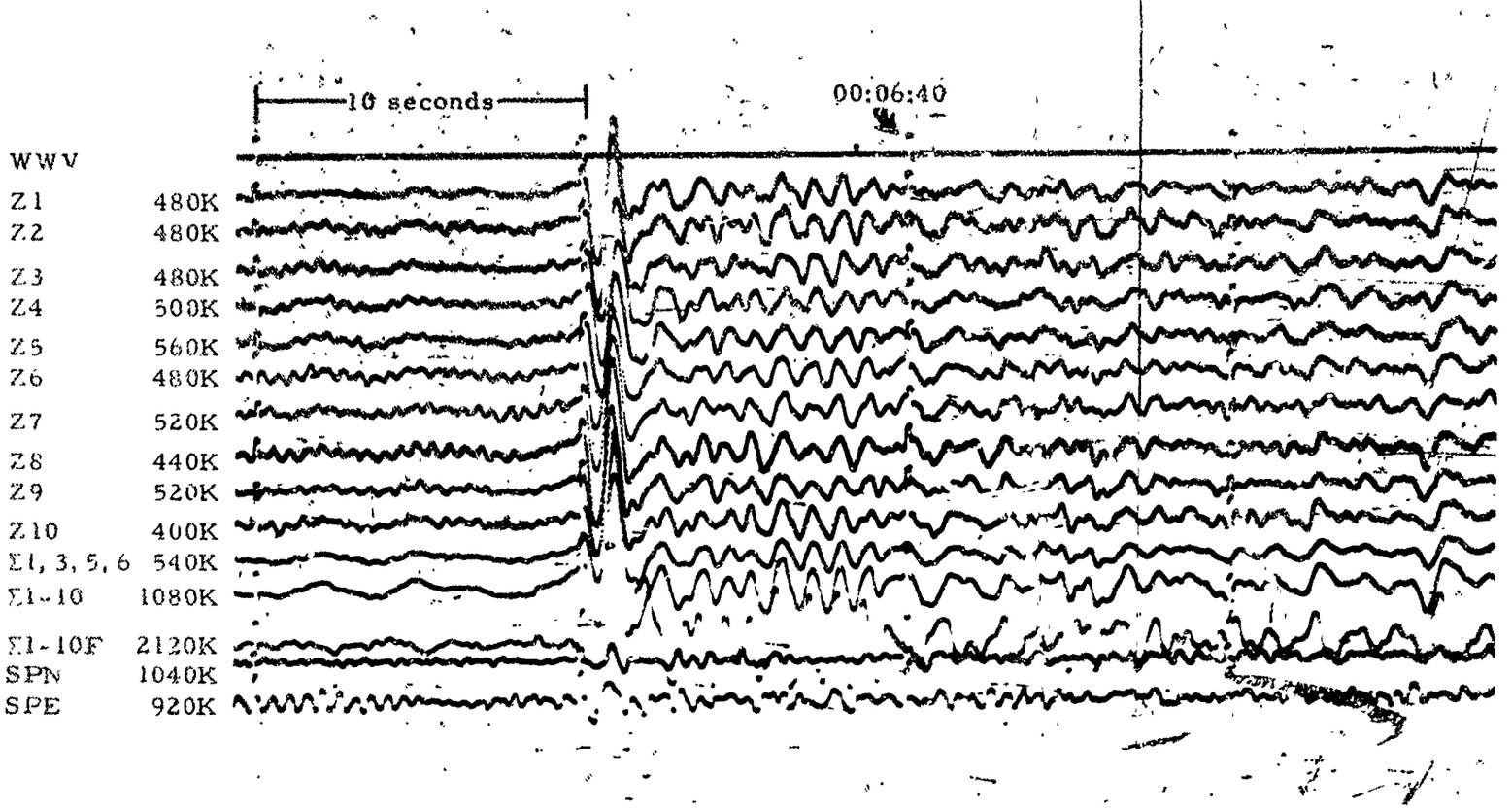

Figure 3-28. WMSO seismogram illustrating a P-phase arrival from the Fiji Islands.
Epicentral data: $\Delta \simeq 92^{\circ}$, h ≃ 515 km, azimuth ≃ 250°, magnitude ≃ 5 2
(X10 enlargement of 16-mm film)

WMSO
Run 217
5 Aug 1963

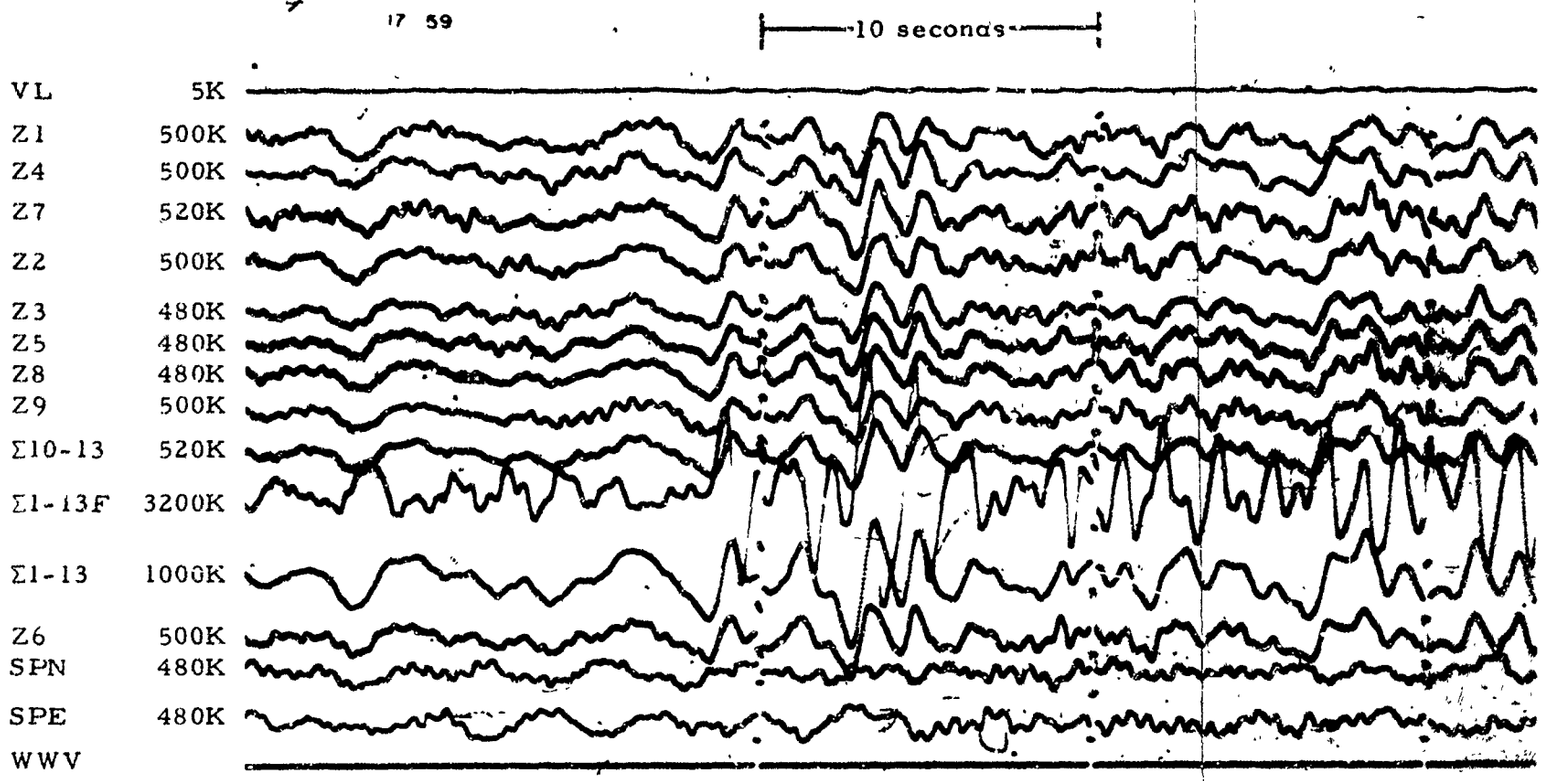

Figure 3-29. WMSO seismogram illustrating a P-phase arrival from off the coast of Turkey. Epicentral data: $\Delta \simeq 94^{\circ}$, h ≃ 41 km, azimuth ≃ 39°, magnitude ≃ 5.3 (X10 enlargement of 16-mm film)

WMSO
Run 030
30 Jan 1964
Data Group 311

3.6 DISTANCE = 101° to 120°

TR 64-50

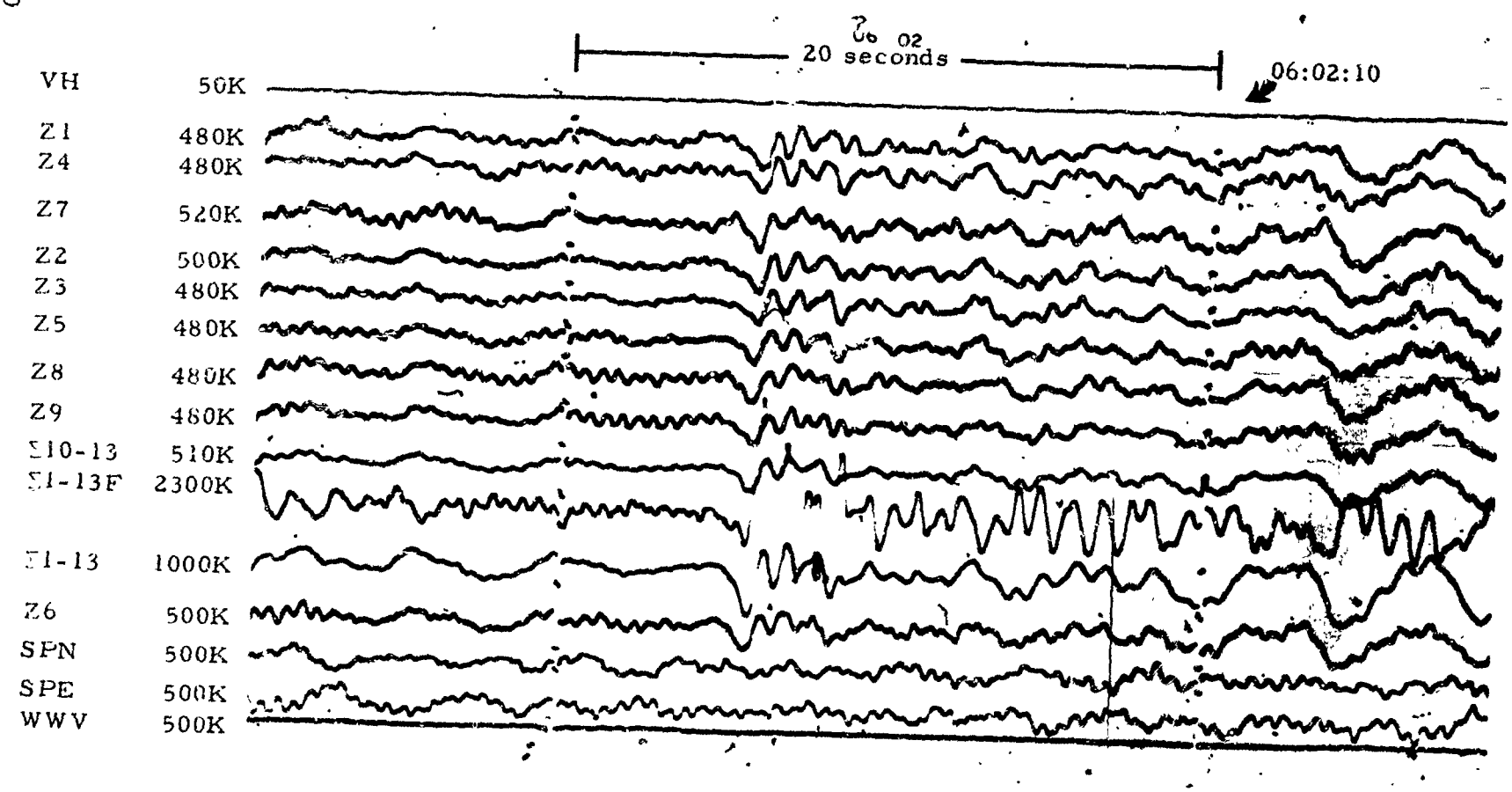

Figure 3-30. WMSO seismogram illustrating a PKP phase arrival from New Britain.
Epicentral data: $\Delta \simeq 112^{\circ}$, h ≃ 33 km, azimuth ≃ 278°, magnitude ≃ 5.1
(X10 enlargement of 16-mm film)

WMSO
Run 028
28 Jan 1964
Data Group 311

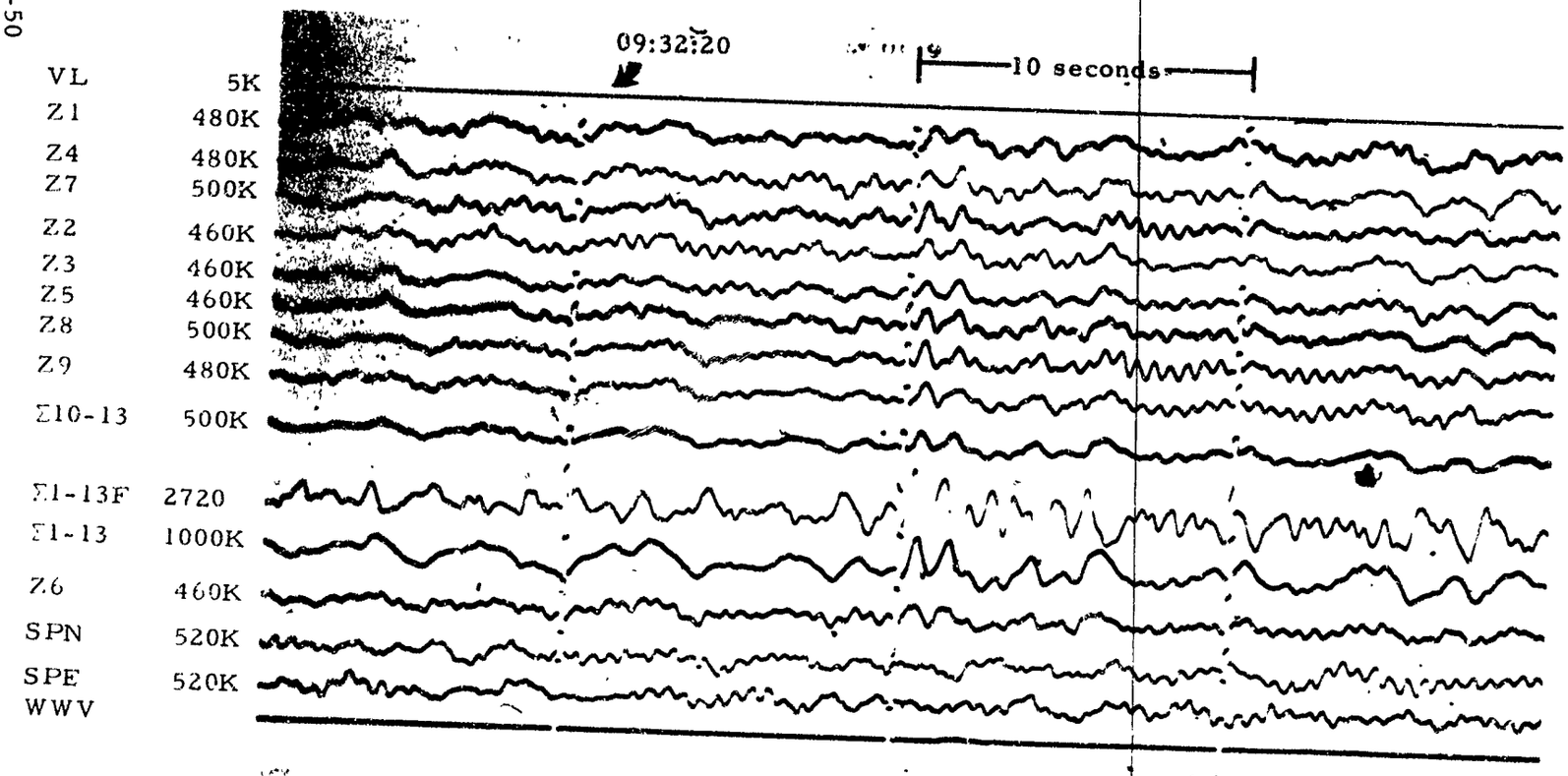

Figure 3-31. WMSO seismogram illustrating a PKP phase arrival. Epicenter: near the coast of Southern Iran, $\Delta \simeq 114^{\circ}$, h ≃ 33 km, azimuth ≃ 27°, magnitude ≃ 5.6 (X10 enlargement of 16-mm film)

WMSO
Run 019
19 Jan 1964
Data Group 311

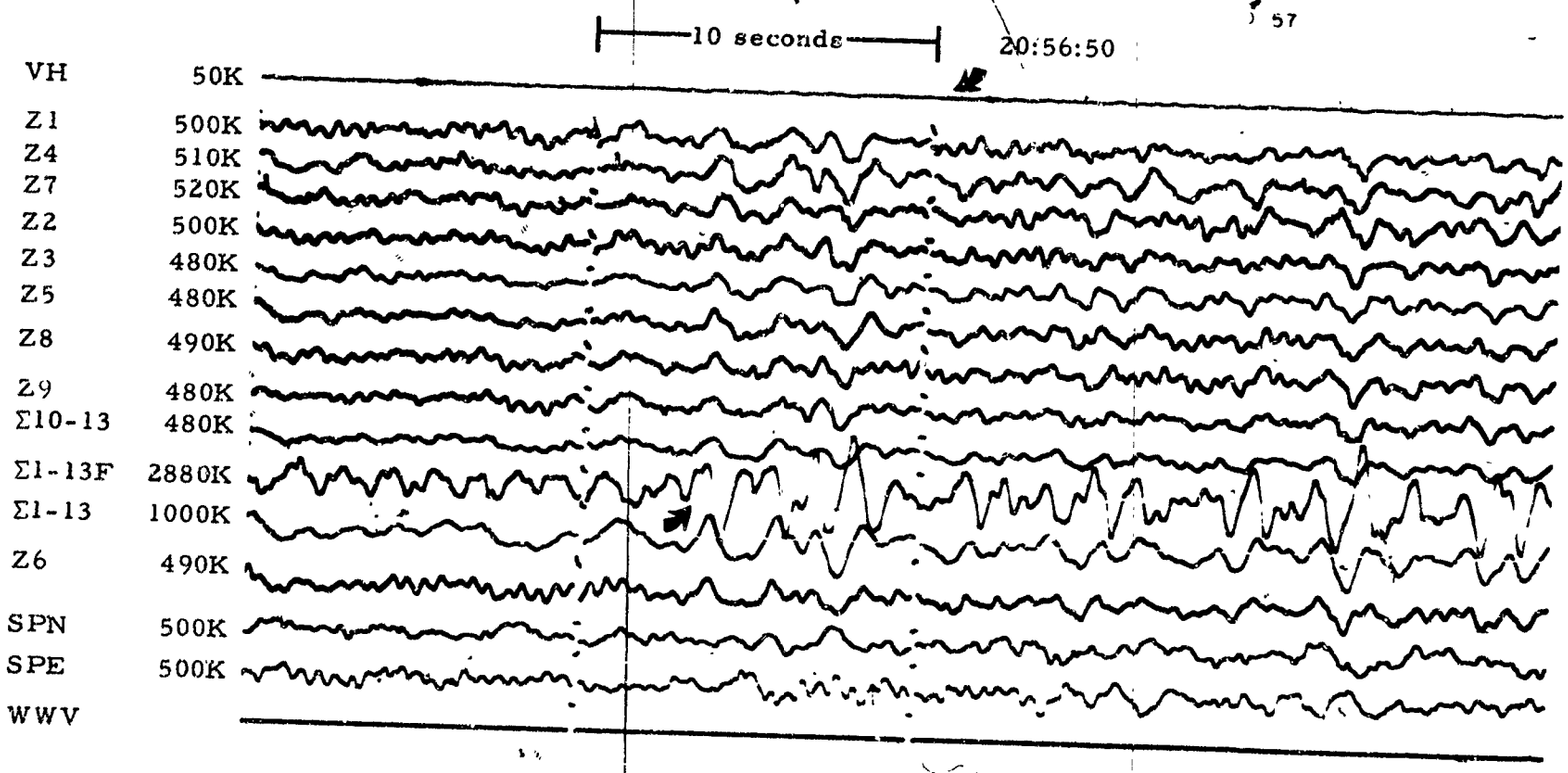

Figure 3-32. WMSO short-period seismogram illustrating a PKP phase arrival. Epicenter: near the north coast of Luzon, $\Delta \simeq 115^{\circ}$, h ≃ 53 km, azimuth ≃ 319°, magnitude ≃ 4.8 (X10 enlargement of 16-mm film)

WMSO
Run 020
20 Jan 1964
Data Group 311

3.7 DISTANCE = 121° to 140°

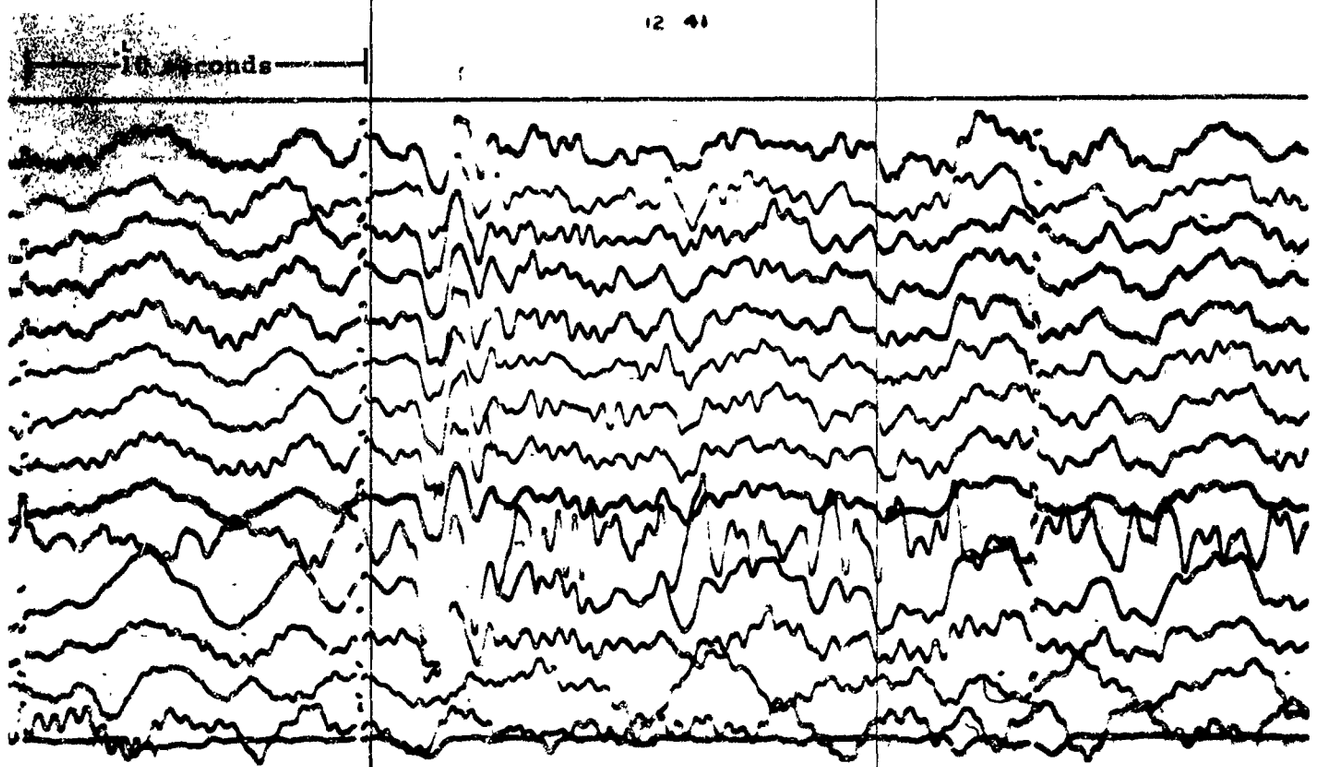

Figure 3-33. WMSO short-period seismogram illustrating a PKP phase arrival from the Banda Sea. Epicentral data: $\Delta \simeq 127^{o}$, h ≃ 96 km, azimuth ≃ 291^{o}, magnitude ≃ 5.7 (X10 enlargement of 16-mm film)

WMSO
Run 001
1 Jan 1964
Data Group 311

3.8 DISTANCE = 141° to 160°

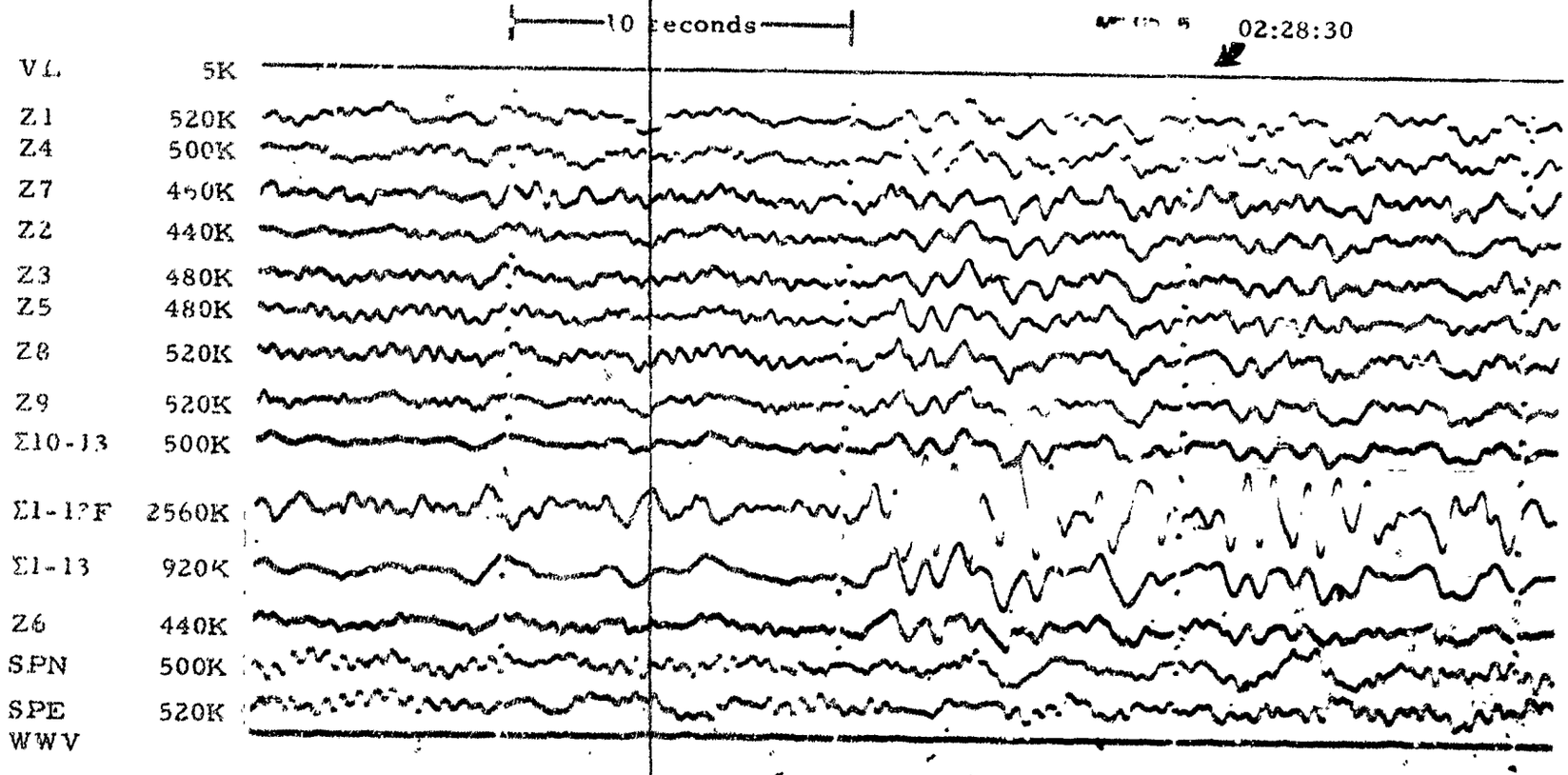

Figure 3-34. WMSO short-period seismogram illustrating a PKP phase arrival. Epicenter: off the southern coast of Java, $\Delta \simeq 143^{\circ}$, $h \simeq 81$ km, azimuth $\simeq 307^{\circ}$, no magnitude data available. (X10 enlargement of 16-mm film)

WMSO
Run 056
25 Feb 1964
Data Group 3003

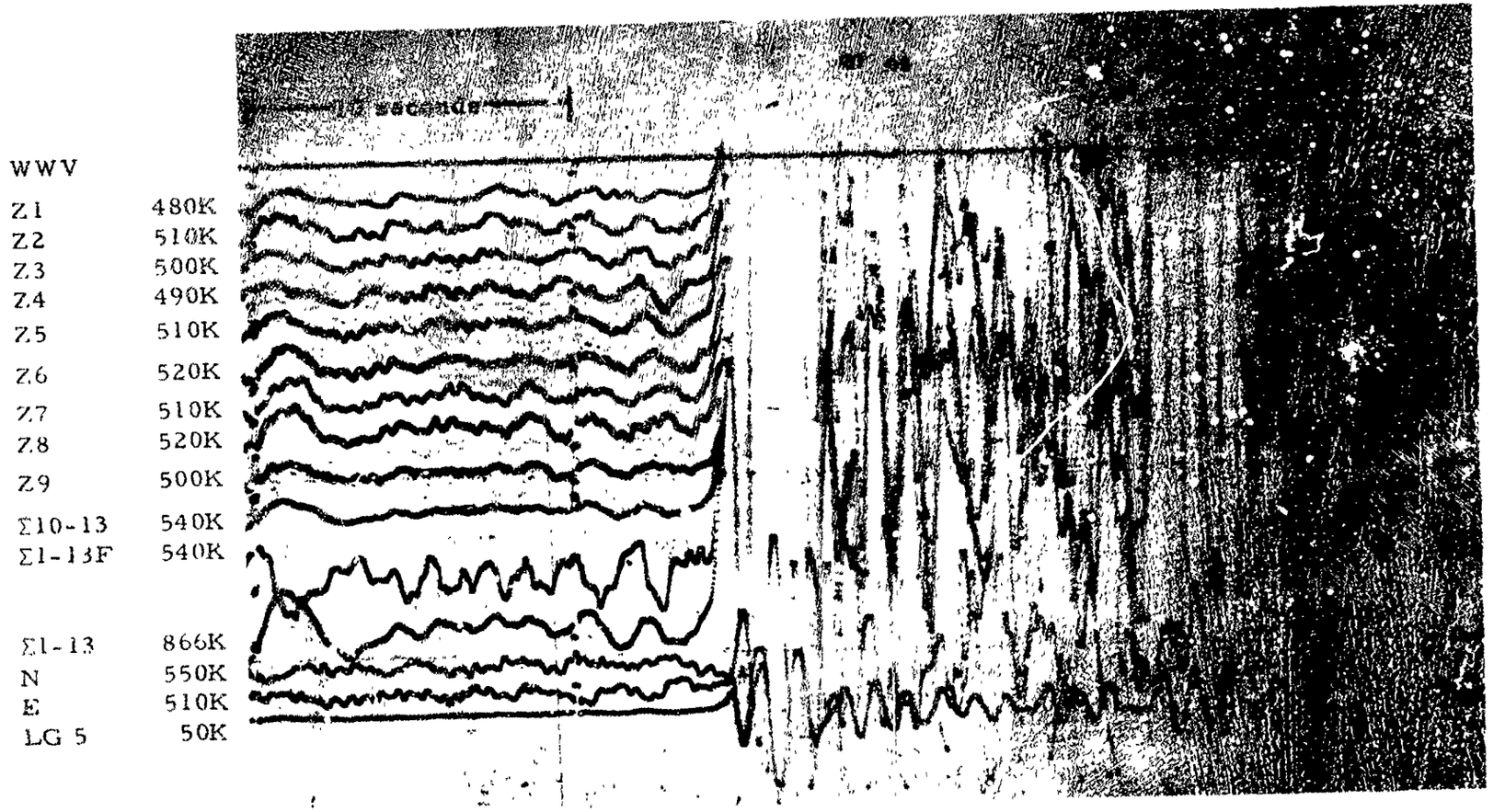

Figure 3-35. WMSO seismogram illustrating a PKP phase arrival. Epicenter: off the southern coast of Sumatra, $\Delta \approx 144^{\circ}$, h ≈ 50 km, azimuth ≈ 321°, magnitude ≈ 6.1 (X10 enlargement of 16-mm film)

WMSO
Run 297
24 Oct 1964

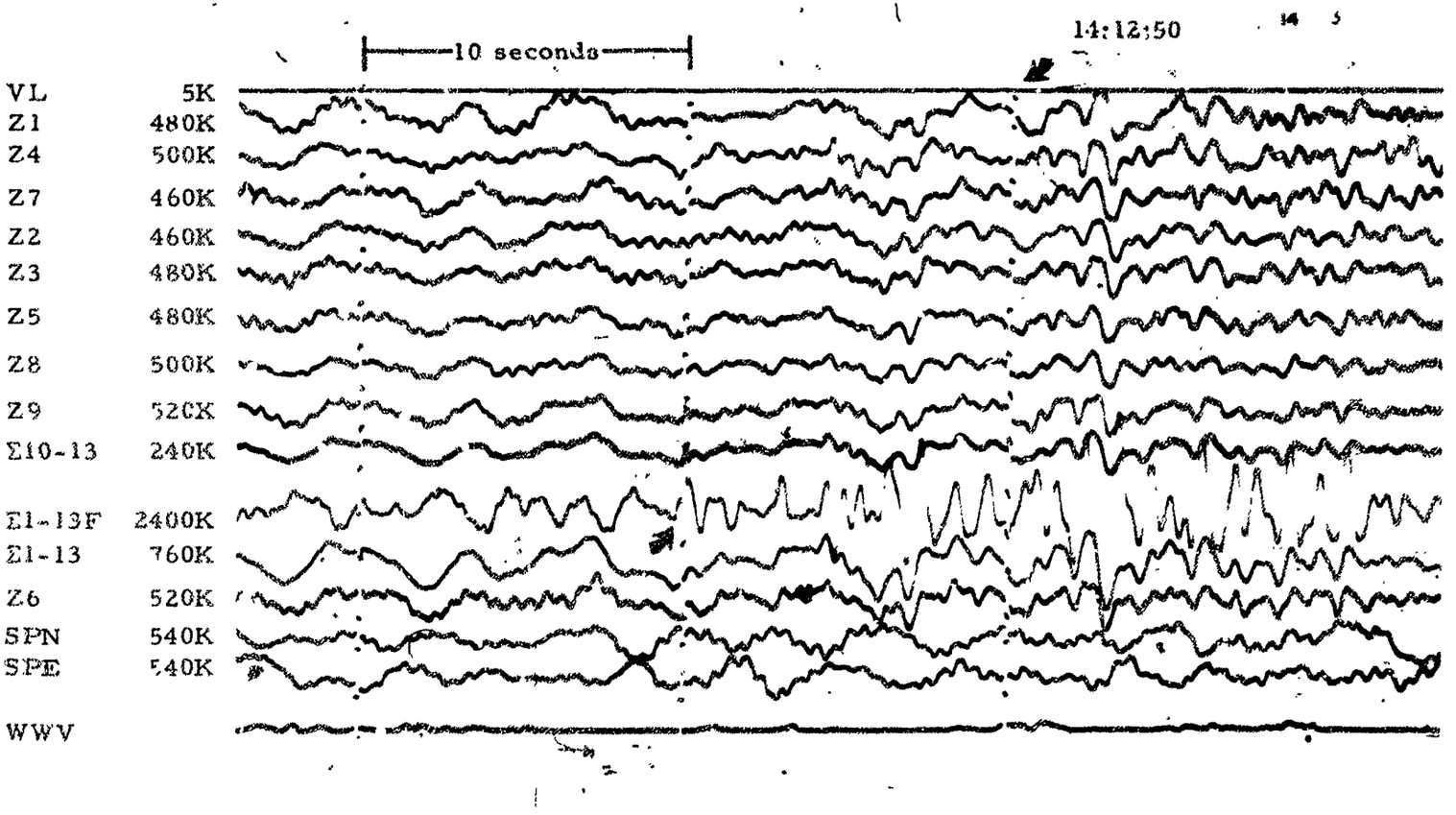

Figure 3-36. WMSO seismogram illustrating a PKP phase arrival from the Sunda Strait. Epicentral data: $\Delta \simeq 144^{\circ}$, h ≃ 33 km, azimuth ≃ 316°, magnitude ≃ 5.2 (X10 enlargement of 16-mm film)

WMSO
Run 052
21 Feb 1964
Data Group 3003

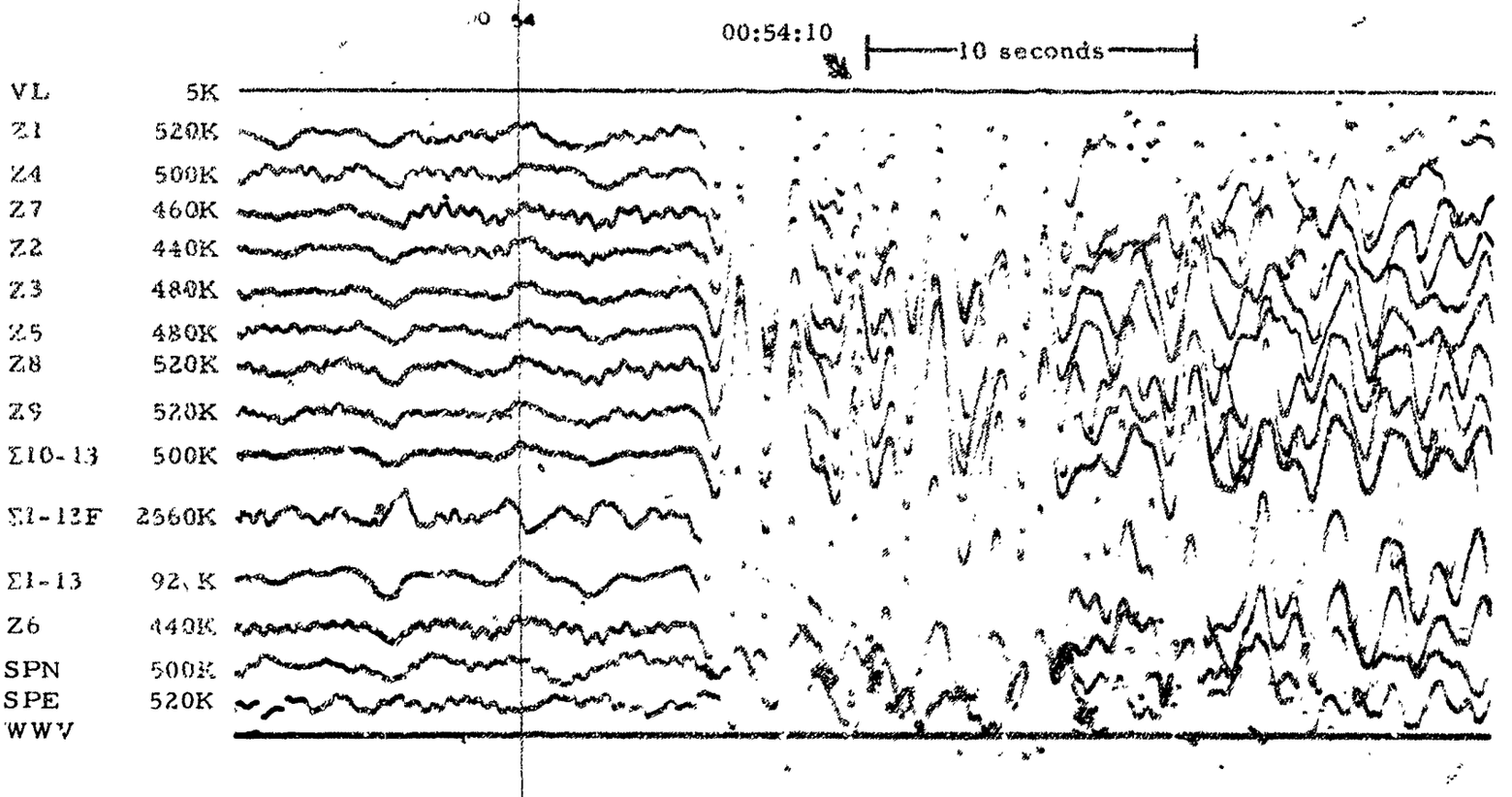

WMSO
Run 056
25 Feb 1964
Data Group 3003

Figure 3-37. WMSO seismogram illustrating a PKP phase arrival from the Prince Edward Island region. Epicentral data: $\Delta \simeq 145^{\circ}$, $h \simeq 33$ km, azimuth $\simeq 120^{\circ}$, magnitude $\simeq 6.7$ (X10 enlargement of 16-mm film)

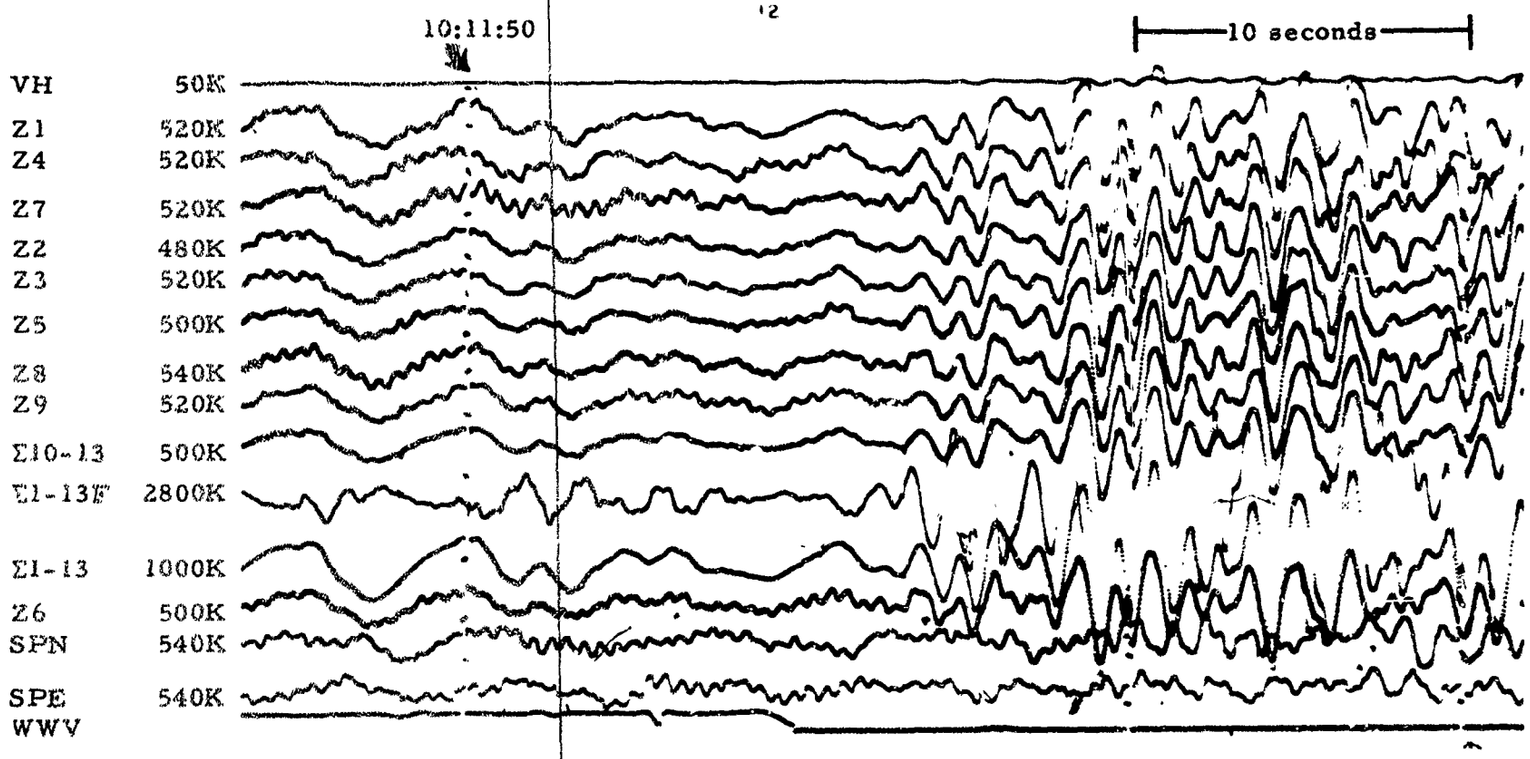

Figure 3-38. WMSO seismogram illustrating a PKP phase arrival from the Chagos Archipelago region. Epicentral data: $\Delta \simeq 150^{\circ}$, h ≃ 33 km, azimuth ≃ 28°, magnitude ≃ 5.2 (X10 enlargement of 16-mm film)

WMSO
Run 055
24 Feb 1964
Data Group 3003

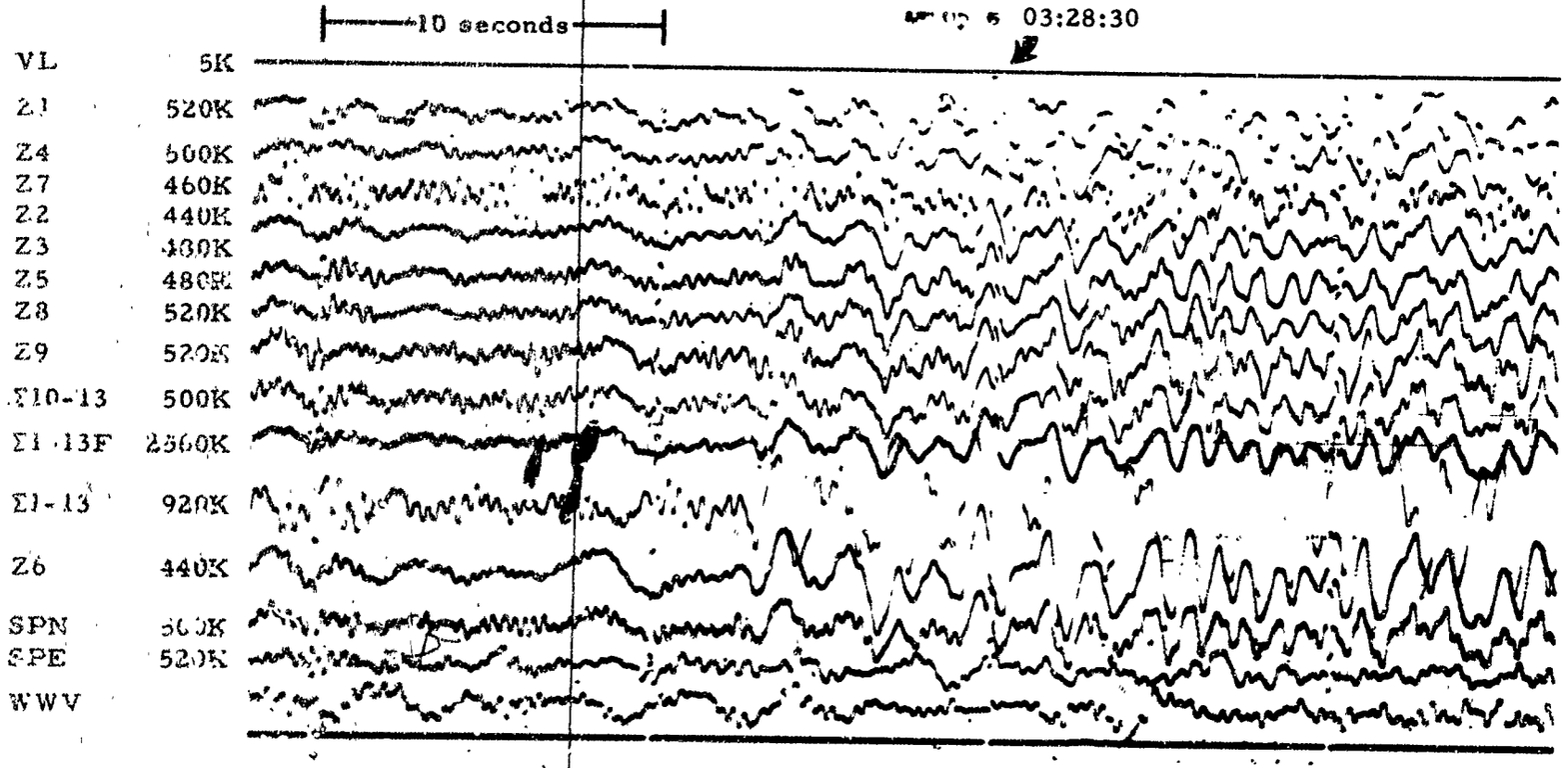

Figure 3-39. WMSO seismogram illustrating a PKP phase arrival. Epicenter: south of Australia, $\Delta \simeq 153^{\circ}$, $h \simeq 33$ km, azimuth $\simeq 227^{\circ}$, no magnitude data available. (X10 enlargement of 16-mm film)

WMSO
Run 056
25 Feb 1964
Data Group 3003

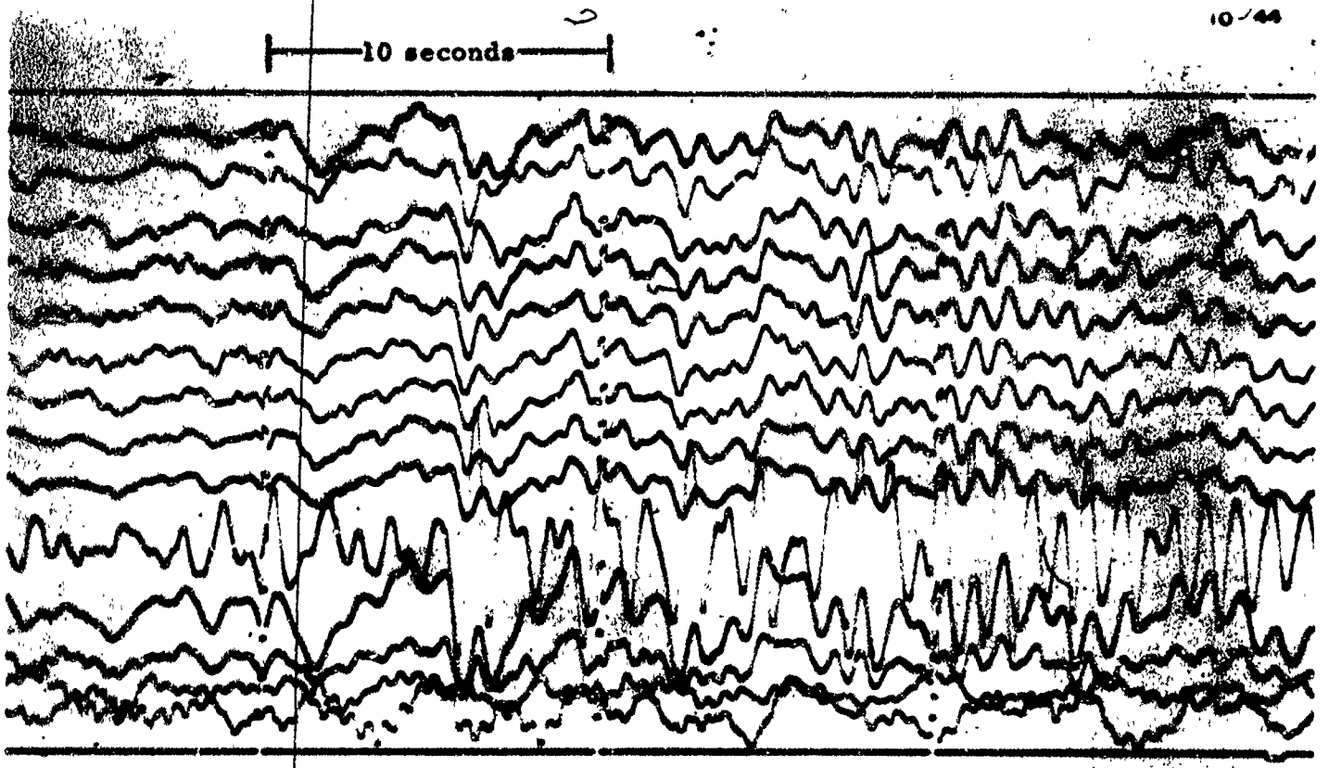

Figure 3-40. WMSO short-period seismogram illustrating a PKP phase arrival from the Indian Ocean. Epicentral data: $\Delta \simeq 155^{\circ}$, h ≃ 33 km, azimuth ≃ 337°, no magnitude data available (X10 enlargement of 16-mm film)

WMSO
Run 011
11 Jan 1964
Data Group 311

4. NOISE SAMPLES

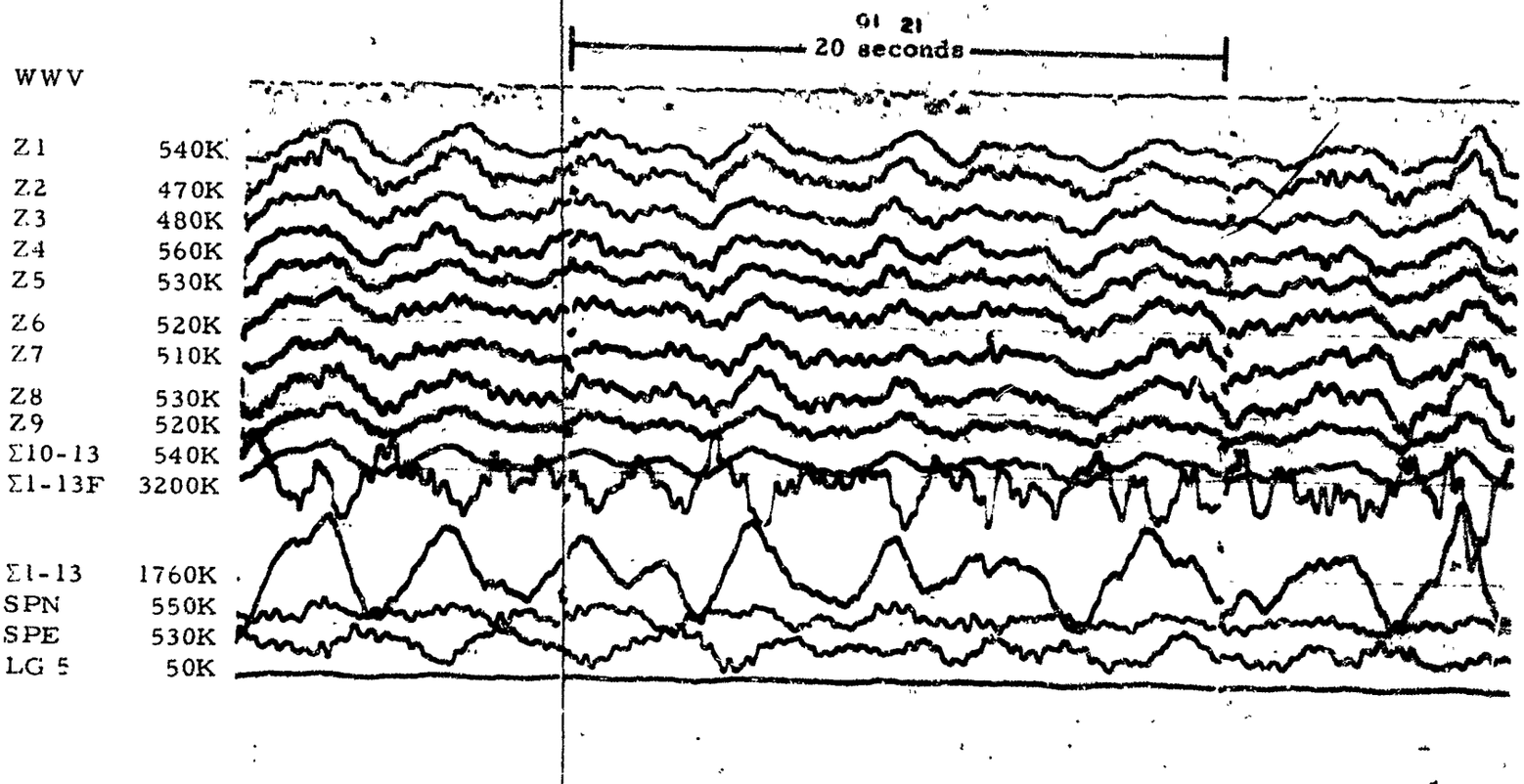

Figure 4-1. WMSO short-period seismogram illustrating 1/2-second microseisms (X10 enlargement of 16-mm film)

WMSO
Run 303
30 Oct 1963

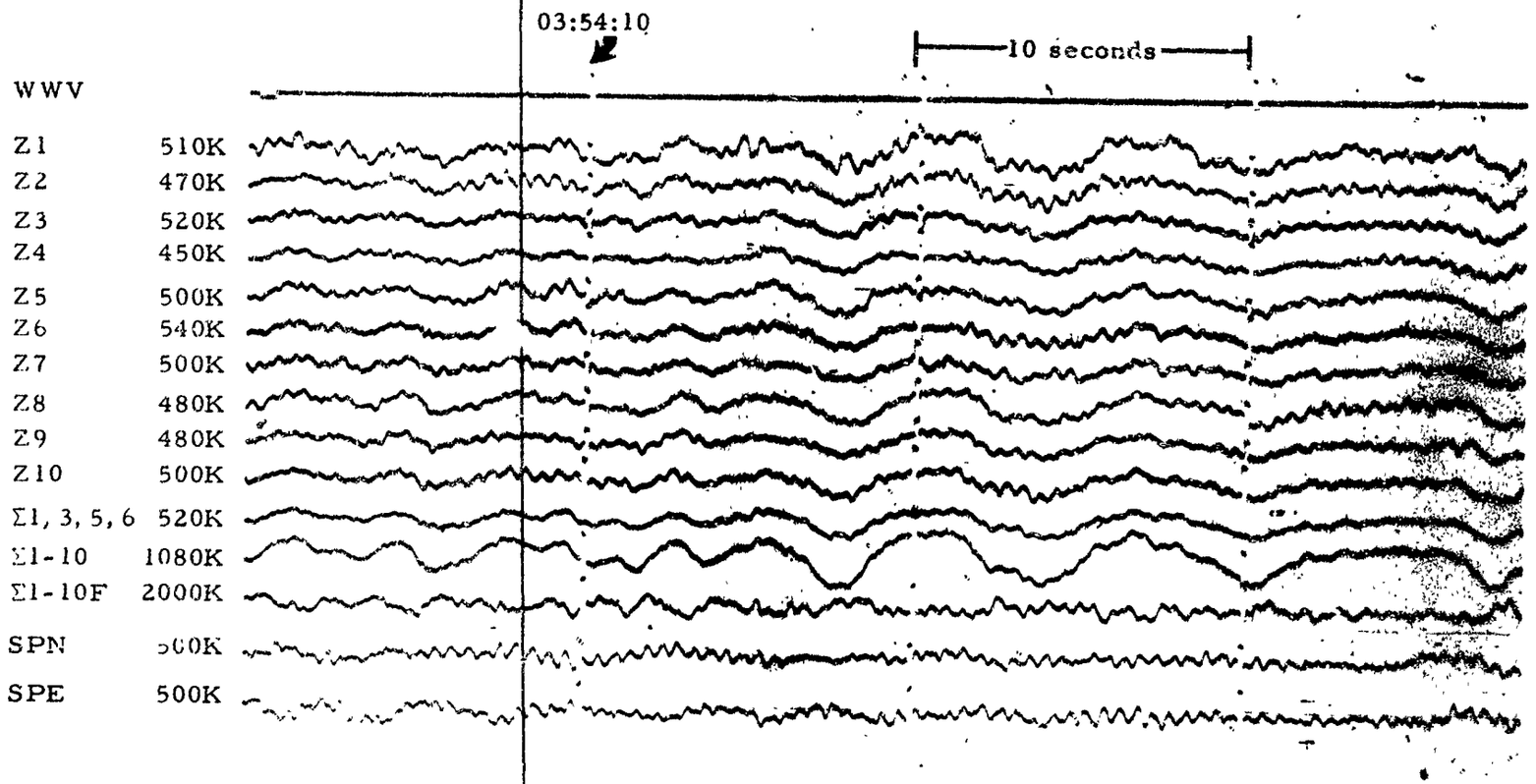

Figure 4-2. WMSO seismogram illustrating the occurrence of 4- to 6-second microseisms at a low level on the short-period system (X10 enlargement of 16-mm film)

WMSO
Run 161
10 Jun 1963

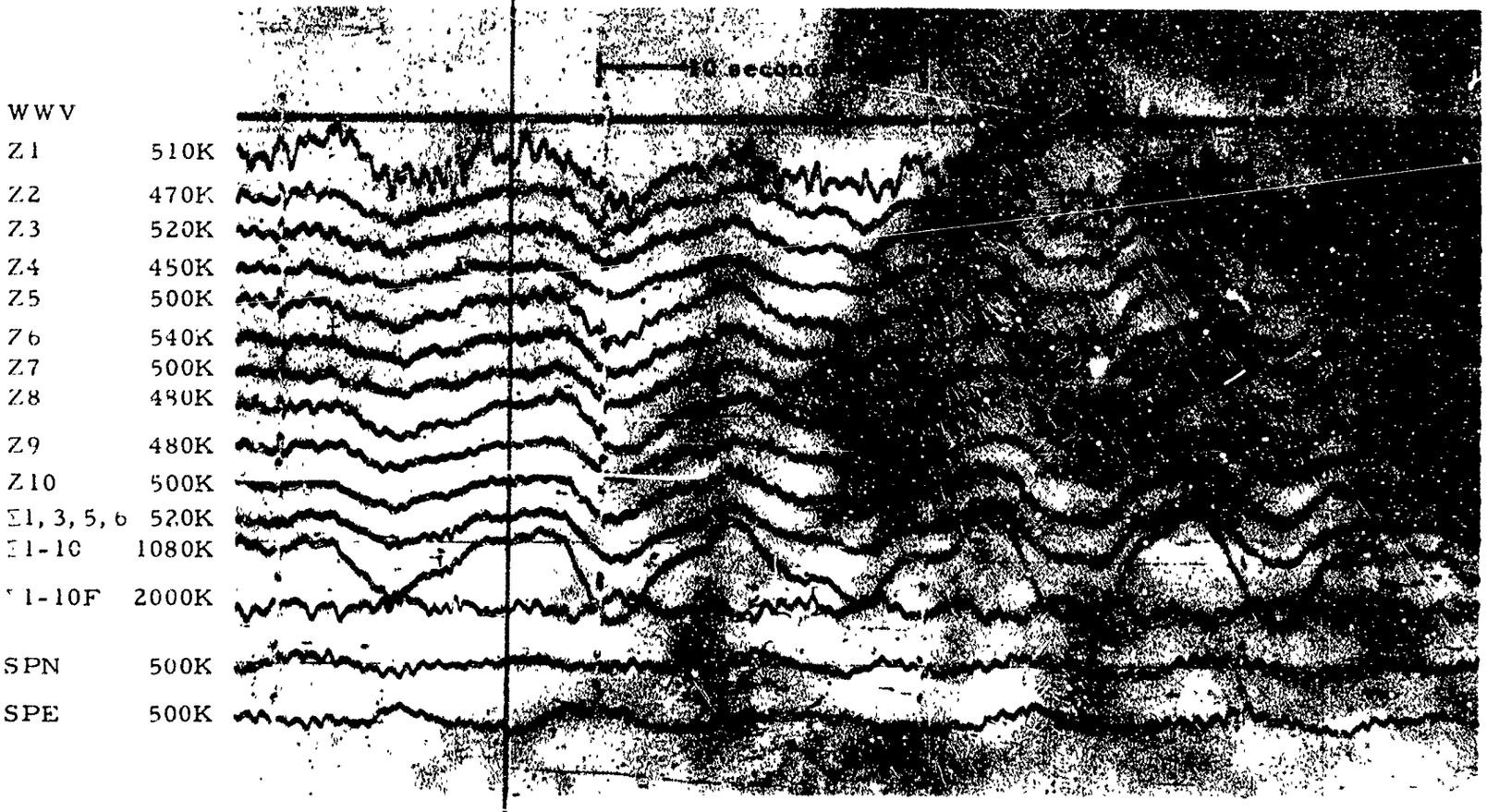

Figure 4-3. WMSO seismogram illustrating the occurrence of 4- to 6-second microseisms at a moderate level on the short-period system (X10 enlargement of 16-mm film)

WMSO
Run 161
10 Jun 1963

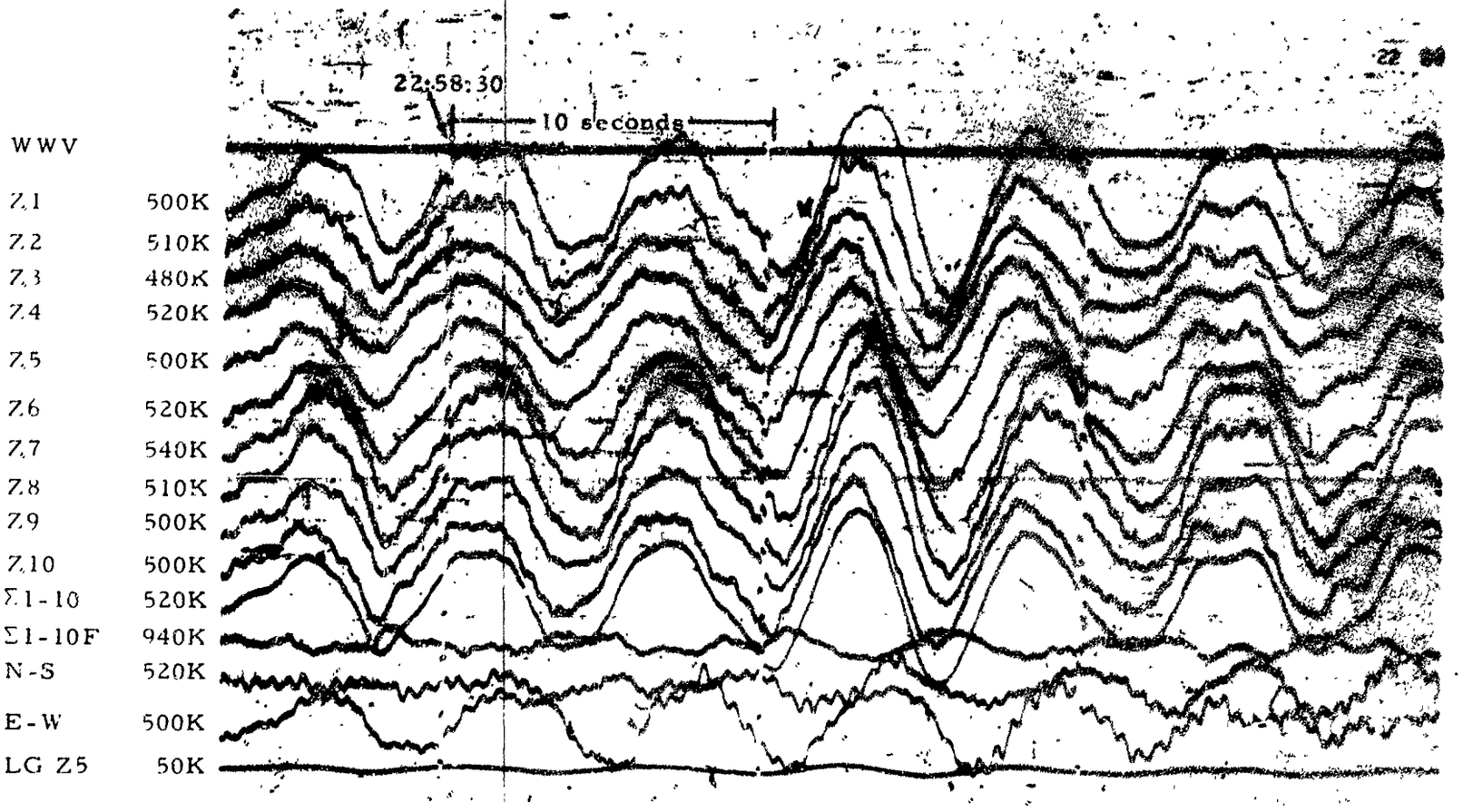

Figure 4-4. WMSO seismogram illustrating the occurrence of 4- to 6-second microseisms at a high level on the short-period system (X10 enlargement of 16-mm film)

WMSO
Run 364
30 Dec 1962

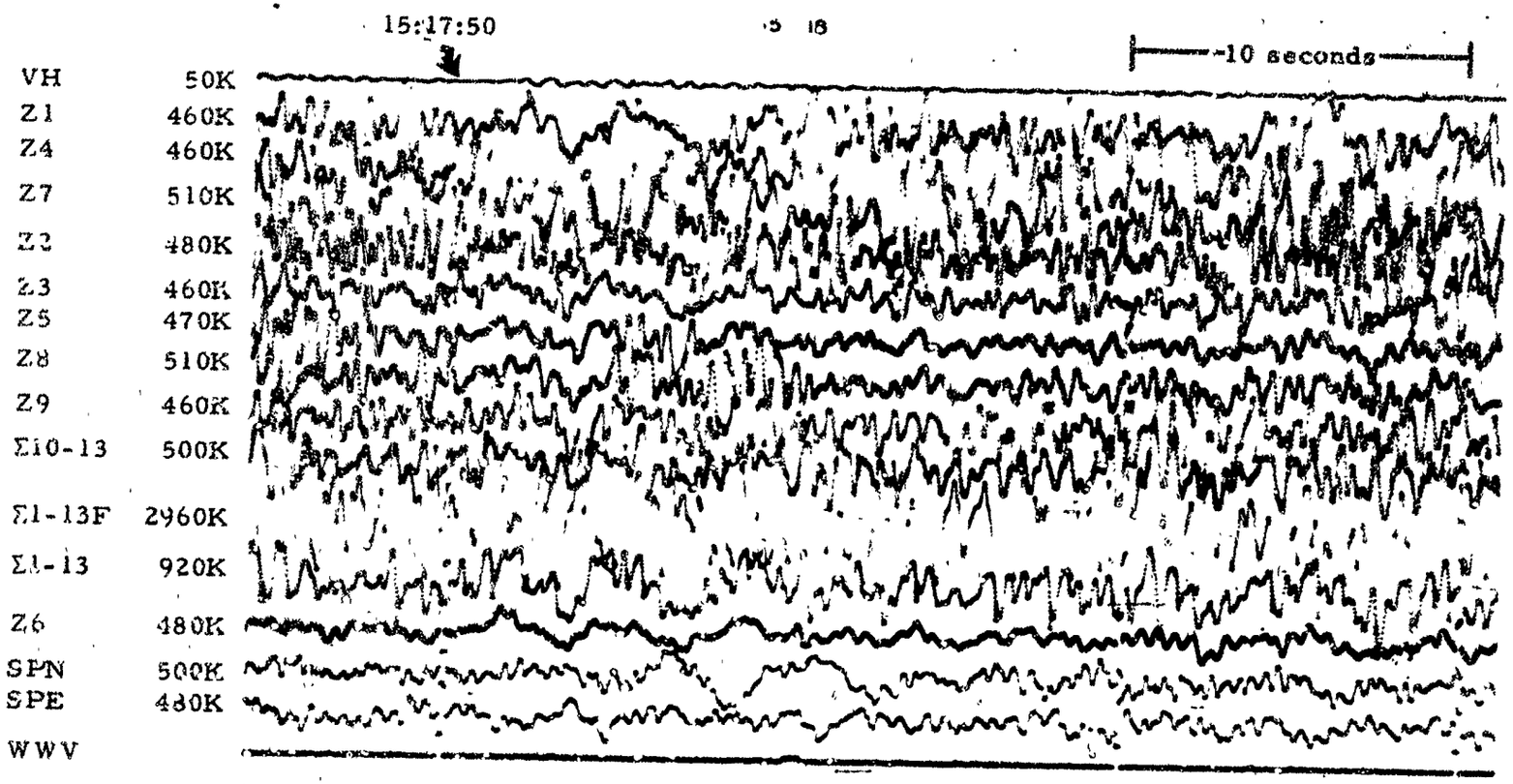

Figure 4-5. WMSO seismogram illustrating wind generated noise on the short-period system. Wind speed is approximately 38 mph (X10 enlargement of 16-mm film)

WMSO
Run 046
15 Feb 1964
Data Group 3003

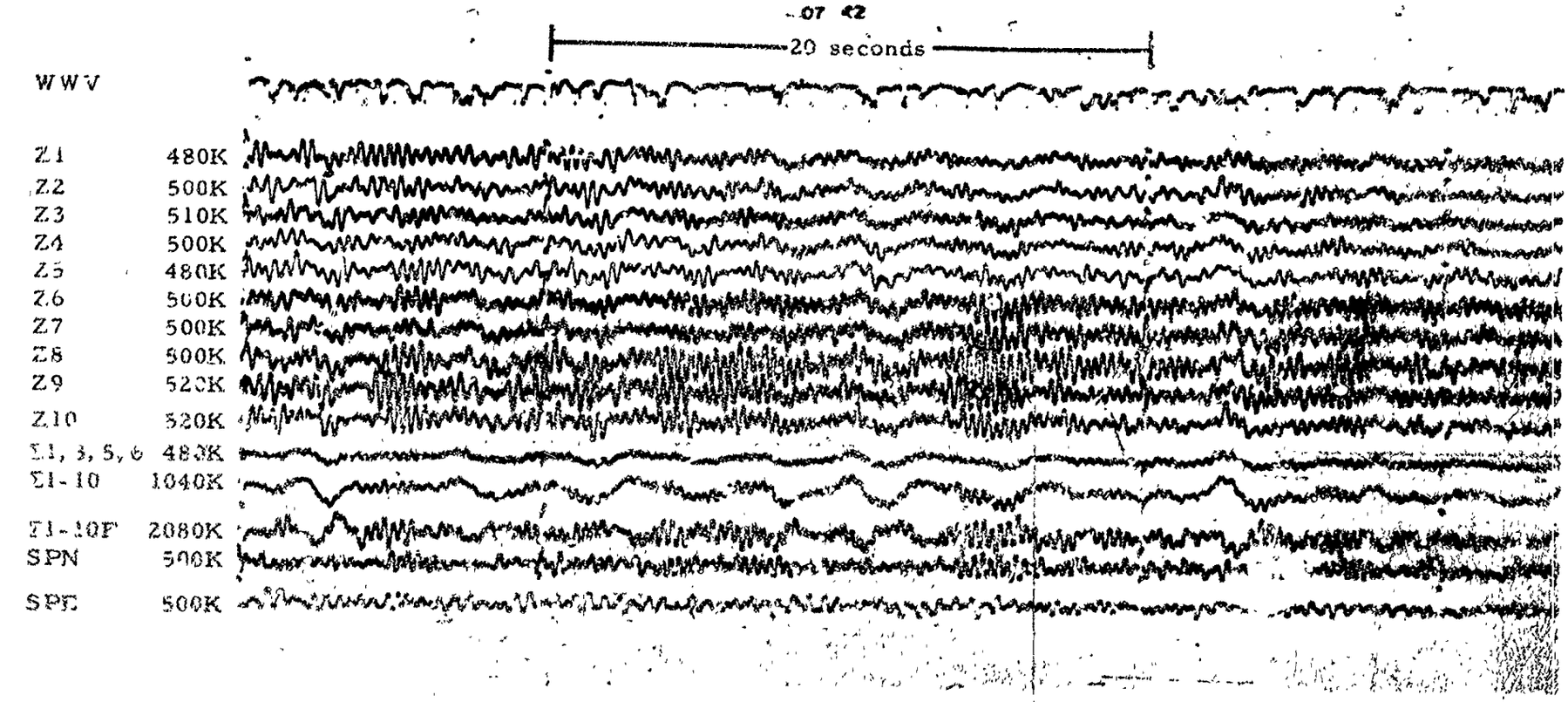

Figure 4-6. WMSO seismogram illustrating the short-period system response to train noise. (X10 enlargement of 16-mm film)

WMSO
Run 145
25 May 1963

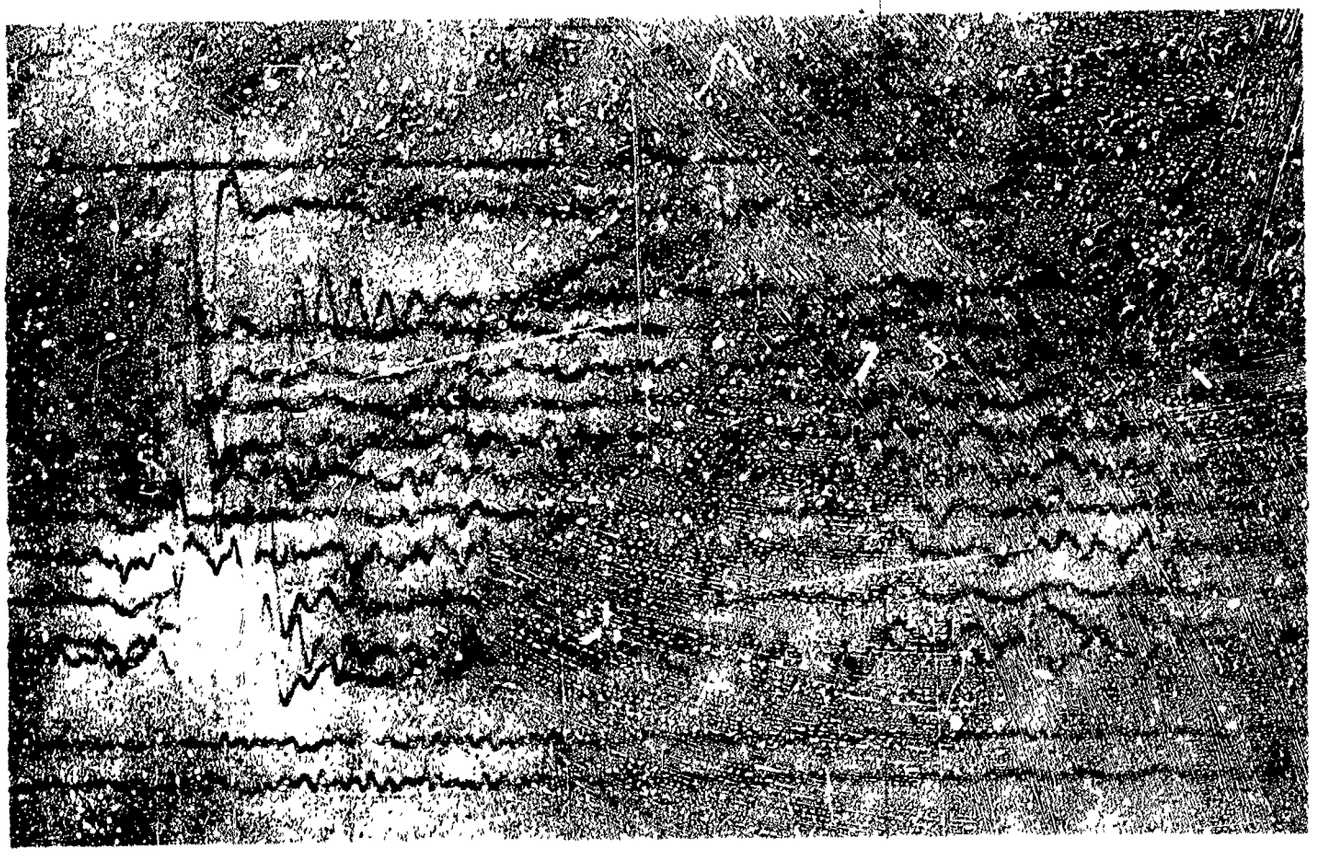

Figure 4-7. WMSO seismogram illustrating lightning spikes on the short-period system (X10 enlargement of 16-mm film)

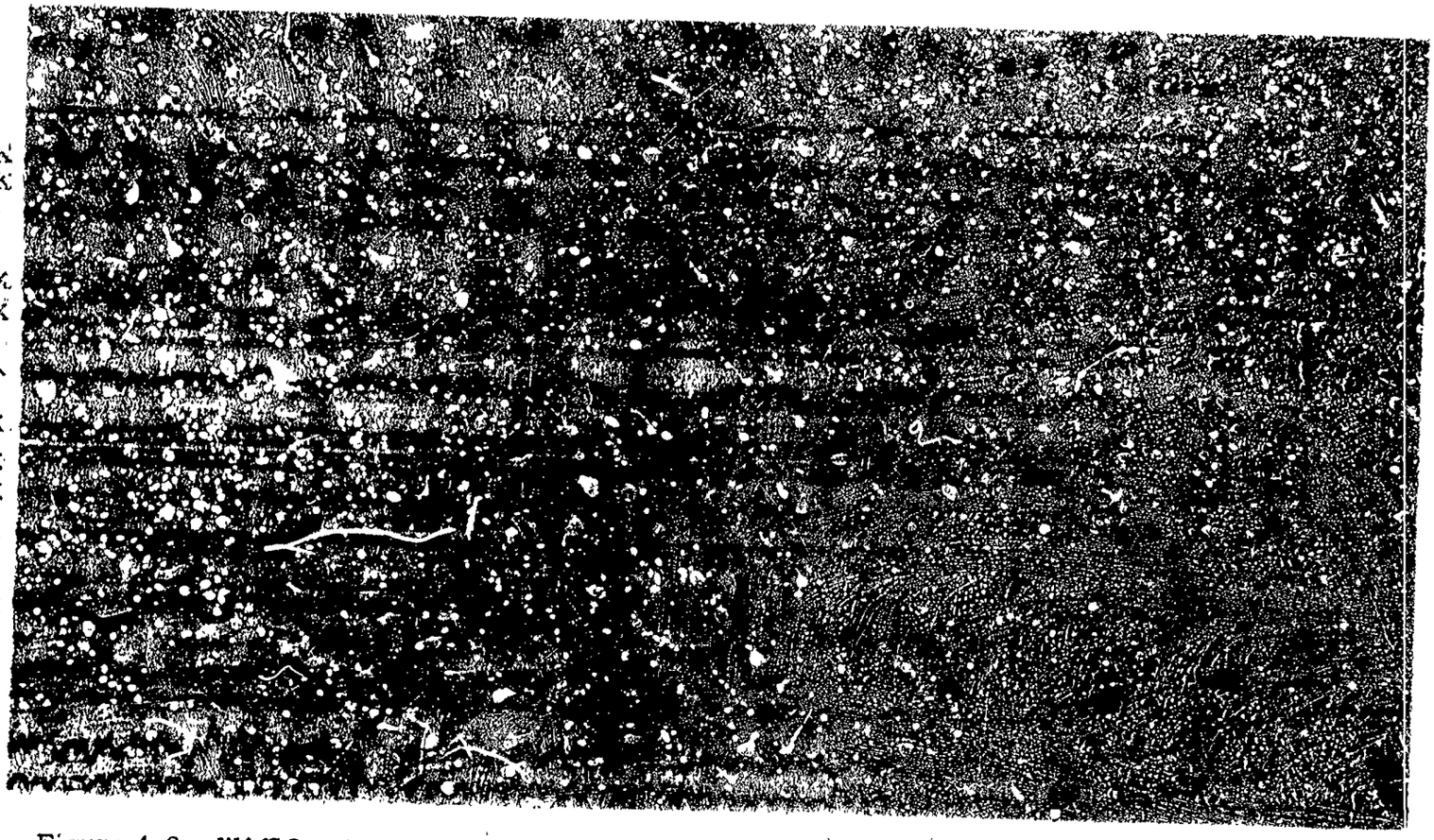

Figure 4-8. WMSO seismogram illustrating overlining and a generally noisy condition caused by barometric pressure changes (X10 enlargement of 16-mm film)

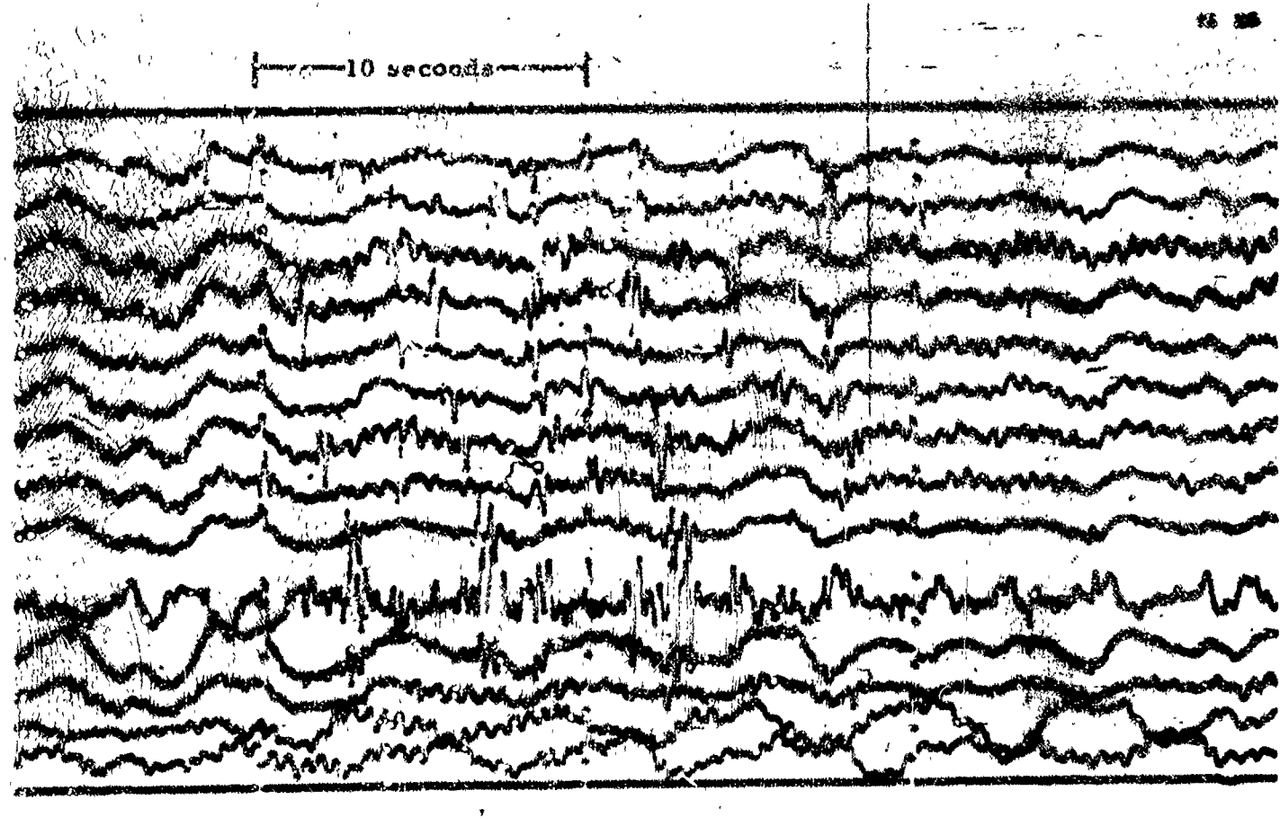

Figure 4-9. WMSO seismogram illustrating artillery generated acoustic signals. No corresponding seismic signals were recorded. (X10 enlargement of 16-mm film)

WMSO
Run 340
6 Dec 1963
Data Group 3:1

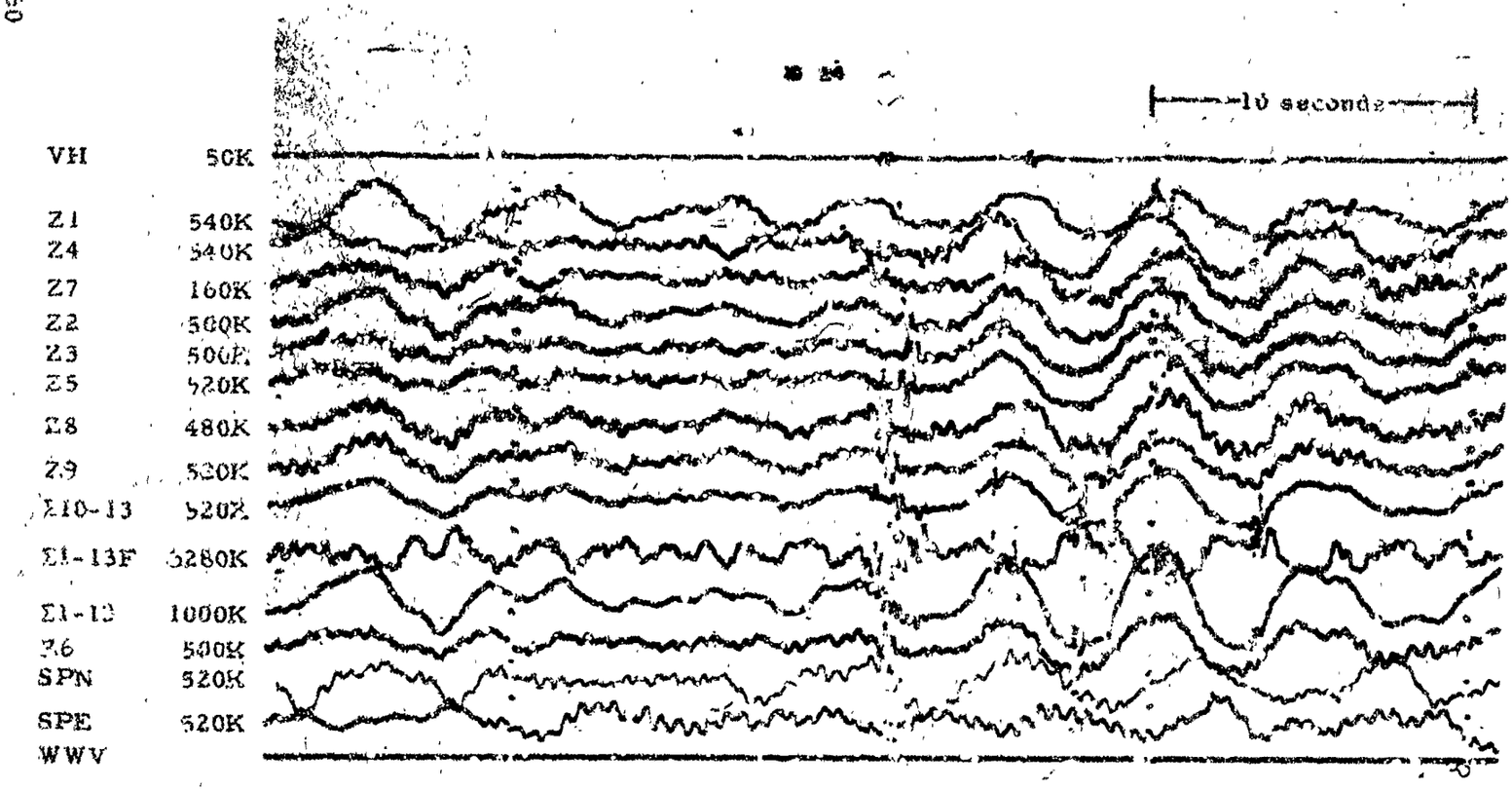

Figure 4-10. Seismic signal and corresponding acoustics from artillery fire as recorded on the WMSO short-period seismogram. (X10 enlargement of 16-mm film)

WMSO
Run 339
5 Dec 1963
Data Group 311

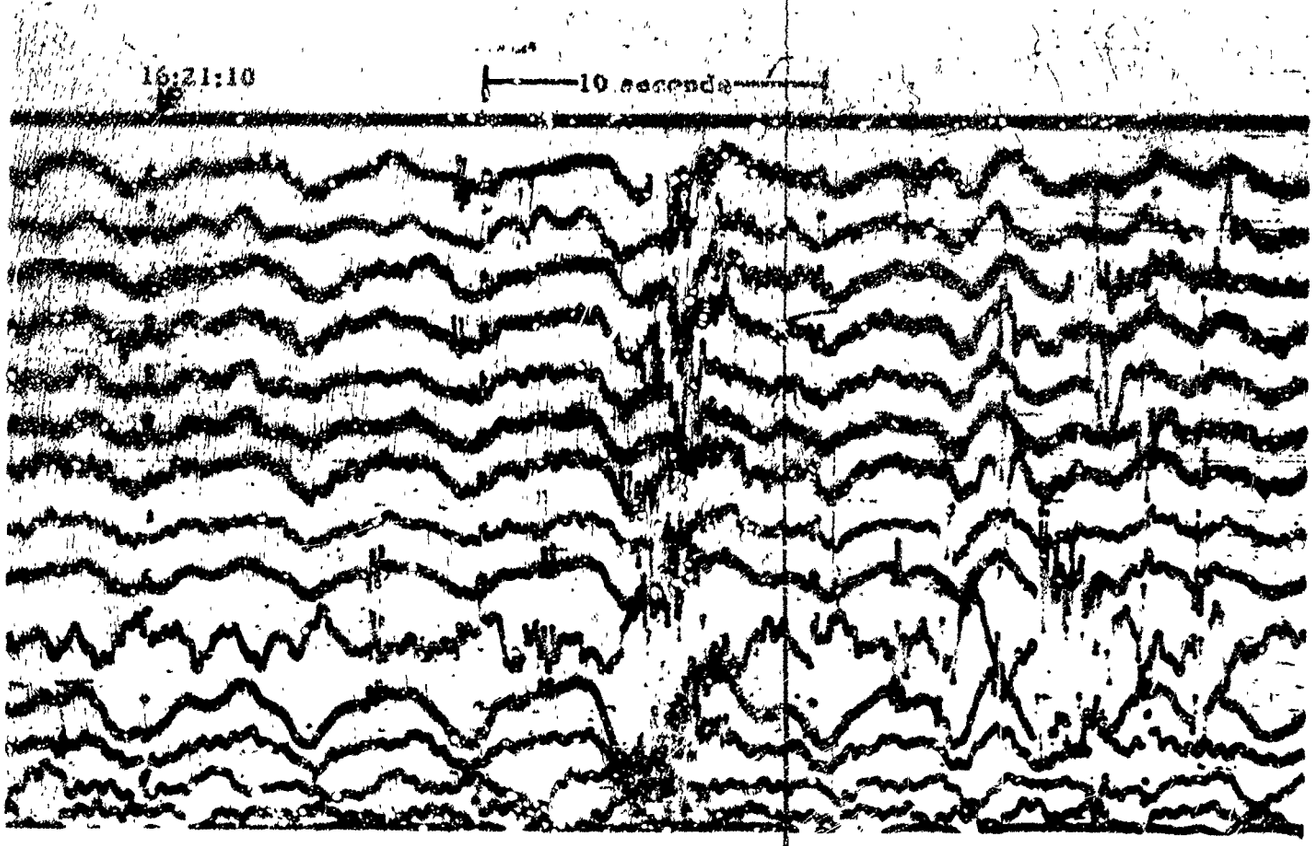

Figure 4-11. WMSO seismogram illustrating the seismic signal and acoustics generated by the demolition of outdated ammunition and artillery duds on Fort Sill. (X10 enlargement of 16-mm film)

WMSO
Sun 314
10 Dec 1963
Data Group 311

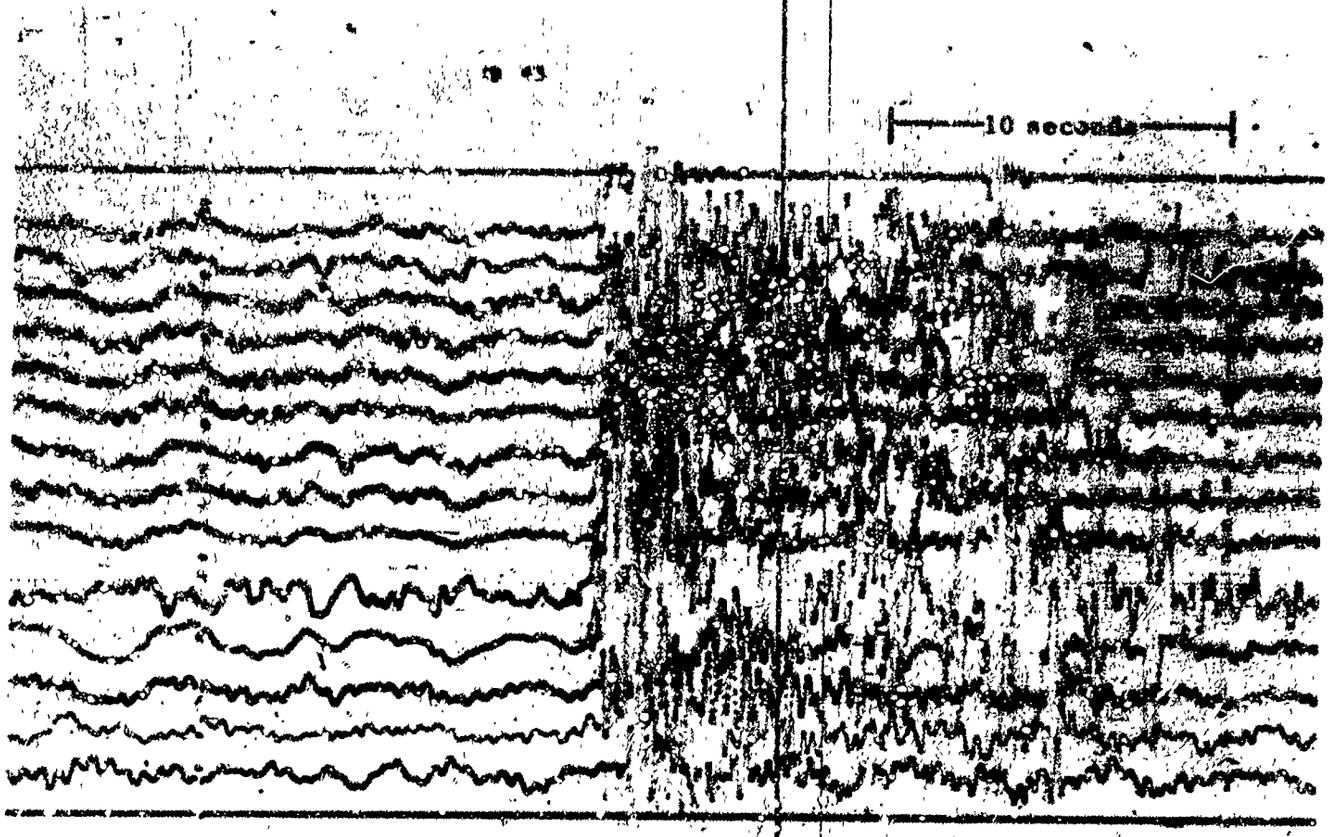

Figure 4-12. WMSO seismogram illustrating a 2500-pound detonation of TNT on Fort Sill. (X10 enlargement of 16-mm film)

WMSO
Run 337
3 Dec 1963
Data Group 311

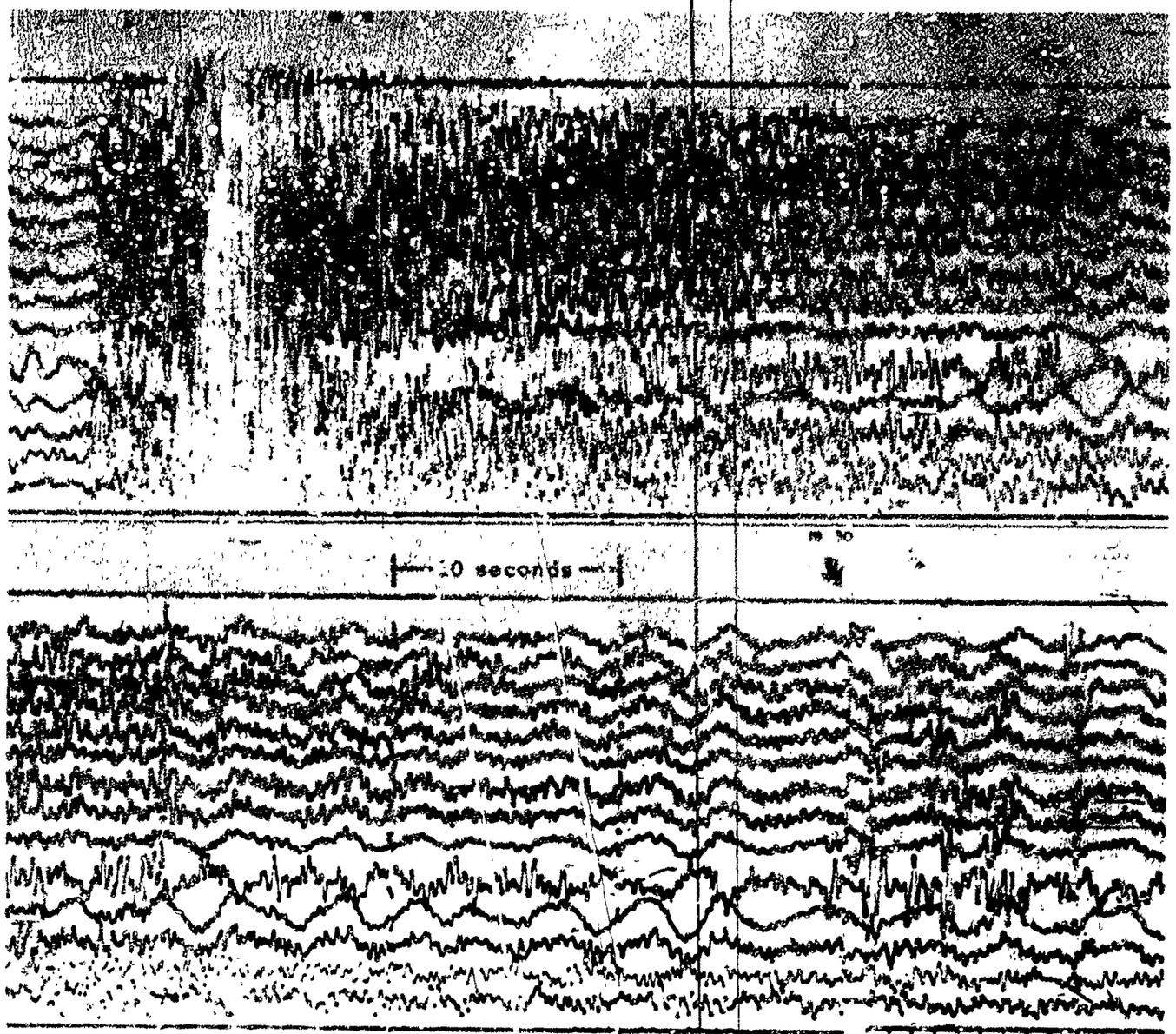

WMSO
Run 337
3 Dec 1963
Data Group 311

Figure 4-13. WMSO seismogram illustrating an acoustical signal generated by a blast at Richard's Spur Quarry. Epicentral data: Δ = 18.1 km, azimuth = 73.9°
(X7.4 enlargement of 16-mm film)

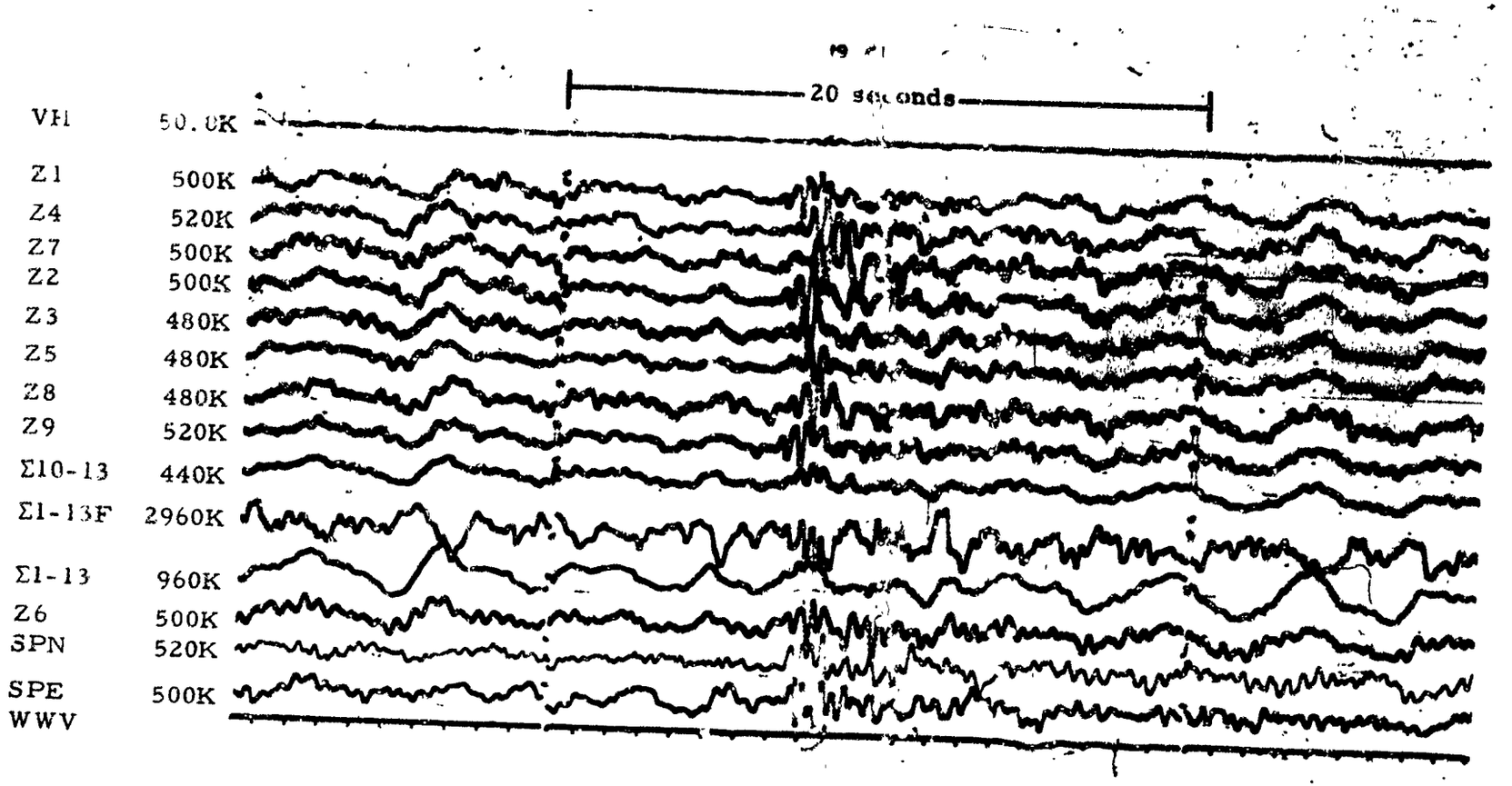

Figure 4-14. WMSO seismogram illustrating the Lg (Sur) phase from a near regional (?) event. The P phase was not recorded (X10 enlargement of 16-mm film)

WMSO
Run 337
3 Dec 1963
Data Group 311

INDEX

Acoustic Signals, 4-9, 4-10, 4-11, 4-12, 4-13

Aegean Sea, 3-26

Andreanof Islands, 3-16, 3-17, 3-18

Atlantic Ocean, 3-13, 3-23

Australia, 3-39

Banda Sea, 3-33

Bolivia, 2-8, 2-9, 2-19, 3-20

Brazil, 3-14, 3-20

California, Gulf of, 3-1

Chagos Archipelago, 3-38

Chile, 2-5, 2-6, 2-7, 2-20, 2-21, 3-11, 3-19

Easter Islands, 2-10, 3-21

Ecuador, 3-12

Fiji Islands, 2-17, 2-32, 2-33, 2-33a, 2-35, 3-27, 3-28

Galapagos Islands, 3-10

Guerrero, Mexico, 3-3

Hawaiian Islands, 3-15

Hokkaido, Japan, 3-24

Idaho, 3-2

INDEX, Continued

Indian Ocean, 3-40

Ionian Sea, 3-25

Iran, 3-31

Jalisco, Mexico, 3-5

Java, 2-23, 2-27, 3-34

Kamchatka, 2-4, 2-28

Kermadec Islands, 2-1, 2-29, 2-30, 2-38, 2-39, 2-42, 2-43

Kurile Islands, 2-3, 2-11, 2-16, 3-22

Lightning Spikes, 4-7

Loyalty Islands, 2-31

Luzon Island, 3-32

Macquarie Islands, 2-24

Mexico, Central, 2-41

Microseisms, 4-1, 4-2, 4-3, 4-4

New Britain, 3-30

New Guinea, 2-14, 2-15, 2-36

New Hebrides Islands, 2-12, 2-13, 2-34, 2-37

Ontario, 3-6

Oregon, Coast of, 3-7, 3-8

Peru, 2-2, 2-18, 2-19

INDEX, Continued

Phases

Lg, 4-14

Love, 2-40, 2-41

P, 2-1, 2-2, 2-3, 2-4, 3-1, 3-2, 3-3, 3-4, 3-5, 3-6, 3-7, 3-8, 3-9, 3-10, 3-11, 3-12, 3-13, 3-14, 3-15, 3-16, 3-17, 3-18, 3-19, 3-20, 3-21, 3-22, 3-23, 3-24, 3-25, 3-26, 3-27, 3-28, 3-29

PcP, 2-18

PcPPKP, 2-31

PKKP, 2-25, 2-26

PKKS, 2-37

PKP, 2-14, 2-22, 3-30, 3-31, 3-32, 3-33, 3-34, 3-35, 3-36, 3-37, 3-38, 3-39, 3-40

PKPPKP, 2-28

PKPPKPPKP, 2-29

PKPPKPPKPPKP, 2-30

PKPPKS, 2-38

pP, 2-1, 2-2

PP, 2-12, 2-13, 2-14, 2-15, 2-16

PPP, 2-16

PPS, 2-34

PS, 2-32, 2-34

INDEX, Continued

Rayleigh, 2-40, 2-42, 2-43, 2-44

S, 2 5, 2-6, 2-8, 2-9, 2-10, 2-11, 2-20, 2-32, 2-41

ScP, 2-19, 2-20

ScS, 2-10, 2-20, 2-21

SKKKS, 2-39

SKKP, 2-27

SKKS, 2-36, 2-37

SKP, 2-23, 2-24

SKS, 2-32, 2-33, 2-33a, 2-34, 2-35, 2-36

SP, 2-11, 2 35

SPP, 2-35

sS, 2-5, 2-7

SS, 2-17

SSS, 2-17

Surface, 2-41

Pressure Noise, Barometric, 4-8

Prince Edward Island, 3-37

Quebec, 3-6

Revilla Gigedo Island, 3-4

Sandwich Islands, 2-25

Santa Cruz Island, 2-26, 2-44

Sonora, Mexico, 2-40

Sumatra, 2-22, 3-35

Sunda Strait, 3-36

Train Noise, 4-6

Turkey, 3-29

Venezuela, 3-9

Wind Noise, 4-5